GEOLOGICAL AND STRUCTURAL ANALYSIS OF THE HWANGE AREA- NORTHWEST ZIMBABWE: USING REMOTELY SENSED DATA AND GEOGRAPHIC INFORMATION SYSTEMS (GIS)

MSc Thesis

By

Mufaro Chivasa

July 1996

Thesis submitted in partial fulfilment of the requirements for the Degree of *Master of Science in Applied Science.*

Department of Surveying & Geodetic Engineering
University of Cape Town

The University of Cape Town has been given the right to reproduce this thesis in whole or in part. Copyright is held by the author.

University of Cape Town

The copyright of this thesis vests in the author. No quotation from it or information derived from it is to be published without full acknowledgement of the source. The thesis is to be used for private study or non-commercial research purposes only.

Published by the University of Cape Town (UCT) in terms of the non-exclusive license granted to UCT by the author.

University of Cape Town

TO:
AMAI, ORIPAH, SHYNETH, EUNICE, OMELIA, BRIGHTON,

NDINOTENDA NOKUNDITSIGIRA KWAMAKAITA. MWARI VAKUKOMBORERE!

Acknowledgements

I would like to thank the Scientific and Industrial Research and Development Centre (**SIRDC**) for sponsoring my studies and the Environment and Remote Sensing Institute (**ERSI**) for supplying the Landsat TM data used in this research.

I am grateful to my supervisor, Prof. M.J. de Wit of the Centre for Interactive Graphics Computing, Department of Geological Sciences, University of Cape Town for his guidance during my research work.

I wish to thank my friend E. Musakwa and my uncle P. Ziwende for their encouragement and for acquiring the maps required for my research project. Special thanks go to my mother and my family members who gave me a lot of support during this time. Mr M. Barry (GIS Course Convenor), Dr M. Doucoure, Mr D. Wilson Mrs S. Binedell and the members of staff in the Surveying and Geodetic Engineering Department, University of Cape Town are also thanked for their technical assistance.

Last but not least, I want to thank my colleagues and friends, Eric Kwabena-Forkuo, Jefferson Chaumba, Samuel Osei, Samuel Yirenkyi, Antwi Adjei Danso, Bandile Mtshatsha, Miss V. Muleya, Mr L. Gatsi, Mr D. Padkin, Joy Gopal and Simon Onywere for their assistance and co-operation during my stay in Cape Town.

Abstract

There is a continuous need to locate more targets for coal exploration and evaluation of geological structures in the north-west coalfields in Zimbabwe. Conventional methods of analysing geological structures and field mapping are being hindered by inaccessibility of some areas and thick covers of Recent sediments. Remote sensing has been found to be a valuable method of identifying lithologic units and geological structures in the area. Integration of the remotely sensed data in a 2D GIS resulted in recognition of spatial relationships between lithologic units, geological structures , coal seams and vegetation patterns.

The Hwange area constitutes the western part of the Mid-Zambezi Karoo basin. The area consist of a wide spectrum of rocks ranging from Precambrian gneisses, Proterozoic schists and granulites, Karoo sediments to Tertiary and Recent sands. The area has been affected by a number of faults and shears some of which post date the Karoo sediments. These faults are an expression of the major tectonic events associated with this area. Some of the faults have been attributed to the effects of the Zambezi Rift System. Fault zones in the area, such as the Deka, Entuba and Inyantue Zones have been recognised as part of this system and these divide the Lower Karoo rocks into different coalfields.

To try and evaluate the outcrop patterns and geological structures in the Hwange area, all the available geological and structural data were captured in a spatial database. The diversity of data incorporated in the spatial database demanded the need for a structured database design approach. The Entity-Relationship model was used to conceptualise the geological data of the Hwange area. This model was transformed into the Relational Model that formed the implementation model of the database.

Landsat 5 TM data covering the area from the Zimbabwean winter (20 June 1984) path 172, row 73 were also analysed for the information required to locate Karoo rift faults and the distribution of lithologic units associated with coal. The use of directional filters in the E-W and NE-SW directions and vegetation reflection characteristics during the dry season (June 1984) proved very effective in mapping fractures in the Karoo rocks.

Landsat TM image enhancement techniques such as principal components analysis, edge enhancement, decorrelation stretching, band ratios; and colour composites made following these techniques, allowed mapping of different lithological units and discrimination between Karoo rocks and the crystalline basement rocks.

Lineament analysis defined E-W, ENE-WSW, NE-SW and NW-SE conjugate sets of lineaments. The first three sets are related to the regional fracture zones of the Zambezi rift system. The Entuba fault zone was found to be associated with most of the fractures affecting the Hwange coalfields. These have a dominant NE-SW and ENE-WSW trend in the Western Areas, Wankie Concession, Chaba, Entuba and Sinamatella coalfields. The E-W trending fracture set is dominated by joint sets in the Karoo basalt covering the north-west portion of the Hwange Coalfields. These show no relationship with the linear features of the Zambezi Rift system. The NW-SE trending lineaments are dominantly developed on tilted bedding planes in the Karoo rocks as well as a few sparse joints in the Karoo basalt.

Overlaying enhanced Landsat TM images on mapped faults and lithology data in a GIS revealed a number of features along the Entuba zone which were not previously known. The south-western part of the Entuba inlier was shown to consist of a synformal fold plunging to the south and bound on both sides by strike slip faults. Several kinematic indicators such as displacement of sedimentary strata have shown that the Entuba fault displays right lateral strike-slip coupled with dipslip movement.

Proximity analysis using borehole data (depth to top and bottom of a coal seam) showed that most of the lineaments in the area are normal faults which have caused considerable displacements of the main coal seam. Comparison of seam depth across most of these faults within coalfields and from one field to another shows that local and regional variations in depths of the main seam is primarily a function of vertical displacements along the faults over and above variations in the morphology of the pre-Karoo floor. The Entuba field was found to have greatest vertical variations over very short distances across faults, with depths varying from 60m to 520m from west to east over distances of

less than 500m. This part of the field has been partly affected by extensive normal faults, some of which can be traced for more than 10km.

In the Hwange area, the Karoo rocks have been down faulted into a rift margin which is in turn divided into smaller fault blocks by intra-rift faulting. The shape of the fault blocks are further controlled by the orientation of the post-Karoo faults which have also down faulted the main coal seam. Exploration activity in the area should also seek to establish the locations of these faults to help further decipher variations in depths of coal seams.

Table of Contents

List of Illustrations

List of Tables

Glossary and List of Abbreviations

ARC/INFO: ESRI GIS software

ARCVIEW: ESRI GIS software.

BCC : Band Colour Composite

BDC :Band Difference Colour Composite

BRC :Band Ratio Colour Composite

Cardinality Ratio constraint: The number of participating entity instances in a relationship between two entities:

CIGC :Centre for Interactive Graphics Computing

Colour Composite: A colour image produced by assigning a colour to each of the images of a scene and digitally superimposing the results.

Contrast Stretching: Increasing the contrast of images by expanding the original range of values or tones to utilise the full contrast range of the display device.

Coverages: ***ARC/INFO*** graphics data files.

Database: A collection of non-redundant data files shared among different applications (a collection of computer programs performing a particular function).

Decorrelation Stretching: A method of stretching highly correlated band images resulting in uncorrelated images.

Digital Elevation Model: A 2.5 D representation of terrain as a function of elevation

Directional filter: A spatial filter applied in a specified direction.

DSCC :Decorrelation Stretch Colour Composite

DISPLAY: Image processing software

Entity-Relationship Model: A conceptual model that takes the real world as composed of things or objects that have independent existence and are related to one another in one way or the other.

Entity: A thing that has independent existence.

ERSI :Environment & Remote Sensing Institute

Foliation: Fracture planes displayed in a highly sheared rock.

Footwall: The bottom part of a coal seam.

Foreign key: The identifying attribute of one entity that is incorporated as an attribute of the other to implement a relationship between the two entities in a relational model.

GIS **(Geographic Information Systems)**: Tools for collecting, storing, manipulating and retrieving data from the real world for a particular purpose.

Granulite: A metamorphic rock subjected to temperatures of over 750^0C.

GRID: The ARC/INFO module for processing cell base data.

Ground control point: A geographical feature of known location that is recognisable on images and can be used during geometrical correction.

Ground truth/data: Supporting data collected on the ground and information derived therefrom as an aid to interpretation of remotely sensed data.

High-pass filter: A spatial filter that enhances high spatial frequencies and as a result sharpens the image.

HSV : Hue. Saturation, Value

Hue: The attribute of colour by virtue of which it differs from grey of the same brilliance and allows it to be classified in different classes such as red, green etc.

IDRISI: Image processing and raster based GIS software developed at Clark University.

Image registration: The process of geometrically aligning two or more sets of image data such that the image data matches its position on the ground.

Karoo Rocks: A generic term of sedimentary sequences deposited from the Carboniferous to the Triassic epochs.

Kernel: A pixel array used for digital image filtering.

Key attribute: An attribute that uniquely identifies a feature.

Landsat: A series of satellites used for remote sensing that were deployed by *NASA* which carry the *MSS* and *TM* imaging system.

Lineament: A large scale linear feature shown on an image that reflects a wide zone of faults and other fractures and zones of weakness in the bedrock.

Lithology: The field description of rocks

Mean Area Length Parameter: A parameter that determines the density of lineaments with a certain length range in a particular area.

Mining Lease: An area where a mining company has mining rights.

Multispectral data: Remotely sensed data in two or more spectral bands.

NASA: National Aeronautics and Space Administration

NDVI: Normalised Difference Vegetation Index

Object-Oriented model: A data model that uses real world concepts instead of computer models: It takes the real world as a system composed of objects with unique identities.

Overburden: The amount of waste material overlying a coal seam.

Porphyroblastic: A metamorphic texture defined by highly deformed large crystal of a certain mineral.

Principal Components Analysis (PCA): A mathematical method of generating a new set of variables for band images that are highly correlated which describe the variance of the original data set but are independent of each other, that is their correlation is zero.

Relation: A two dimensional table used to store data in a Relational data model.

Relational Model: A data model that uses a table to represent an object in the real world.

Remote Sensing: The use of electromagnetic radiation sensors to record images of the environment which can be interpreted to yield useful information: i.e obtaining information about the physical features without any physical contacts with the features.

RGB : Red, Green, Blue

Safari Area : Hunting Area

Saturation: The purity of a colour or the degree to which all the wavelengths correlate to the dominant wavelength (hue).

Spontaneous ignition/combustion: Ignition of coal measures as a result of pyrite oxidation.

Structured Query language (*SQL*): A language used in documentation of tables, definitions and retrieval of data tables using structured statements.

Tectonics: Movement of faulted blocks relative to each other.

Thematic mapper(*TM*): A second generation imaging system used on board the Landsat satellites.

TIN - **Triangulated Irregular Network**: A triangulation method that uses x,y,z co-ordinate triads to fit a set of triangles to all data points and interpolating intermediate values of z from known values at the corners of triangles.

Training sets: The data samples of known identity used to determine decision boundaries as part of a supervised classification of a digital image.

Type Locality : A place where the lithologic units of a certain group of rocks are fully represented.

Value: Intensity of the colour.

Chapter 1

Introduction

1.1 Introduction

The ability to merge spatial data sets from different sources, display and manipulate combinations of these data often leads to an understanding and interpretation of spatial phenomena that are not apparent when individual spatial data types are considered in isolation. For this reason, Geographic Information Systems (GIS) technology has seen a rapid development in earth sciences where merging and manipulation of cartographic and remote sensing data is required to support decision making as well as identification of potential mineralised areas and environmentally sensitive areas (Bonham-Carter 1994).

In geology, Remote Sensing is a valuable method to help identify and analyse lithological distributions, outcrop patterns and structural features. It also provides multispectral data covering large areas. GIS provides the analytical tools that allow integration, manipulation and inference of the meaning of such data sets. Inference is carried out by performing measurements, statistical computations and fitting of models to data values as well as visual assessment of such manipulated data.

Integration of the two technologies (GIS and Remote Sensing) has been recognised as a powerful tool that can help in understanding geological structures, lithological distribution, and improve efficiency in delineation of exploration and mining target areas. For this reason, these technologies were chosen for the analysis of the geology, structure and coal potential of the Hwange Area in Zimbabwe. The area is the only current source of bituminous coal in Zimbabwe and is the target for ongoing coal exploration. Identification of possible areas for coal exploitation is becoming a problem because of unavailability of detailed geological maps and because of the inaccessibility of some potential mineralised areas. Mining in the already evaluated coalfields has intersected a number of geological structures such as faults which have not been detected by conventional

geological mapping procedures. This underscores the real need for using remotely sensed data in the area as described in the later sections of this thesis.

The thesis comprises eight chapters. Chapter 1 is an introduction to the study area ; the geology of the area and aims of the thesis. Chapter 2 gives an overview of the mapped geology and geological structures of in the Hwange area as given by earlier researchers such as Lockett (1979) and Watson (1960). The third and fourth chapters describe the design and structure of the spatial database constructed for this study. The chapter also gives a brief description of all the data sets incorporated in the Hwange database. Chapter 5 is concerned with digital image processing techniques and extraction of spatial data from remotely sensed data. Integration of map data and interpretation of lithologic distributions and geological structures are discussed in Chapter 6. Chapter 7 outlines conclusions and recommendations of this study.

1.2 Location of the Study Area

The study area is about 9600 square kilometres and is located in the western part of Zimbabwe, in the Hwange District, Matebeleland North Province. The area centred at the coal mining town of Hwange located 335km north-west of Bulawayo, is bound by the following geographic co-ordinates: $26^0$15E; $18^0$00S, $27^0$10E; $18^0$00S, $27^0$10E; $18^0$45S, $26^0$15E; $18^0$45S. On Landsat 5 the area falls within path 172 row 73, quad 1. Figure 1.1 below shows the location of the study area.

The area covers the mining leases of Wankie Colliery Company, Kamativi Tin Mines and several special grants and exclusive prospecting orders (EPOs) for coal, lead-zinc, copper and diamonds. The southern half of the study area is covered by the Hwange National Park and the Deka Safari Area, the west by the Matetsi Safari Area and the south-east by the Sikumi Forest Land. The central and northern parts are used for communal farming. The Bulawayo-Victoria Falls railway line passes through the southern part, and the main road connecting Victoria Falls to Bulawayo runs through the central part of the area.

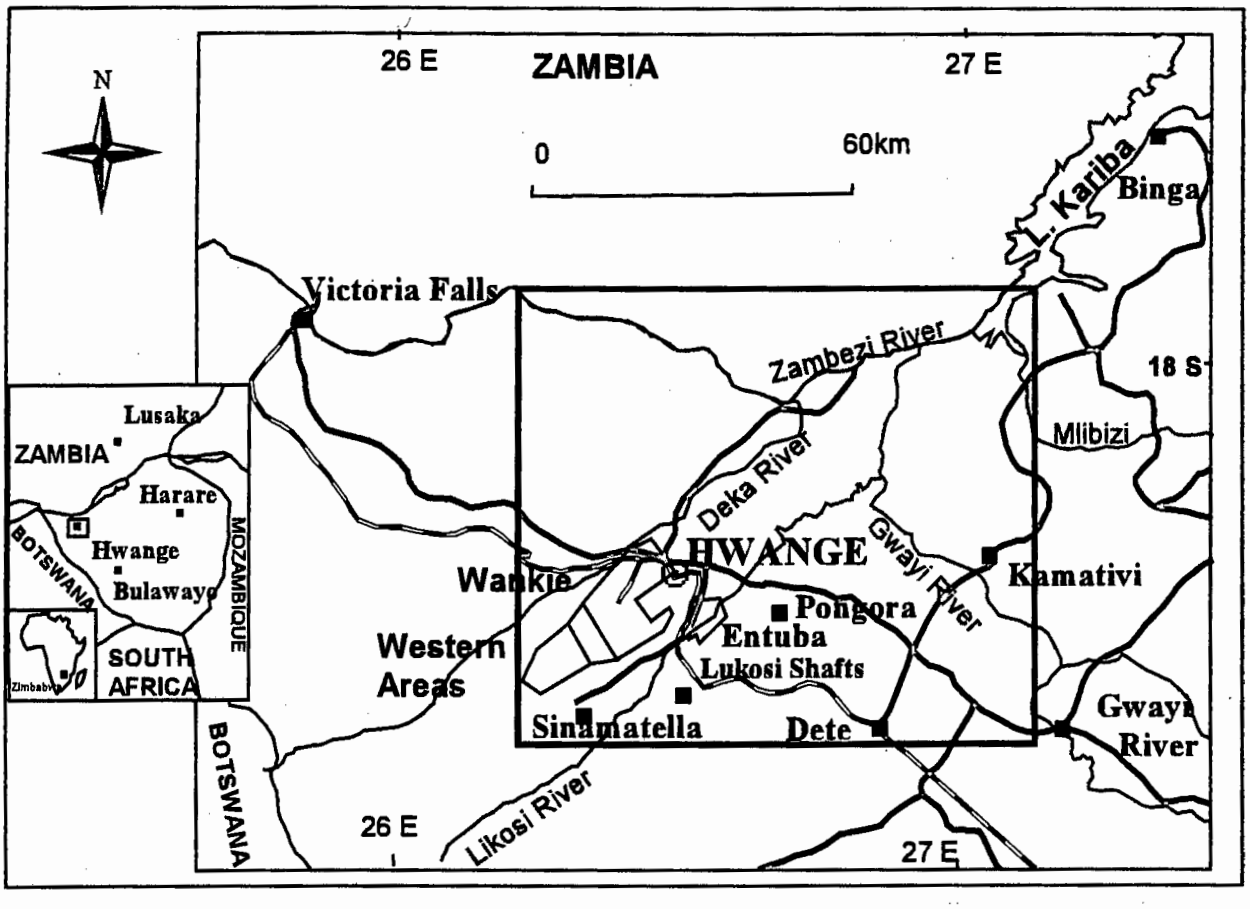

FIG 1.1: Map Showing the location of the Hwange Area and major coalfields.

The box define the extent of the study area

The two main power lines (330kv) from the Hwange Power Station to Bulawayo and Kwekwe also pass through the central part of the study area.

1.3 Geological Setting

The lithologies of the study area constitute parts of the Mid-Zambezi Karoo Basin, the Magondi and Zambezi metamorphic belts. The western part of the area is covered by the coal bearing Permo-Triassic Karoo sediments and Jurassic basalts; the southern part by the Kalahari sands; the central and eastern sector by metamorphic rocks belonging to the 2.0 Ga Magondi and Zambezi Mobile Belts. The area was affected by post-Karoo faulting which is responsible for a complex array of faults and shears in the area. This deformation, as well as the sporadic cover of Kalahari sands, has resulted in a complex outcrop pattern throughout the area. The major faults trend NE-SW and some extend for distances of over 60km (Stagman 1978, Lockett 1979). The major faults divide the coal bearing Karoo sediments into several coalfields, namely: Wankie Concession; Western Areas; Entuba; Sinamatella; Lukosi and Inyantue coalfields. Currently the bituminous coal seam is mined in the Wankie Concession coalfield only. A detailed overview of the geology of the area is discussed in Chapter 2.

1.4 Topography, Climate and Vegetation

The study area consists of three well defined geomorphologic units, the Kalahari plateau of recent sands, the metamorphic basement inlier, and the relatively flat Karoo terrain. The Kalahari plateau is generally flat and covered with unconsolidated sand that supports dense woodlands dominated by Zimbabwean teak and mopane.

The metamorphic inlier, which covers the central and eastern parts, falls gently towards the north and is deeply dissected in the north-east to give rise to several peaks with altitude up to 1207 metres near Kamativi Mine. Vegetation on this inlier is dominated by brachystegia species.

The Lower Karoo sediments which consist of sandstones, fireclay, carbonaceous shales and glacial beds are characterised by low-lying flat country and the Upper Karoo sediments (escarpment grits

and ripple marked flags), by well wooded flat elongated hills tilted towards the north. Mopane and thorny species are the major vegetation types growing on Karoo sediments.

Climatic conditions are mainly semi-arid with average summer temperatures of up to 45 ° C. Average rainfall of 630mm per annum is restricted to the summer months (November to March). Drainage of the area is effected mainly by the Inyantue, Lukosi, Deka, Gwayi and Zambezi Rivers. The sources of the Deka, Inyantue and Lukosi rivers are close to the Kalahari sand contact with Karoo sediments in the southern sector of the area. These three rivers all flow towards the north to drain into the Gwayi and Zambezi Rivers.

1.5 Previous Geological Work

To date much of geological work done in the Hwange area has been mainly concerned with delineation of the coalfields, copper deposits and the pegmatite hosted tin deposits. Because of the potential of the area for coal, gas and base metals, certain parts of the area have been more extensively studied during detailed mapping and drilling that produced 1:25 000 scale maps of the Wankie, Western Areas and Entuba coalfields and 1: 100 000 maps of the Dete-Kamativi inlier.

Geological mapping in the Hwange area dates back to 1895, when Giese pegged a coal concession of about 600 square kilometres centred at the present location of Hwange town. Exploratory work started in 1901, and a shaft was sunk at Wankie which was used for underground exploration (Watson 1960). Detailed mapping around the present Hwange town was done by Hooper for the Wankie Coal, Railway and Exploration Company prior to coal production in 1904 (Watson 1960). Detailed regional geological mapping was done by Lightfoot in 1912. His work resulted in production of the first 1:100 000 geological map of the Hwange area. Lightfoot revised his map in 1928 to cover the area beyond the coal concession and depicted occurrence of granites and heavily sheared and faulted rocks in the Hwange Area (Lockett 1979). A short report by Maufe in 1931 was the first report that described the complex fault pattern of the area although it was compiled mainly for the Lower Inyantue valley.

Discovery of tin, fluorite and copper in the eastern part of the area resulted in a number of researchers remapping the area. From 1938 to 1979 several reports were compiled by Ferguson (1939), Maufe (1943), Watson (1960; 1962), Swift (1951), Ewart (1959) and Lockett (1979). The reports concentrated mainly on lithological distribution and put very little emphasis on structural interpretation and distribution of coal reserves with relation to geological structures.

The period, 1979 to 1981 saw a major oil and gas exploration-activity undertaken by Shell Developments (Pvt) in the Hwange area. This involved intensive diamond-core-drilling in the Entuba and Western Areas coalfields. Results of these activities are summarised in reports by Shell Developments (1981) and Palloks (1984). These reports show a positive correlation between depth to coal seam, orientation, coal quality and geological structures. The reports also highlight the occurrence of faults similar to those mapped underground and on surface in the Wankie Concession area. These newly discovered faults have not been fully investigated because of inaccessibility and lack of remotely sensed and geophysical data.

1.6 Outstanding geological problems of the Hwange Area

Because of the lack of detailed large scale geological and structural maps, the following outstanding problems in the Hwange area have not been resolved:

1. The nature of the contacts between the Karoo sediments and the Precambrian inliers is not clear. Effects of fault displacement along the contacts are not fully understood. Perhaps analysis of regional satellite imagery and geophysical data offers ways of understanding the relationships.

2. The central problem in the area remains that of identifying fault patterns in the weathered Karoo rocks covered with superficial sediments. These faults are difficult to identify in the field, so if any of the coal reserves in the Entuba, Western Areas and Sinamatella fields are to be upgraded to mineable reserves, faults in these areas should be identified and their displacements of the coal seam established.

3. Easily accessible coal deposits in the Wankie Coalfield are being depleted and some are becoming sub-economic due to increasing depth and unstable ground conditions. Future mining areas need to be located in the relatively inaccessible surrounding areas.

4. Some parts of the Hwange area have been affected by spontaneous ignition probably due to pyrite oxidation and have not been identified. Therefore analysis of remotely sensed data of the area facilitates identification of these areas prior to mining.

1.7 Objectives of the present study

The main objectives of the present study are:

1. To design and implement a geographically referenced database containing information required to establish spatial relationships between lithological distribution, coal seam properties and geological structures in the Hwange area.

2. To determine the combinations of Landsat TM bands that best discriminate between rocks associated with coal (Permo-Triassic sediments) from the surrounding igneous and metamorphic rocks.

3. To use GIS and image processing techniques to map lithologic units, localised fracture patterns, regional lineaments (folds, faults and shears) and attempt to establish their relationships with lithologic units and coal seam characteristics in the Hwange coalfields.

4. To identify target areas for coal exploration and further investigation of geological structures.

1.8 Research Methodology and Project Sequence

This section outlines the methods used in this research to capture, integrate and analyse geological and structural data of the Hwange area in a GIS. The methods include:

1. Design and construction of a database using 1:100 000 geological and topographic maps of the Hwange Area. Database implementation and digitising of maps using ***ARC/INFO*** software

2. Building of digital elevation models using topography and drainage data.

3. Rectification, registration and processing of Landsat TM images from the Zimbabwean winter season (20 June 1984), path 172 row 073 quad 1, using the following image processing techniques of ***IDRISI, DISPLAY*** and ***ARC/INFO's GRID*** and ***IMAGE INTEGRATOR*** software.

   (a) Principal Component Analysis (PCA)
   (b) Decorrelation Stretching
   (c) Edge enhancement
   (d) Image filtering
   (e) Band ratioing and Compositing
   (f) Band difference
   (g) Image classification

4 Visual interpretation of enhanced Landsat TM images and updating the geological maps of the Hwange Area and the spatial database.

5. Lineament analysis using histograms of frequency orientations and lengths. Calculation of mean area parameter and overlay on mapped faults.

6. Draping of Landsat TM processed images, lithology and structural features onto the digital elevation models and interpretation of geological data and topographic features on the composite images and lineament maps.

7. Evaluation of the location of the coalfields in relation to geological structures (faults, folds, shear zones) identified on Landsat TM scenes and digitised geological maps. Proximity analysis to determine the effects of faulting on coal seam depth and quality.

8. Construction of structural and geological models for the Hwange area showing the effects of each deformation phase on different rock types.

9. Geological modelling in a GIS to facilitate identification of possible coal exploration target areas.

1.9 Limitations of the present study

(i) Geophysical data was not available to support some of the interpretations made from the Landsat TM images. Geophysical data together with borehole data would allow more robust interpretation of subsurface geology.

(ii) Software used in the research had limited image processing capabilities because it was running on low memory platforms, thus it did not have enough disk space to support processes that require large memory such as principal components analysis.

(iii) There was limited time for fieldwork and ground truth data to support interpretations made from the Landsat TM images covering the northern part of the study area.

Chapter 2

An Overview of the Regional Geology and Tectonic setting of the Hwange area.

2.1 Introduction

This chapter is concerned with reviewing the regional and local geology as well as the tectonics of the Hwange area.. The overview is a summary of the tectonic models and geology shown in Figs 2.1 to 2.5 based on the work done by Lightfoot (1929), Watson (1960), Petters (1991), Leyshon and Tennick (1988), Osterlen (1990), Stagman (1978) and Lockett (1979) Orpen et al (1990) and interpretation of Landsat TM data.

2.2 Regional Geological Framework

The Hwange Project area lies within three geological terrains, viz. the Zambezi Mobile Belt, Magondi Belt and the Mid-Zambezi basin (Stagman 1978). The area has suffered two periods of Precambrian orogenic activity and a major Palaeozoic rifting event (Zambezi Rift system). The two orogenic events have resulted in high grade gneisses and schists which have been a focus of research on several fundamental questions of pre-Karoo tectonics.

Some of the high grade gneisses and schists in the Hwange area have been recognised as the western extension of the 2.1 Ga Zambezi Mobile belt (Stagman 1978). In the study area the Zambezi belt is represented by strongly deformed garnetiferous and granitic gneisses containing a pronounced WSW-ENE trending tectonic fabric (Lockett 1979). These rocks have been intruded by late Proterozoic granites, serpentinites and dolerite dykes. The Zambezi belt continues beneath the Kalahari sands blanket westward (Fig 2.1) into Botswana and Namibia to link up with the Damara belt.

The Magondi belt is represented by the Piriwiri and Malaputese Groups. The Piriwiri Group consists of black graphitic and ferruginous slates and highly metamorphosed schists whilst the Malaputese Group comprises granulites, quartzite and other paragneisses. Munyanyiwa et al (1995) recently dated high grade rocks of the Magondi Belt at 1930-1960 Ma . These are interpreted to represent major magmatic activity in the south-east part of this belt. This has linked the rocks of the Piriwiri and Malaputese Groups to a major crustal disturbance along the edge of the Zimbabwe craton during the Mesoproterozoic. The belt has also been extrapolated to extend beneath the Kalahari sand cover, and has been correlated by Stowe (1989) to represent the northern extension of the Namaqua Mobile belt. Fig 2.1 below shows the regional tectonic setting of the Hwange area as interpreted by Stowe (1989) and Orpen et al (1990).

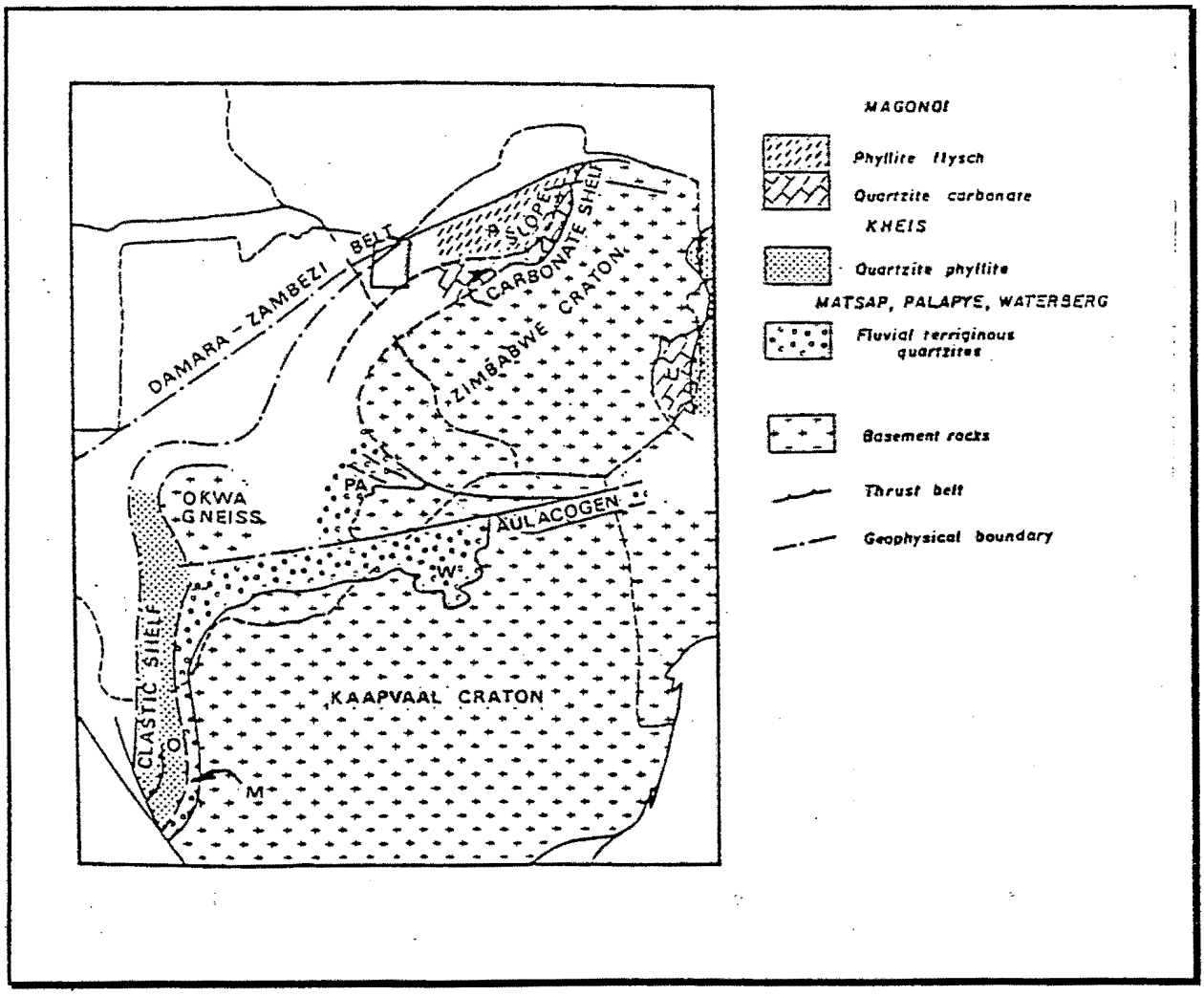

FIG 2.1: **Map showing the regional tectonic setting of the Hwange area and extrapolation of the Zambezi belt into Botswana and Namibia. The box shows the location of the study area.** (*Modified After Stowe 1989*)

Three phases of deformation have been identified by Leyshon and Tennick (1988), and Stowe (1989) to be responsible for the strong foliation, folding and high grade metamorphism characterising the Piriwiri and Malaputese rocks.

The central, western and northern portions of the Hwange area are part of the western extension of the Mid-Zambezi basin, filled with rocks of the Karoo Supergroup. In Africa the Karoo sequence is used as a collective term for a series of rocks deposited during a time from late Carboniferous to early Jurassic preserved as continental sequences. The Mid-Zambezi basin is one of the rifts that resulted from a long period of regional crustal extension preceding the fragmentation of Gondwana during the Permo-Triassic period (Petters 1991).

The basin forms the southern extension of the African Rift system and sediments in this basin show the variety of tectonic, magmatic and climatic conditions that have influenced the sedimentary environments along the African Rift valley. The sediments range from clastic, organic and chemical facies deposited as accumulations of blocks and conglomerates to fine sandstones, siltstones and clays. These represent the many depositional environments of the rifts during the Permo-Triassic period (Tiercelin, 1990; and Kogbe, 1990) which include piedmont areas, alluvial fans, fan deltas, fluviatile systems and lucustrine basins (Tiercelin, 1990). Clastic sediments are more frequent in the East African Rift valley including the Mid-Zambezi basin because of the existence of steep and rejuvenated topography that encouraged rapid erosion, therefore, resulting in thick layers of Permo-Triassic clastic sediments, that constitute the Ecca, Beaufort and Stormberg Groups of the Karoo Supergroup (Kogbe et al, 1990).

Continued crustal extension during late Triassic to early Jurassic resulted in extrusion of voluminous basalts throughout southern and eastern Africa including the western part of the Hwange area. This gave rise to the Drakenberg Group basalts which are well represented by the Drakensberg Mountains in South Africa and the Lesotho Highlands. These basalts form the only volcanic and youngest layer of the Karoo Supergroup in Africa. Fig 2.2 below shows the distribution of Karoo sediments and the Karoo basalts in Southern Africa.

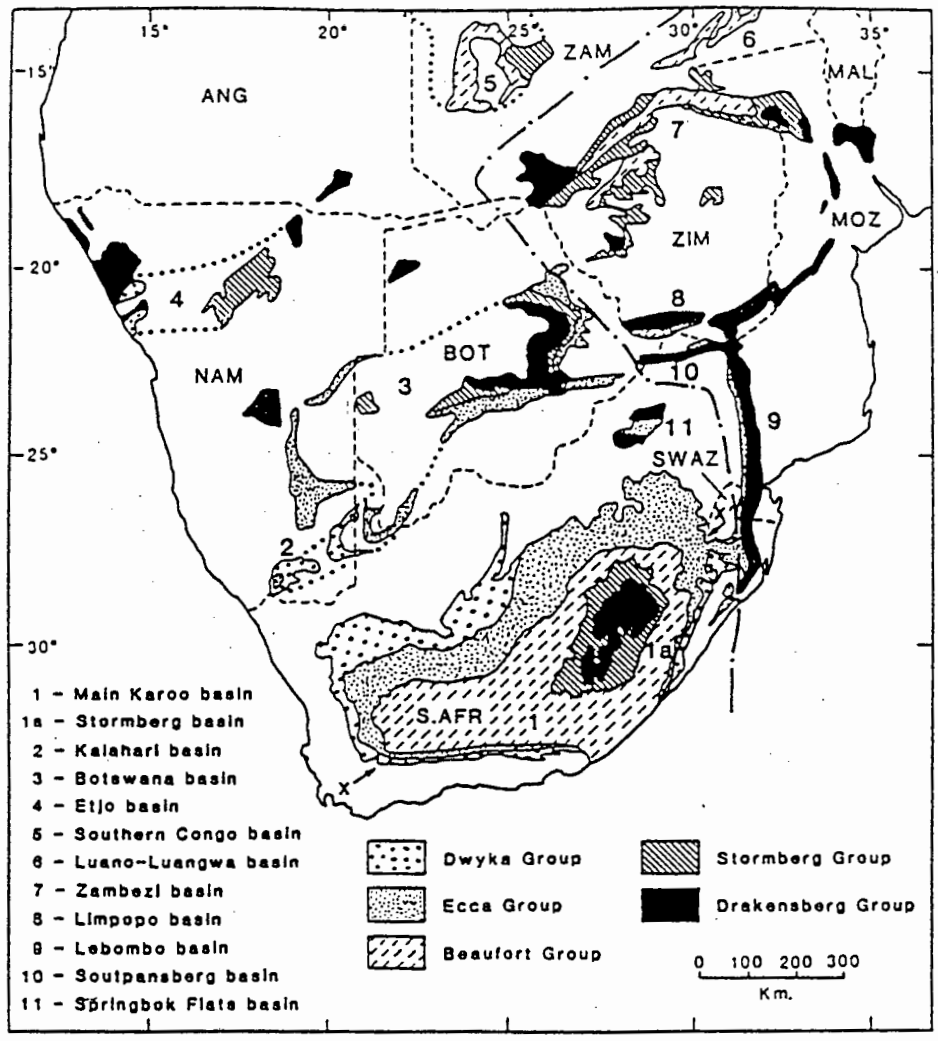

FIG 2.2: **The Karoo basins of southern Africa, showing outcrop and sub-crop stratigraphic units** *(Adapted from Smith et al 1993)*

Trans-tensional movements along the rift faults during and after the deposition of the Karoo sediments resulted in complex fault patterns characterising the Karoo sequence in the Mid-Zambezi basin. Similar movements in the East African Rift valley gave rise to a complex array of smaller internal faults within the regional rifts with NW-SE and NE-SW trends (Chorowicz,1990). Numerous major faults of this age have been recognised in the Hwange area such as the Deka, Entuba and Inyantue faults as shown in Fig 2.3 below (Orpen et al 1990; Petters, 1991). Figure 2.4 shows the distribution of rift faults in East, Central and Southern Africa and their extensions in the Hwange area . Rift faults in the Hwange area and the rest of the Mid-Zambezi basin are still active, therefore resulting in earth tremors occasionally felt along the Zambezi Valley.

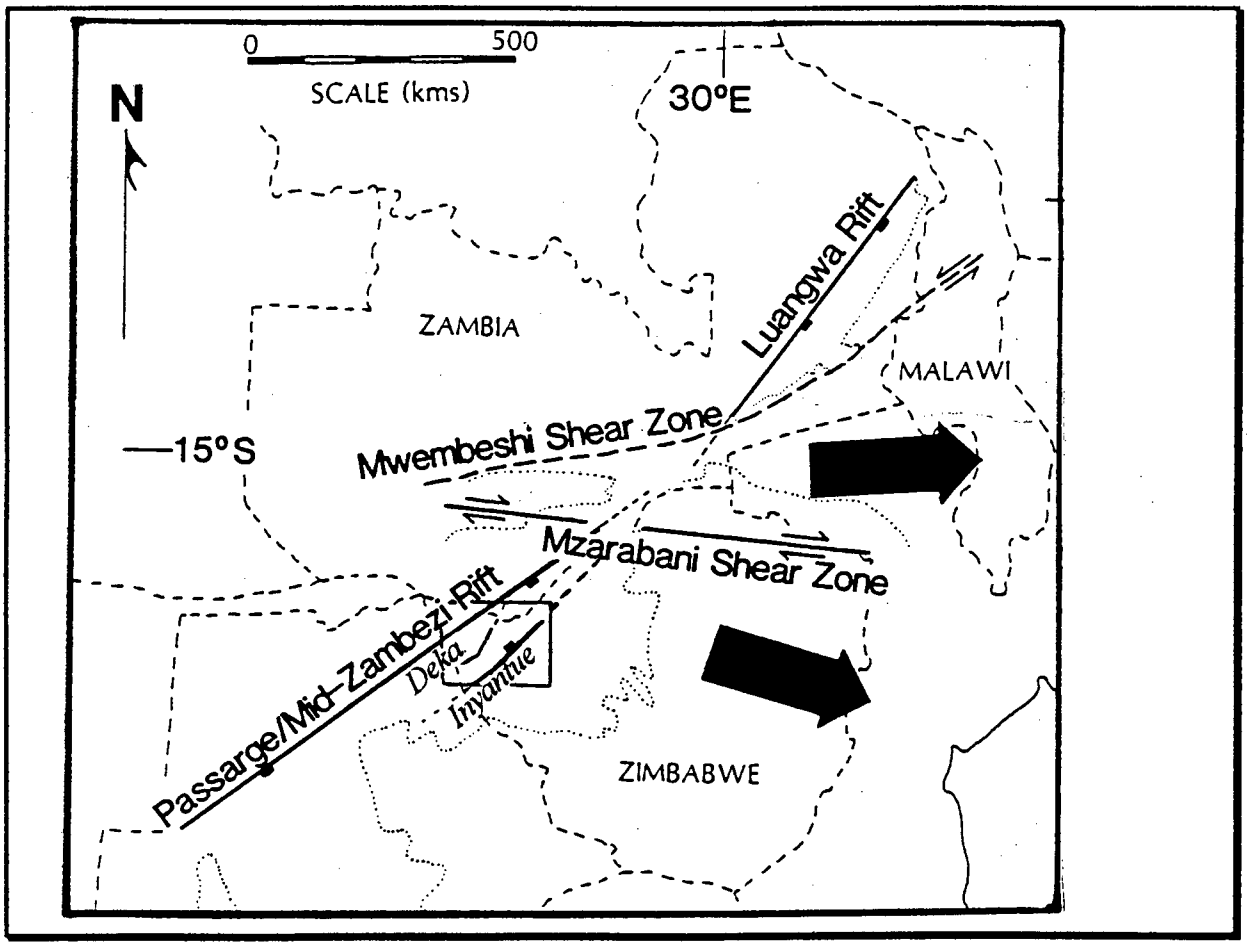

FIG 2.3: Diagram showing possible crustal movements in Central Africa during and after Karoo basin development. *(Orpen et al 1990).* Box shows the location of the study area.

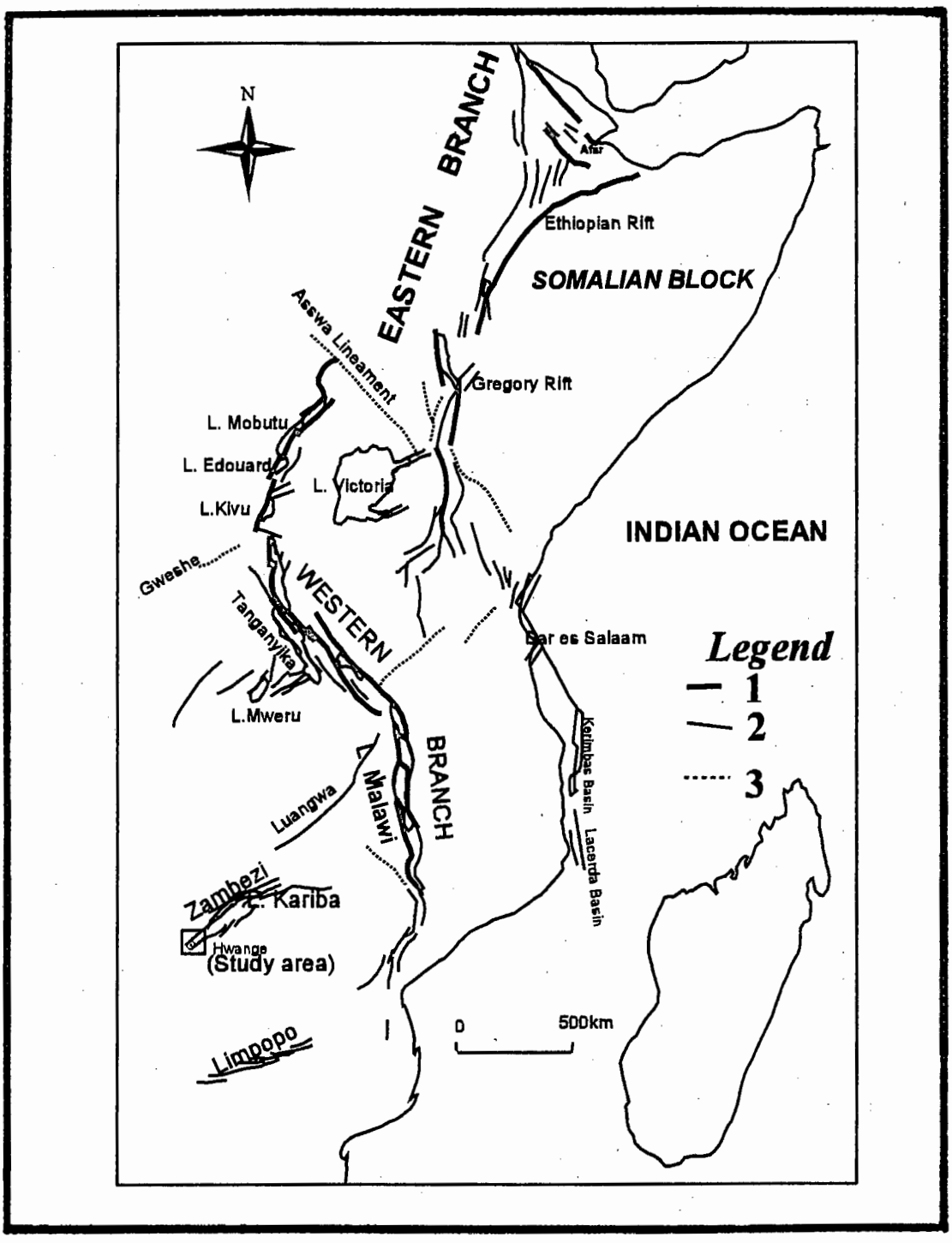

FIG 2.4 : Map showing the present activity in the East African Rift Valley: 1: Major active fault zones; 2: Active fault zones; 3: Inactive fault zones.
(Adapted and modified after Chorowicz, 1990)

2.3 Local Geology

The geology of the Hwange area is made up of the Zambezi Belt Gneisses, the Malaputese Group, the Piriwiri Group, Granites, the Sijarira Group and the Karoo Super Group. The following sections describe the formations and lithologic units representing each of these groups in the Hwange Area.

2.3.1 The Zambezi Belt Gneisses

The Zambezi belt in the Hwange area (see Fig 2.5) consists of Precambrian granitic gneisses which constitute about 60 percent of the crystalline rocks in the area. These rocks occupy a major part of the central part of the study area.

The Zambezi belt gneisses together with the Malaputese granulites, Proterozoic granites and the Piriwiri schists covering the central and eastern parts of the Hwange area are locally known as the Dete-Kamativi inlier (Stagman 1978, Lockett 1979) and those to the south of Hwange town, the Entuba inlier.

The Precambrian gneisses have been divided into three types, porphyroblastic and augen-gneiss, biotite-rich gneiss and migmatites. The biotite-rich gneiss is strongly sheared and occur mainly along the contacts with the strongly deformed supracrustal rocks of the Piriwiri Group. Tectonic layering strikes ENE-WSW and in the east these gneisses are in intrusive contact with the rocks of the Malaputese Group. The porphyroblastic gneisses have a gradational contact with migmatites. In the Entuba fault zone, (Fig 2.5), the sheared porphyroblastic gneisses are in faulted contact with the Karoo rocks, and have a predominant mylonitic texture. Foliation is variably developed and generally dips to the south-east and contains a gently plunging down-dip lineation. Foliation intensity increases towards the centre of the fault zone in the Entuba zone and towards the intrusive contacts with the Proterozoic granites in the Dete-Kamativi inlier.

FIG 2.5: Geological Map of the Hwange Area

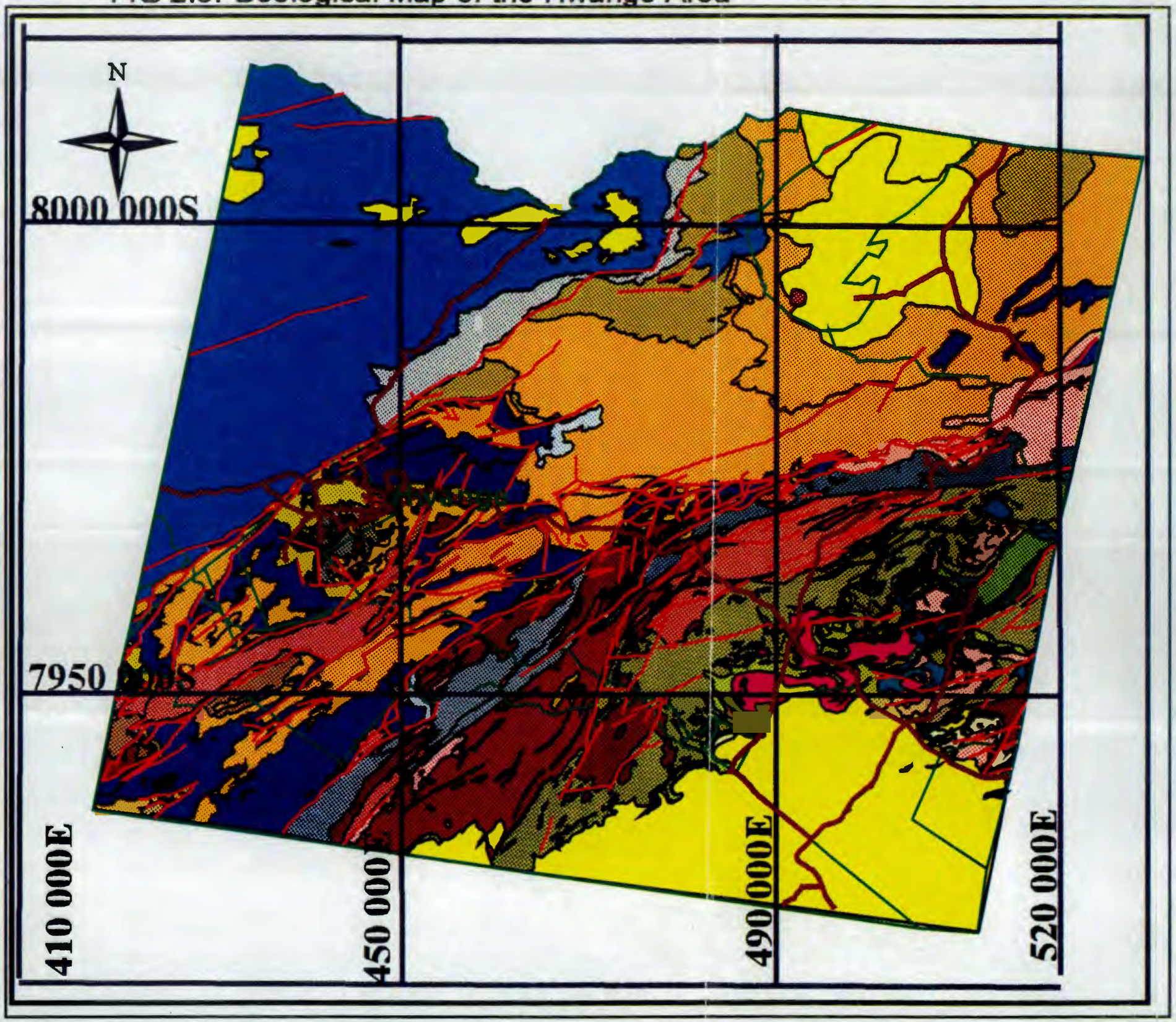

Road
Road
Border
Faults
Farms
Hwange
Lower Wankie Sandstone
Alluvium
Altered basalt
Amphibolites
Andalusite Gneiss
Batoka Basalt
Biotite Gneiss and Migmatites
Burnt Coal
Carbonaceous Shale
Dolerite Dyke
Escarpment grit
Fault breccia
Fireclay
Garnet-Biotite Gneiss
Glacial sediments
Graphitic Schists
Kalahari sand
Lower Wankie Sandstone
Madumabisa Mudstone
Mafic and calcareous amphibolites
Mafic and metapelites
Massive Granite and Nebulitic gneiss
Massive granite
Metapelites
Mine dump
Mixed mafic and metapelites
Pink Paragneiss
Porphyritic Granite
Quartz rich gneiss
Quartzite
Ripple marked flags
Serpentinite
Sijarira sediments
Silcrete
Sillimanite Gneiss
Strongly Foliated gneiss
Tourmaline -garnet pegmatite
Tourmaline-mica schist
Tourmaline-mica-garnet schist
Undifferentiated Karoo sediments
Upper Wankie sandstone
Veined tourmaline-garnet schist
Veined tourmaline-garnet schists
calc-silicate rocks, marble
metapelites
mixed mafic and metapelites

24 0 24 48 Kilometers

2.3.2 *The Malaputese Group*

The Malaputese Group consists of mafic granulites, metapelites, quartzites, paragneisses calcareous and magnesian rocks intercalated with marble (Lockett 1979, Watson 1962). These lithologies are part of the 2.0 Ga Deweras Group of the Magondi Belt. Similar to the Deweras Group in the Chinhoyi-Lomagundi area, these rocks are generally undifferentiated. The most extensive lithologic units of the Malaputese Group are the mixed mafic granulites and metapelites (see Fig 2.5). These are mainly composed of undifferentiated metapelites, mafic granulites and amphibolites. These rocks cover the area extending from the Gwayi River Mine towards the south-west through Dete and are blanketed by the Kalahari sands. Towards the east and north-east of the Gwayi River Mine, the mixed rocks grade into metapelites referred to by Lockett (1979) as the Eastern domain. These are characterised by elongated ridges of chlorite-sericite, biotite-quartz schists and graphitic schists. The metapelites are enfolded with pink paragneiss and quartzite. The quartzite form low-lying elongated ridges to the south-east of Gwayi River Mine, and these rocks are strongly foliated and interfolded with the paragneisses.

The metamorphic conditions of the Malaputese rocks have been evaluated by Lockett (1979), who found that an early high-grade metamorphism attained the granulite facies resulting in garnet, cordierite, sillimanite, andalusite mineral assemblages in the metapelites. Chlorite and sericite in both mafic granulites and metapelites are a result of retrograde metamorphism.

Large scale isoclinal folds with axial traces parallel to foliation can be recognised in all the groups. Three large scale synclinal folds have been traced, south of Kamativi Tin Mines, around the village of Dete and north of the Hwange Airport covering the area around Gwayi River mine (See Fig 4.2).

2.3.3 The Piriwiri Group

The 2.0 Ga Piriwiri Group delineates a ENE-WSW trending belt cutting diagonally across the study area (See Fig 2.5). The group consists of supracrustal formations made up of garnetiferous mica schists, phyllites, impure quartzites, sillimanite gneiss, calcareous, mafic and graphitic schists. These rocks have been divided by Lockett (1979), Leyshon and Tennick (1988), Watson (1962) and Stagman (1978) into three major Formations. The Tshontanda Formation (which occurs around Tshontanda siding), the Inyantue Formation, which is the belt along the Inyantue river, and the Kamativi Formation. The high grade rocks in these belts have been subjected to intense deformation and are intruded by granites dolerite dykes, garnet-tourmaline pegmatites and tin pegmatites.

2.3.3.1 The Inyantue Formation

The Inyantue Formation forms the main belt of the Piriwiri Group in the Hwange area. The belt is flanked on both sides by strongly foliated gneisses, parallel to the west by the Tshontanda Belt. As the belt emerges from beneath the Kalahari sand cover it narrows northwards where it merges with the schists of the Kamativi Formation. The Inyantue Formation consists of garnetiferous gneiss and schists incorporating intercalations of calcareous, graphitic, magnesian and arenaceous rocks (Lockett 1979). These have been distinguished into seven categories namely, garnetiferous gneiss and schist, calcareous rocks, graphitic schists, dark-blocky metapelites, biotite-hypersthene granulites, quartzite and magnesian rocks.

Pressure and temperature paths analysed by Lockett (1979) and Watson (1962) shows that the rocks have been subjected to granulite facies metamorphism and subsequently to retrograde metamorphism, as evidenced by the presence of tremolite-chlorite schists in the area. Foliations and lineations are sub-parallel to those occurring in the surrounding gneisses. Sporadic pegmatites have been found to intrude the Inyantue Formation. There are a greater number of (10-15 dykes per five square kilometre) dolerite dykes than in other Formations. Schists of the

Inyantue Formation are covered in the area south-east of RHA mine by Lower Karoo sediments which have been recognised to host very good coal seams (See Fig 2.5).

2.3.3.2 The Tshontanda Formation

This Formation comprises garnetiferous mica schists, sillimanite gneiss with intercalations of quartzite, meta-arkose and tourmaline garnet-biotite schist. The Tshontanda Belt emerges from beneath the cover of Karoo sediments in the north and trend south-west where it is covered by the alluvium and the Karoo sediments. The rocks (Lockett, 1979), were subjected to temperatures of about 750 °C during granulite facies metamorphism. Foliations and lineations trend ENE-WSW and are sub-parallel to the garnet-tourmaline pegmatites.

2.3.3.3 The Kamativi Formation

The Kamativi Formation consist of tightly folded muscovite schists, fine-grained biotite schists and intercalations of metasediments similar to those in the Tshontanda Belt. The schists are cut by garnet-tourmaline pegmatites and discordant sheets of lithium and tin-bearing pegmatites. The south-west end of the Kamativi Belt is covered by the outliers of the Karoo sediments and the southern contact with the gneisses is heavily faulted. Faulting is more intense towards the contact between the Kamativi belt and the Inyantue belt (see Fig 2.6 below) where a NE-SW array of faults filled with quartz veins is prominent (Watson 1962).

2.3.4 Granite

The Granites of Meso-proterozoic age occur in the central and western parts of the Dete-Kamativi inlier. These are mainly granodiorites (Lockett 1979). A porphyritic granite forms a prominent elongated zone of intrusions along the Piriwiri and Zambezi Belt gneiss north of Pongora siding (see Fig 2.5). In the area north of Dete the granites show a NNE-SSW trend, with post-intrusion deformation. The granites are associated with a rugged terrain of boulders and castle kopjes.

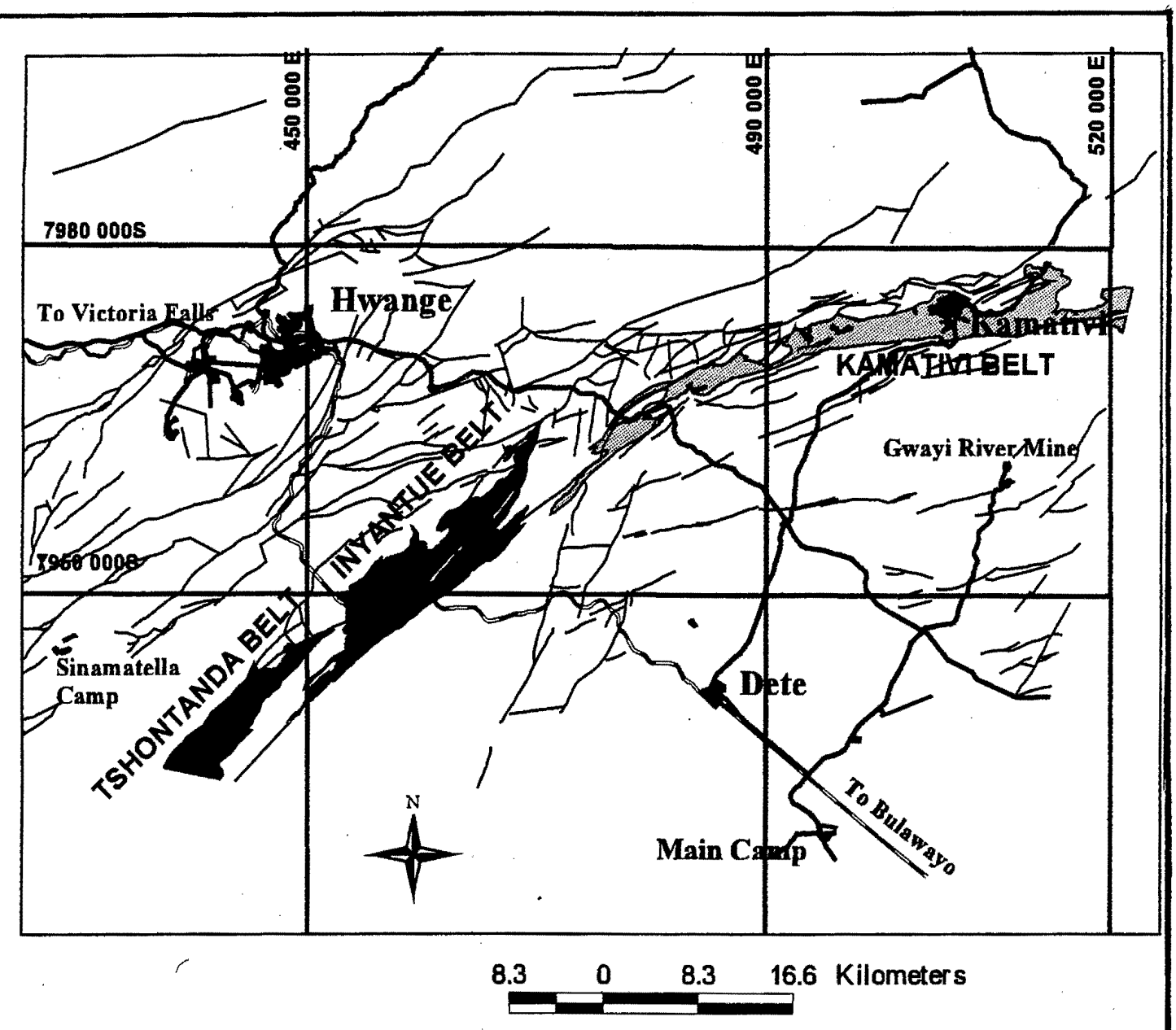

FIG 2.6: Map showing the Tshontanda, Inyantue and Kamativi Belts and the faults associated with each belt.

.2.3.5 *The Sijarira Group*

The Sijarira Group consist of hard flaggy purple shales, sandstone and red-brown quartzite occurring along the Entuba Fault zone. The most extensive exposure of these rocks is in the area north of Sinamatella Camp and south-west of the Western Areas coalfield where they occur as purple shales and sandstones. The sediments are unfossiliferous and have faulted contacts with the Karoo sediments and the granitic gneiss (Watson 1962).

2.3.6 The Karoo Supergroup

The major part of the Hwange Project area is covered by the rocks of the Karoo Supergroup. These rocks have been subdivided into a three fold division of Permo-Carboniferous, Triassic, and Jurassic sequences by Lightfoot (1928), Stagman (1978) on the basis of their fossil content. Locally the rocks have been classified into two sections, the Lower and Upper Karoo Supergroups. In the Hwange area, the nomenclature used throughout Southern Africa has been adopted by dividing the two Groups into the Dwyka, Ecca, Beaufort and Stormberg and Drakensberg Goups. These Groups are all well-represented in the area, and the area has been declared the type locality of the Karoo rocks in Zimbabwe.

Figure 2.7 shows the stratigraphic column of the Karoo and Table 2.1 shows the Karoo succession in the Hwange area and drawn using the field relations of the units as observed in the field. The nomenclature used in Fig 2.7 and Table 2.1, are adapted from Lightfoot (1929), Kogbe and Burollet (1990).

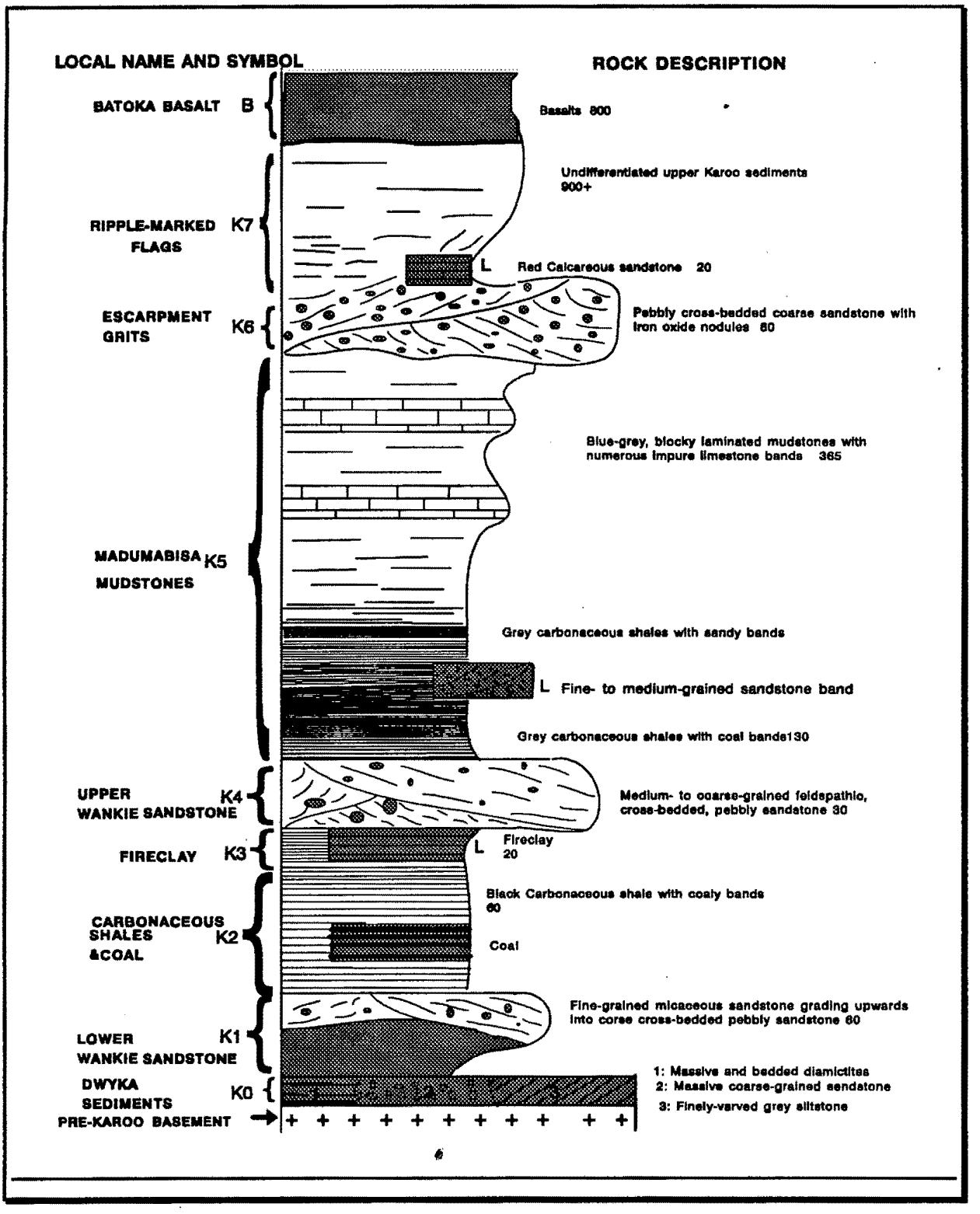

FIG 2.7: Stratigraphic column of the Karoo units in the Hwange area. Numbers represent thicknesses in metres, "L" denotes locally developed beds *(Modified after Lightfoot 1929 and Lockett 1979)*

TABLE 2.1: Table showing the stratigraphic units of the Karoo Supergroup in the Hwange Area.

SUPER GROUP	GROUP	AGE	FORMATIONS	CODE	THICKNESS
UPPER KAROO	Drakens-burg	Jurassic	**Batoka Basalts:** Amygdaloidal lavas	B	800m+
	Stormberg	Triassic	**Ripple Marked Flags** Maroon shales, ripple marked silt, grey limestone and sandstone	K7	900m
		Triassic	**Escarpment Grit** Grit, weathering red	K6	60m-
LOWER KAROO	Beaufort	Triassic	**Upper Madumabisa Mudstone:** Grey mudstones with nodular limestone	K5	365m+
	Ecca	Permian	**Lower Madumabisa Mudstone:** grey-mudstones with coal bands	K5	130m+/-
		Permian	**Upper Wankie Sandstone:** Coarse White, feldsparthic sandstone	K4	30m-
		Permian	**Fireclay**	K3	20m-
		Permian	**Carbonaceous Shale and Coal:** Black carbonaceous mudstones with the main coal seam at the bottom	K2	60m-
		Carbo-Permian	**Lower Wankie Sandstone:** Fine grained sandstone	K1	60m-
	Dwyka	Carbonife rous	**Fluvio-Glacial Beds**	K0	72m-

2.3.6.1 The Dwyka Group

The Dwyka Group comprises glacial sediments which directly overlie the Precambrian basement gneisses. These sediments occur in two areas in the Hwange Area, to the south-west of the town of Hwange along the south-western edge of the Western Areas coalfield and along the Pongora river, about 50 km south-east of Hwange (see Fig 2.8). In both areas the sediments have been exposed and/or intersected by exploration drillholes. Four lithofacies have been distinguished, namely, massive and bedded diamictites, massive sandstone deposited in a fan delta, fine grained glaciolacustrine clastic sediments and finely varved grey siltstone (Oesterlen 1990). In the Pongora area, south-east of Hwange the sediments attain a maximum thickness of 55 metres and in the Western Areas coalfield, a maximum thickness of 72.4 metres has been intersected by boreholes (Oesterlen 1990). In the Western Areas coalfield the glacial sediments overlie the quartzites of the late Precambrian Sijarira Group, but in the Pongora area, the sediments are in discordant contact with the Precambrian gneisses. In both areas the sediments dip shallowly towards the north-west, and paleocurrent analyses have been done by Osterlen (1990) and Lepper (1985) who suggested that deposition was from the south-east.

2.3.6.2 The Ecca Group

The group consists of occasional beds of coal, carbonaceous shales and feldspathic sandstones. In the Hwange area it is made up of the lower Wankie sandstone, coal and carbonaceous shale, fireclay and the upper Wankie sandstone.

The Lower Wankie sandstone

This is a fine grained, well sorted, pale coloured massive sandstone with occasional mica and pebbles occurring below the main coal seam and above the glacial sediments. Borehole intersections of the lower Wankie sandstone in the Wankie and Entuba fields have shown that in these areas the sandstone occurs as fine grained micaceous sandstone (Watson 1960). Outcrops of the lower Wankie sandstone occur throughout the areas covered by the Wankie, Entuba, Inyantue

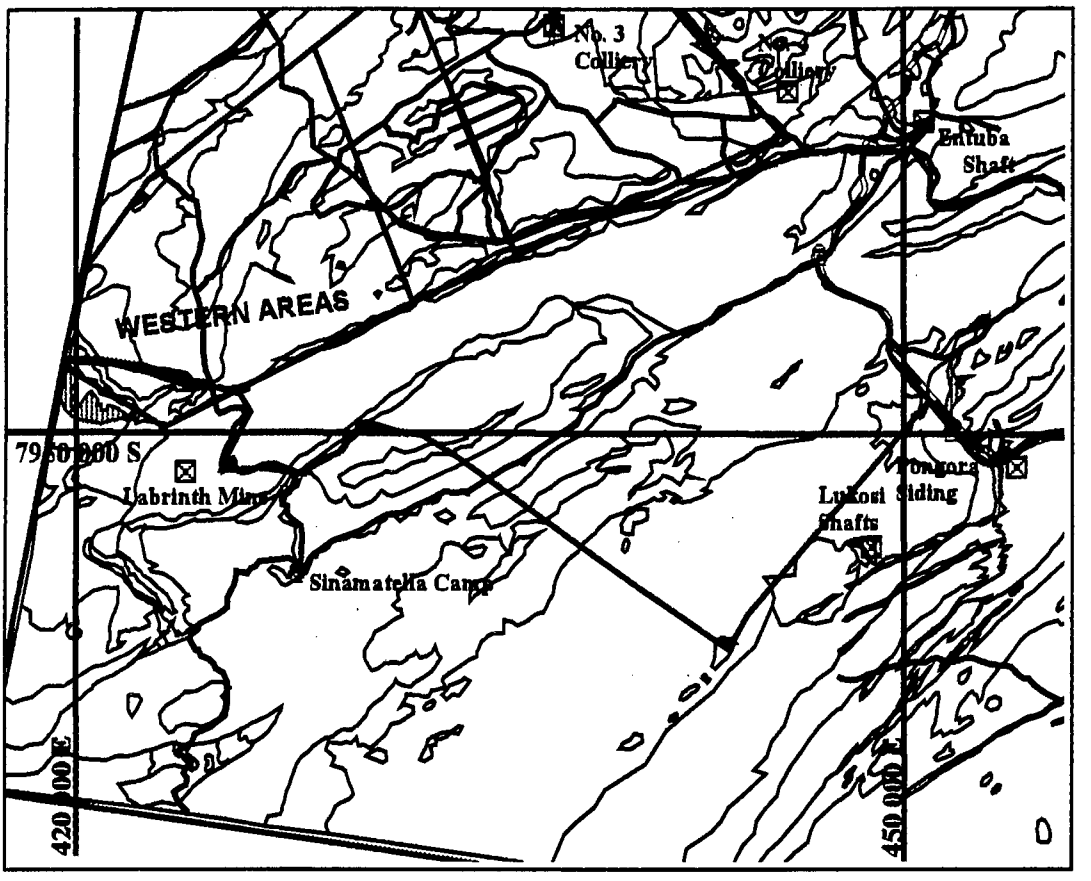

N

2.3 0 2.3 4.6 Kilometers

KEY

Gravel Road

Lithological Boundary

Railway Line

Camp/Rail Siding

Mine/Shaft

Dwyka Sediments

FIG 2.8: Map showing the distribution of the Dwyka Group in the Hwange Area

and Western Areas coalfields. Along the south-east Karoo-basement contact, Lockett (1979) has mapped outcrops from the Pongora river to the Gwayi River.

The lower carbonaceous shales and coals.

The lower carbonaceous shales are well bedded, friable rocks composed of dark carbonaceous and pale coloured shaly layers. The bottom of these shales contains the main seam, which attains a thickness of 20m in some parts of the Wankie Coal field. The shales are poorly exposed except in areas around Hwange, Dinde School and Inyantue field where the carbonaceous shales occur as outliers on the Precambrian rocks. Watson (1960) noted that where these shales and the main coal seam have been faulted and exposed, the areas have been affected by spontaneous combustion. This has produced burnt areas occurring in the Wankie Concession area, Inyantue and the Entuba field adjacent to Entuba fault.

The Fireclay

This is a high-grade raw refractory material locally replacing the higher horizons of the lower carbonaceous shales. Fireclay is exposed in the central part of the Wankie Concession, Western Areas and Inyantue fields. Outcrops are hard, cream-yellow in colour and weather into small angular fragments. In some areas, and with depth, the fireclay grades to hard, greyish to pale grey rock (Watson 1962). The fireclay attains maximum thickness of 20 - 30 metres in the Wankie Concession area.

The Upper Wankie sandstone

This sandstone is exposed in all the coalfields with more extensive exposures in the Wankie Concession, Western Areas, Entuba and the Inyantue area. The upper Wankie sandstone consists of medium to coarse grained, pebbly, cross bedded feldspathic sandstone which weathers to flat topped rounded boulders. The sandstone overlies the fireclay and carbonaceous shales and attains a maximum thickness of 30m in the Wankie Concession and Entuba fields.

2.3.6.3 The Beaufort Group

The Group consists of thick layers of mudstones with thicknesses of up 1500m. The lower part of the sequence is Permian and upper part is Triassic (Kogbe and Burollet 1990). The Madumabisa mudstone represents the Beaufort Group in the Hwange area.

The Madumabisa mudstone

This forms the major part of the Lower Karoo cover. The mudstone comprises a 500 - 600m thick layer of grey to black mudstones which has been divided by Lightfoot (1929) and Lepper (1995) into, lower Madumabisa (upper carbonaceous mudstone), middle Madumabisa and upper Madumabisa mudstone. The upper carbonaceous mudstones occur above the upper Wankie sandstone. They are poorly exposed and only occur in small areas along the Lukosi and Inyantue valleys and the Entuba field. The carbonaceous layer contains impure coal seams rich in iron oxide with one attaining a thickness of more than one metre and locally known as the Madumabisa seam.

The mudstone above the carbonaceous mudstone consists of argillaceous beds and comprise the bulk of the mudstone exposed in the Hwange area. The mudstone is exposed in the entire area south of the Victoria Falls road and between the Dete inlier and Deka fault. The Madumabisa mudstone is very fine grained and weathers to small angular fragments with very thin bedding planes. Layers of sideritic mudstone and calcareous beds occur occasionally. The mudstone also forms cliff exposures in several parts of the Hwange area as shown by the spectacular Madumabisa Hill next to Colliery No.3. The Madumabisa mudstone marks the upper limit of the Lower Karoo sediments.

2.3.6.4 The Stormberg Group

This is a sequence of sandstones and mudrocks that overlie the Beaufort Group. The Escarpment grit and Ripple-Marked flags in the Hwange area represent the remnants of this Group.

The Escarpment grit and Ripple-Marked Flags

These are the only Upper Karoo (Triassic) sediments exposed in the Hwange area. The Escarpment grit forms elongated, flat topped ridges bound by steep slopes (escarpments) throughout the central part of the study area. To the south-west of Wankie Collieries, the grits cap the Madumabisa mudstone and form the woody-flat tops of the plateaux in the area. The entire area north of the Victoria Falls main road is covered by the grits and in places by the ripple-marked flags (Watson 1960). The grits are highly oxidised, fractured and silicified giving a rugged and red appearance to the steep slopes bordering plateaux in the area.

2.3.6.5 The Drakensberg Group

The Drakensberg Group is the topmost and youngest group of the Karoo Supergroup. The rocks in this Group are Jurassic in age and comprise basalts, rhyolites and pillow lavas. The basal part contains interbedded sediments of late Triassic age (Smith et al 1993). In the Hwange area, the Drakensberg Group is referred to as the Batoka basalt.

Batoka basalt

The Karoo basalts cover the western part of the study area. The basalts are separated from the Karoo sediments by the Deka fault. These basalts have been observed to contain zones of crystalline calcite and abundant ilmenite (Stagman 1978, Watson 1960). The rocks form a flat terrain west of Hwange cut by several gorges along the Zambezi, Deka and Matetsi rivers.

2.3.7 The Kalahari sands

The Kalahari beds of Tertiary to Recent age cover the south-east and parts of the northern zone of the Hwange project area. These consist largely of unconsolidated wind-blown sand with silcrete and some horizons of silicified sandstones. The sands attain a maximum thickness of 110m south-east of Dete.

2.4 Geological Structures

2.4.1 Folds

The two metamorphic belts forming the Dete-Kamativi inlier can be structurally divided into: (1) an open cross-folded terrain in the south-east zone and (2) linear terrain comprising elongate supracrustal formations and gneissic terrain. Three fold phases have been recognised within both terrains by Lockett (1979) and Watson (1962). These have produced complex interference fold patterns seen around Dete and Gwayi River Mine. Folding in the Tshontanda and Inyantue Formations is not extensive, but interference fold patterns have been noted around Illambo dam where the Inyantue Formation merges with the Kamativi Formation.

2.4.2 Shear Zones

Localised ductile deformation is characteristic of linear zones in the Hwange area and is attributed to regional heterogeneous shear strains. The major shear zones occur along the Entuba fault zone and along the margins of the Piriwiri rocks. Foliations are steeply dipping to the south-east and stretching lineations are sub-horizontal and parallel to the foliations.

2.4.3 Faults

Numerous major faults in the area are oriented NNE-ENE, trending sub-parallel to the Zambezi belt rocks. The main faults are the Deka, Entuba and Inyantue, Malaputese and Mambanje faults. The Deka, Entuba and Inyantue faults have been recognised as being western extensions of the Zambezi rift system (Stagman 1978). Local branching faults from these major faults cut across the Karoo sediments, resulting in complex fracture patterns in the coalfields.

2.5 Economic Geology

2.5.1 Base metals

The Dete-Kamativi inlier is the host to major tin, copper and tungsten deposits in Zimbabwe. Tin occurs in the pegmatites intruding the Piriwiri Group. The tin-bearing pegmatites extend from the

Tshontanda belt in the west to Kalinda Mine east of Kamativi Mines, over a distance of 70km (Lockett 1979). Total tonnage of ore hosted in these pegmatites is not known. The Kamativi Tin mine has been the major producer of tin in the area. Production started in 1950 and rose steadily from the time the mine opened to over 4000 tonnes of tin concentrate with 70 % tin per year by the time the mine closed down in 1994. Mining was also carried out using both opencast and underground methods at other mines such as Lutope, Kamalala, Kapata, Kalinda and Kapami. The mines produced an average of 300 - 500 tonnes of tin concentrate each year together with other base metals such as tungsten, lithium and tantalum. Most of these mines closed down in the mid-70s. It has been noted that there are still huge tin deposits which are not exploited in the area although the actual tonnage is not known.

Copper is another mineral that was mined in the Hwange area. The metal is hosted in mafic granulites of the Malaputese Group. Production was only at Gwayi River Mine which produced an average of 170 000 tonnes of copper ore per annum from 1969 until its close down in 1975. The rest of the area covered with the Malaputese Group was prospected for copper and results show that there are other areas such as around Fin Mine and Evvan claims that have a potential for economically viable copper deposits.

Tungsten was also produced from the Dete-Kamativi inlier. The mineral is hosted in woframite-bearing tourmaline-quartz veins occurring in parts of the Tshontanda and Kamativi belts. Economic deposits of tungsten were only discovered about 5 kilometres north of the Tshontanda siding. Mining was carried out at the RHA mines from the early thirties to 1972 when the RHA mines closed. The mine produced an average of 2000 tonnes of ore per month with a grade of 2kg of 70% WO_3 per tonne of ore (Lockett 1979).

2.5.2 Coal

The economic importance of the Hwange area lies in its huge deposits of coal currently mined at Hwange. The area has been extensively drilled and six coalfields have been delineated (See Fig 1). These are the Western Areas, Wankie Concession, Entuba, Lukosi, Sinamatella and Inyantue

Fields. There are two coal seams in the Hwange area, the poorly developed Madumabisa seam and the Wankie main seam. The main seam is developed in all the coalfields but is currently only mined in the Wankie coalfield because of its occurrence at shallow depths and high quality.

2.5.2.1 The Wankie Concession Coalfield

The Wankie coalfield is centred at the Hwange town and has produced more than 1.5 billion tonnes of bituminous coal since 1903. The average thickness of the main seam in the Wankie field is about 6.5m. The seam is mined in two portions, the top part with ash content greater than 15% and volatile content less than 25% is mined as steam coal and the lower portion with low ash content and high volatile content as coking coal. The total reserves for the Wankie Concession area are estimated to be more than 1 billion tonnes of insitu coal. Of this, more than 500 million tonnes are of bright coking coal and will be mined using underground methods. The opencastable reserves (depth less than 100m) amount to about 100 million tonnes insitu coal, of which half is bright coal. Most of the opencast reserves, which stood at 225 million tonnes by 1987 (Palloks, 1987) have been mined, therefore, raising the need to look for similar reserves in neighbouring fields.

2.5.2.2 The Western Areas Coalfield

The Western Areas coalfield lies to the south-west of the Wankie Concession field. Extensive drilling in the southern part of the coalfield was carried out by Shell Developments from 1978 to 1981. A total insitu coal reserves of about 1.2 billion tonnes of which only 77 million are opencastable were delineated. The average coal seam thickness is 7.9 m with an average ash content of 18%. Mineable coking coal evaluated to date stands at 46 million tonnes (Palloks and Broderick, 1982). Drilling of the northern parts of the coalfield towards the Wankie field can increase this tonnage as the quality of coal increases towards the Wankie Concession. No coal has been produced from this field and exploration in the field has been limited because of its occurrence in the Hwange National Park and Deka Safari areas, which are protected areas.

2.5.2.3 The Entuba Coalfield

The Entuba coalfield lies to the south-east of the Wankie Concession and is separated from this field by a zone of strongly sheared gneisses. Total insitu coal reserves found in the Entuba field amounts to 183 million tonnes with an average seam thickness of about 10.3m. The opencast reserves in the field constitute 77.3 million tonnes and underground reserves, the remaining 106 million tonnes (Palloks 1984, Watson 1960). More than 152 million tonnes of coal have been delineated as coking coal and 31 million tonnes as steam coal. The mineable reserves in the Entuba field could be much less than these tonnages because of extensive faulting and occasional spontaneous combustion. The field is the smallest of the three main fields, covering only about 12 km^2.

2.5.2.4. The Lukosi, Inyantue and Sinamatella Coalfields.

No evaluation has been done for the Lukosi, Inyantue and Sinamatella coalfields although coal measures have been mapped on the surface (Lockett, 1979, Stagman, 1978, Watson, 1960). Five boreholes drilled in the Sinamatella field intersected a heavily faulted seam with an average thickness of 5 metres. In the Lukosi and Inyantue fields the seam is only exposed in the Lukosi and Inyantue valleys. Boreholes drilled in the southern shallow end of the Lukosi field did not intersect any coal. No drilling has been done in the Inyantue field, but there are records that coal has been mined at a small scale in the Inyantue Valley where the sediments occur as outliers in the Inyantue schists, south-east of Hwange town.

2.6 Discussion

The geology of the Hwange Area has been studied in detail in the coalfields and the areas around the major mines such as the Gwayi River Mine and the Kamativi Tin mines. Regional correlation of the lithologic units in the area has not been done in detail but from an attempt made in this section it shows that the Zambezi Belt rocks, the Magondi Belt and the Karoo rocks occurring in this area correlates well with similar rocks in the East African Rift valley and the rest of Southern Africa.

The eastern part of the Hwange area has a high potential of base metals such as tungsten, copper, tin and lead. However, because of the small sizes of deposits found to date and low prices for these metals on the world market most of the exploration in the area has concentrated on coal which has been produced in the area for almost a century. This, therefore has prompted detailed study of the geology and structure of the Hwange coalfields and extensive diamond drilling for bituminous coal and methane gas in the Wankie Concession, Western Areas Coalfield, Entuba and other surrounding areas covered with Karoo sediments.

Geological structures are cited in the reports by Palloks (1984, 1987) and Shell Developments Exploration Report (1981) as the major problems in the Hwange coalfields if any of the more than 3 billion tonnes of coal reserves in these fields are to be mined. Faults affecting the Hwange coalfield have been attributed to the trans-tensional movements along the African rift faults represented in the area by the Deka and Entuba fault zones. Fault splays from these faults have been intersected in the Wankie Collieries where they have affected underground operations in some parts of the coalfield.

Chapter 3

Conceptual Design of the Hwange Database

3.1 Introduction

The core of a GIS is the database, that contains data as spatial and attribute data files. A GIS database can be defined as the a shared non-redundant collection of interrelated, spatially referenced data designed to meet the needs of a user (McCloy, 1995). The database is created and accessed by a software system linked to a GIS called a Database Management System (DBMS). This software system provides the facilities to store, retrieve, modify and delete data files from the GIS system (Burrough, 1986; McCloy, 1995). Information stored in a database can only be manipulated and interrogated to meet the user's needs if it is captured and stored in a structured format. The process of defining and structuring processing needs and data that are entered in a database is called database design (Fernandez, 1993).

The process of designing a spatially referenced database is similar to the design of any alphanumeric information system and can be divided into two broad phases; conceptual design and physical design. Conceptual design is the conceptualisation of the real world or integration of the requirements of the users in a database structure that supports the views and processing needs of the applications. This process produces a conceptual model of the real world being modelled in the database. For instance a geological database conceptual model would contain all the rock types, economic minerals, mines, faults and other features required for a geological analysis. Physical design refers to the implementation, choice of storage structures and access methods to the database (Navathe and Schkolink, 1978).

Digital databases of geological maps, structural maps and mineral distributions can be combined with other data sets such as satellite imagery, hydrology, soil, vegetation, land use and topography in a GIS. This facilitates modelling of processes like mineral deposition, tectonic processes, ground water flow and evaluation of variations of vegetation and relief with sub-surface geology. Inclusion

of these other non-geological data sets together with geological data in a GIS can potentially yield a comprehensive database. Creation of this extensive database, however, demands the need for a structured approach to database design. For this purpose, the structured approach was used to design the Hwange Database used in the evaluation of the geology and structure of the Hwange Area as described in later sections of this chapter. The Entity-Relationship (ER) model was used as the conceptual data model. This model was mapped into a Relational model (implementation model) which allowed implementation of the database in a 2D GIS *(ARC/INFO* and *ARCVIEW)* and use of ***Structured Query Language (SQL)*** to retrieve the data from the database as illustrated in later sections by the geological part of the Hwange Database.

3.2 The Hwange Geology Database

Analysis of the complex outcrop pattern and geological structures in the Hwange area requires several functionalities in the database. The functionalities should allow integration, manipulation and interpretation of geological and structural data from the Hwange Area. The following sections describe the main objectives and functionalities built in the Hwange Geology database and concepts used to design the database.

3.2.1 Objectives of building the Hwange Geology Database

The Hwange Geology database design and construction was done mainly to facilitate integration of data for the following purposes:

1. Ground truthing, registration and classification of Landsat TM images to correlate with known geology and geochemistry.

2. Creation of digital elevation (DEM) for structural analysis.

3. Evaluation and mapping of deformation features.

4. Delineating areas with coal reserves potential.

5. Demarcation of areas affected by the Magondi and Zambezi belt metamorphic events.

7. Analysis of areas affected by spontaneous combustion due to surface and subsurface processes.

8. Analysis of outcrop and fracture patterns and their relationships with regional tectonics.

9. Location of coal seams.

3.3 Database design and Entity-Relationship model concepts used to design the Hwange Database

This section presents the steps taken in the process of designing the database and a brief review of the entity-relationship model concepts.

3.3.1 Database design concepts

Database design is the development of framework of the optimal structure of the database as well as the definition of its contents and specification of constraints to be placed on the validity of the data (Fernandez and Rusinkiewicz,1993). Database design is aimed at achieving the following the following:

i) Ensuring that all data needed to satisfy the processing requirements are included in the database.

ii) Integrating the intended uses of the database in a single schema by developing a conceptual model.

iii) Ensuring that the data included in the database is structured in a way that makes the querying process efficient.

iv) Implementation of the conceptual model into a database management system used by a particular GIS package.

Figure 3.1 below is a diagrammatic representation of the steps in the process of database design adapted and modified from Fernandez and Rusinkiewicz (1993).

Phase 1 involves collection and analysis of data related to intended uses of the database. The purposes of constructing the Hwange Geology database outlined in the previous section illustrate this step and gives a framework to guide the entire process of database design.

Phase 2 is the development of the conceptual schema and evaluation of different relationships between different entities. During the design of the Hwange Geology database, this step involved analysis of the relationships between different rock types, geological structures, and surface features. The model developed represent the semantics of the database and the structure of the data used to describe other data (meta-data).

Phase 3 is the step at which the conceptual model is translated into the implementation model of a particular database management system (data-model mapping). For the design of the Hwange Geology database, this stage involved mapping of the entity-relationship model in the relational model (implementation model).

Phase 4 can be considered as the stage where the specific storage structures are designed. The sizes and types of the attribute table columns are defined according to their relationships to each other in the relational data model.

Phase 5 is the actual implementation of the database. This step involved input of attribute values in the database management system used in ***ARC/INFO*** and ***ARCVIEW*** software.

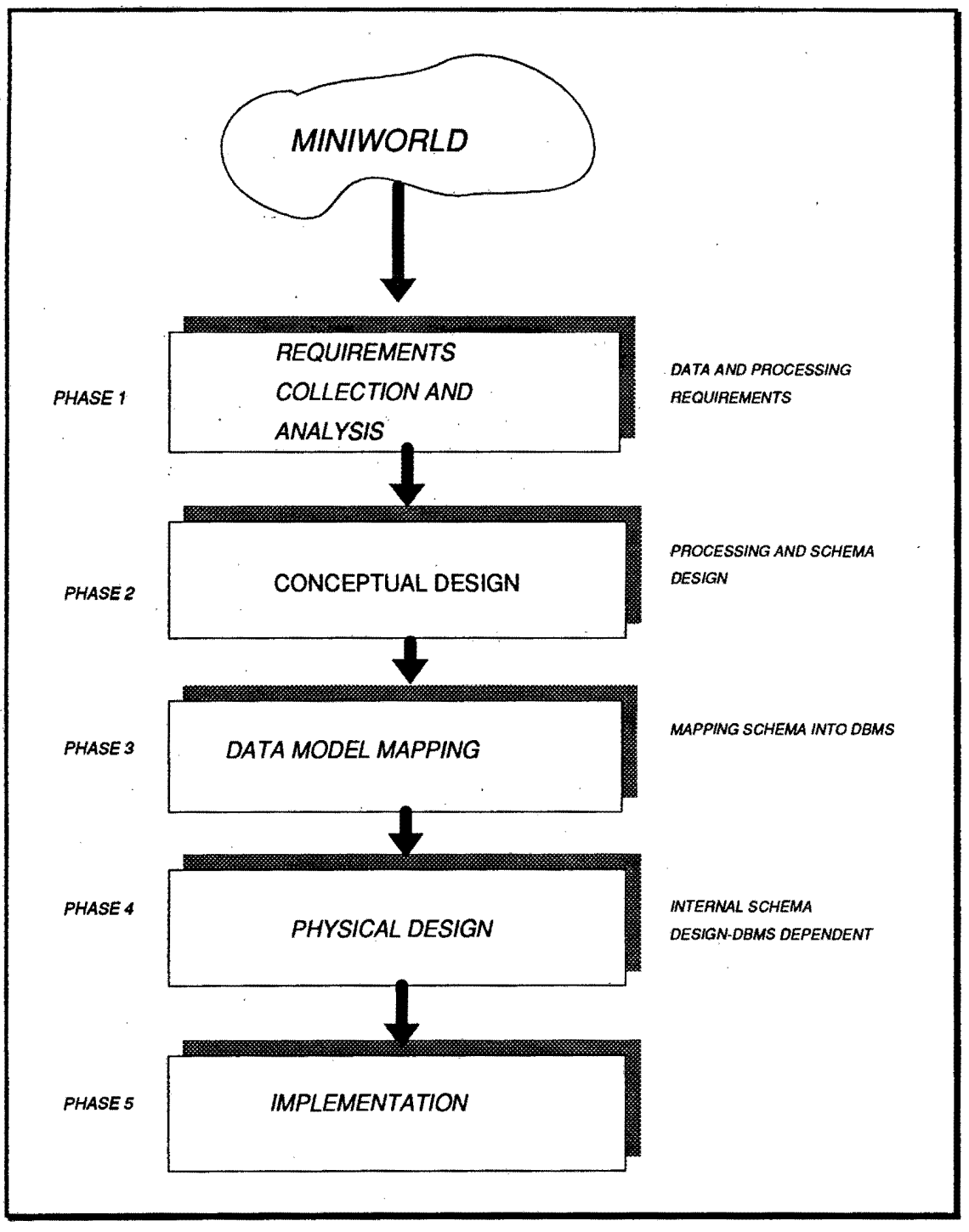

***FIG 3.1*: Diagram showing typical steps in database design**

(Modified After Fernandez et al 1993)

3.3.2 Concepts of the Entity-Relationship and Relational Models

3.3.2.1 The Entity-Relationship Model

The Entity-Relationship model uses the concepts of an entity, relationship and attribute to represent a real world. An entity is a thing or object in the real world with an independent existence such as a rock, person etc. (Date 1981). Each entity has characteristic properties that describes it and it's relationships to other entities such as the age, colour, mineral composition of a rock. Entities characterised by the same attributes can be grouped to form entity sets/types. An entity set has a unique identifying attribute called a ***key attribute.***

Relationships are linkages between objects or entity sets. They can be classified according to the numbers of entities from one entity set which can be associated with entities of another set. These relationship numbers define the cardinality ratio constraints of a database. A relationship between two entity types is called a ***binary*** relationship and that between more than two entities is an ***n***-nary relationship (Fernandez ,1993).

Relationships between two entity sets can be a ***one-to-one*** (1:1), relationship, (that is a relationship in which for each entity in either set there is at most one associated member of the other set), ***one-to-many*** **(1:M)** and ***many-to-many*** **(M:N).**

Participation constraints determine whether the existence of an entity depends upon its being related to another through a relationship. There are two types of participation constraints, ***total*** and ***partial*** (Marble 1983). Partial participation is where some of the entity instances of a particular entity type relate to entity instances of another type. Total participation is where all the entity instances of an entity set relate to the entity set instances of another.

3.3.2.2 Entity Relationship Diagram

Fig 3.2 below is a representation of the entity relationship diagram concepts used in modelling the Hwange geological data. The relationship shown in the diagram is the commonest among the geological features in the Hwange Area. On the diagram, entity sets are shown by rectangles. Ovals

or ellipses represent attributes, and relationships are represented by diamonds. A double line shows total participation and a key attribute is underlined.

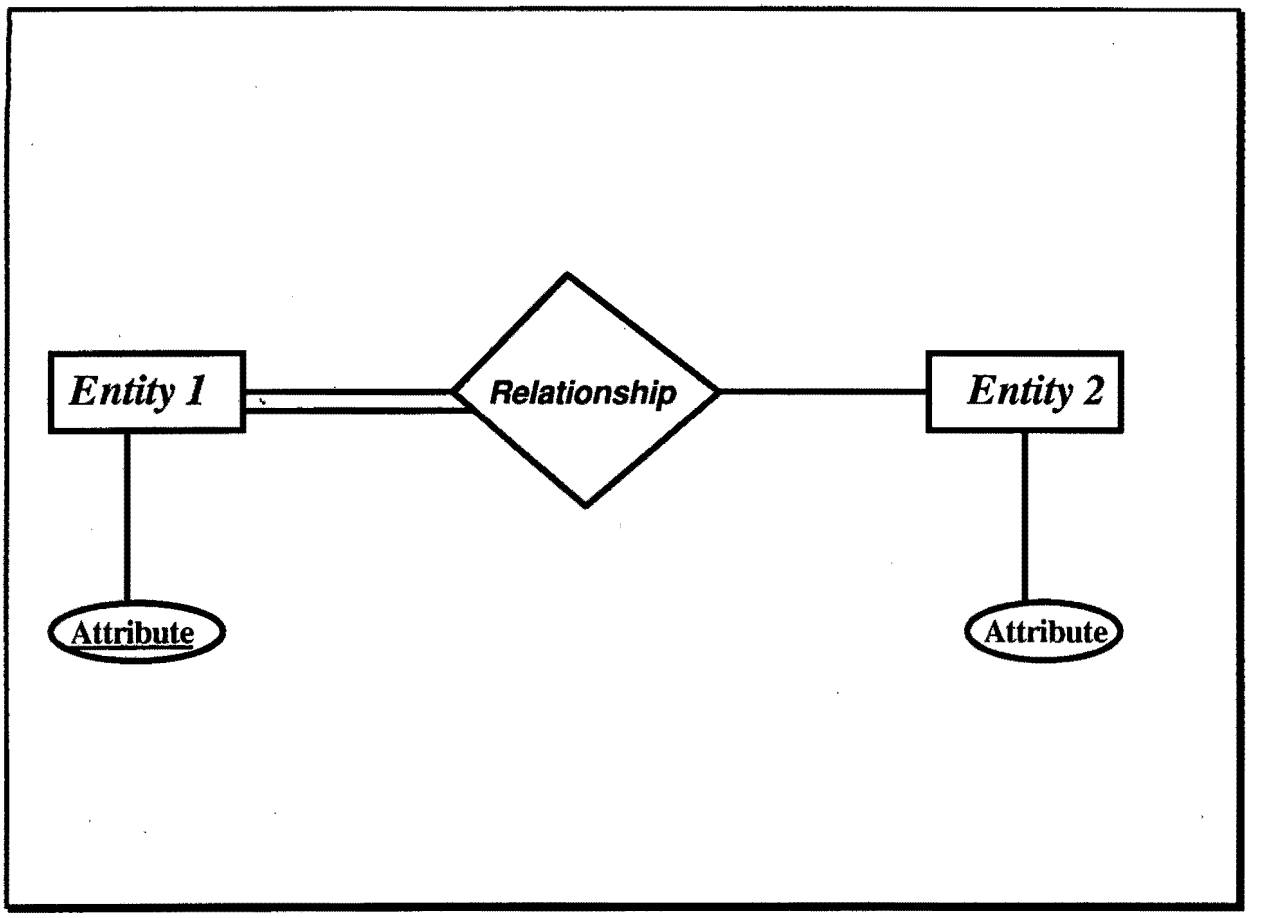

FIG 3.2 : **Diagram showing a 1: Many relationship between Entity 1 and Entity 2. Entity 1 totally participates in the relationship** *(Modified after Elmasri and Navathe 1989)*

3.3.2.3 The Relational Data Model

The Relational data model is a model that employs a two dimensional table of data (Bonham-Carter, 1994) as first proposed by Codd in 1970. In the model, each table is referred to as a ***relation.*** A row in the table is a ***tuple*** (or record) and a column is a ***field.*** Each record has a set of attributes and the range of possible values (domain) is defined for each attribute. A tuple is analogous to a data record in a flat file and contains a collection of data items that describe an

object or entity (Date 1981). A ***key attribute*** in a relation is an attribute that uniquely identifies tuples and provides a link between two or more relations. A key attribute of one relation appearing in another relation is called a ***foreign key***. These concepts are illustrated diagrammatically in Fig 3.3 below.

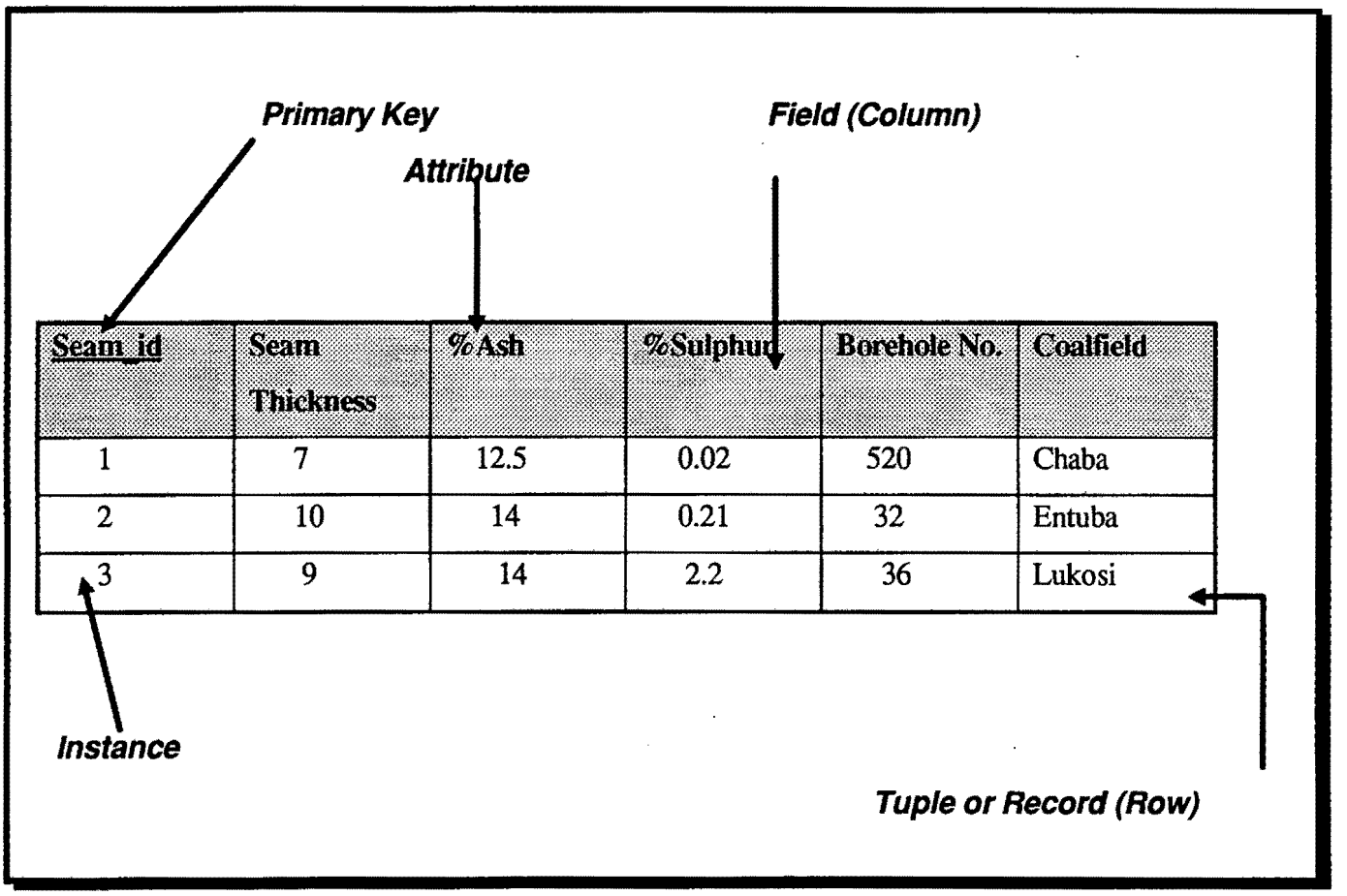

Seam_id	Seam Thickness	%Ash	%Sulphur	Borehole No.	Coalfield
1	7	12.5	0.02	520	Chaba
2	10	14	0.21	32	Entuba
3	9	14	2.2	36	Lukosi

FIG 3.3: **Diagram showing the Relational Data Model concepts.**

3.4 Conceptual Modelling of the Hwange Geological Data

3.4.1 Structure and organisation of the Hwange Geological Maps

The geological maps from which most of the data for the Hwange database were captured are organised into map units of rock Supergroups, Groups, Formations, and lithological units (Lockett

1979). Supergroups and Groups represent areas with rocks which are grouped together according to one of their key attributes. This can be the mode of formation, age or mineral content.

A Supergroup of rocks may consist of one or more Groups. These are defined in the Hwange area by a time break in the formation or deposition of similar rocks, such as the erosional surface (unconformity) separating the four Groups of the Karoo Supergroup (Dwyka, Ecca, Beaufort and Stormberg Groups) which are shown on the map as separate map units. Each Group is made up of Formations which are also divided into individual Series. On the map, each one of the Series is represented by the dominant surface lithology or exposed layer of the succession. Lithological units represent the fundamental units shown on many geological maps; they are rock units distinguished on the basis of their grains and mineral make-up. Most delineations shown on Hwange geological maps represent lithological units and these represent the geological entities modelled in this GIS study.

The extent of the Karoo rocks in the Hwange area defines the minimum extent of the sedimentary basin (Mid Zambezi) in which they were deposited. Areas covered by the metamorphic rocks are divided into metamorphic belts according to their metamorphic history.

To model the Hwange area geology, all the lithostratigraphic units (groups, lithologies, subgroups) and areas associated with individual rock types shown on the maps such as, coalfields, basins and metamorphic belts were converted to closed polygons during digitisation (See Fig 3.4). Attributes of interest to geological modelling such as rock names, rock types, mineral composition, economic minerals, coal-seams ages, tectonic structures, basin and belts they occur in, were used to characterise these polygons. Figure 3.4A and B below show a part of the Hwange geological map before and after digitisation respectively. Each geological entity became a polygon with a unique number and a set of attributes assigned to it.

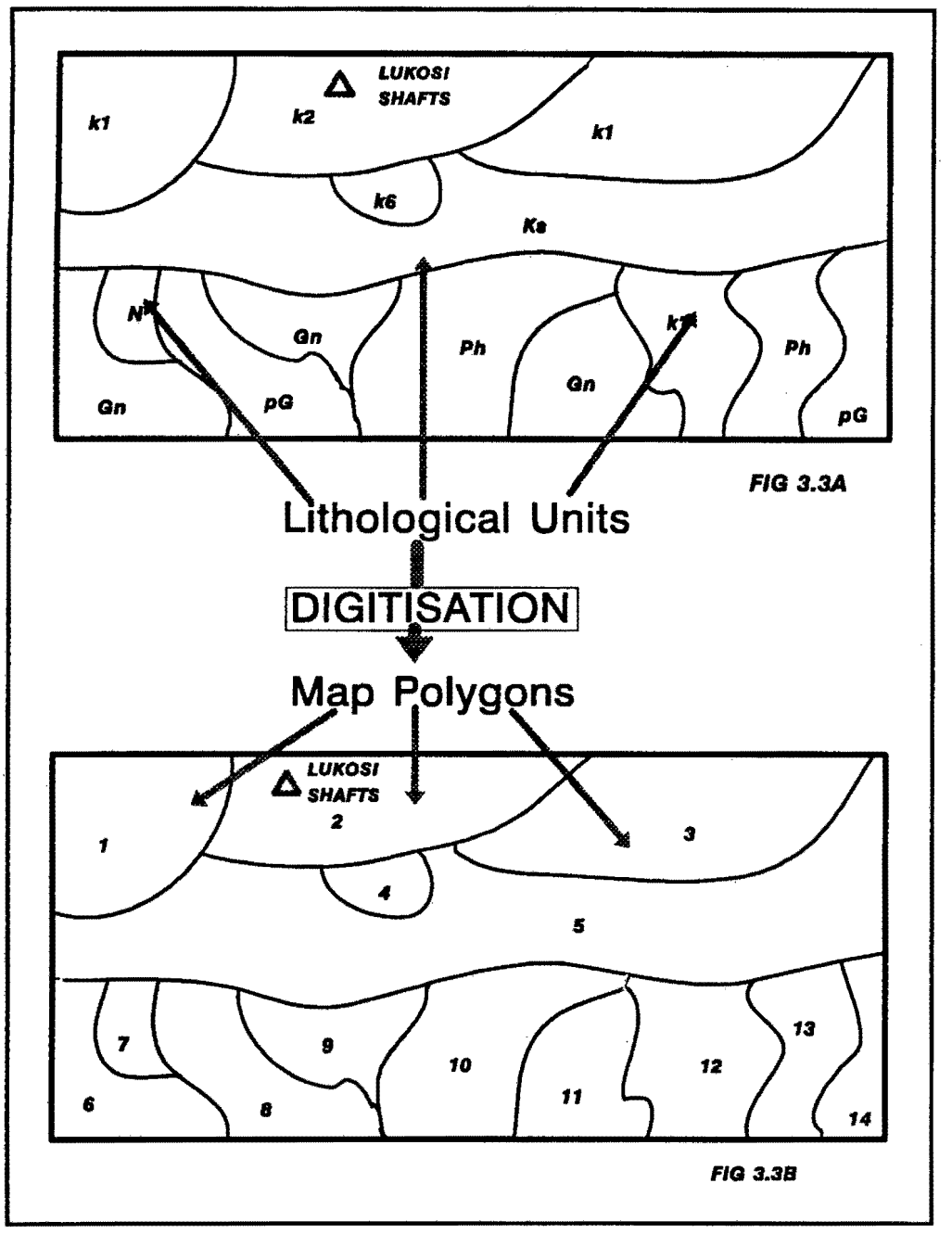

FIG 3.4: **Portions of the Hwange geological map. ABOVE (A): Before digitisation BELOW (B): After digitisation .** The symbols in FIG 3.3A represent lithologic unit codes. After digitisation these are replaced by polygon numbers (FIG 3.3B) that represent lithologic units.

3.4.2 *Entity Relationship Representation of the Hwange Geological Data*

The entity-relationship notation discussed in section 3.3.2.2 was used to capture all the semantics of the Hwange Geology database. Cardinality ratio constraints were used to indicate the type of relationship sets (***1:1, 1:M, M:N***). From the structure of the Hwange geological map described earlier and any other information collected in relation to structural and geological evaluation the following entities were identified:

Map_Polygon
Borehole
Coal seam
Lithology
Coalfield
Series
Formation
Group
Supergroup
Fault
Sedimentary_Basin
Metamorphic_Belt
Farm

Using these entity sets and their attributes, the Entity-Relationship diagram shown in Figure 3.5 was drawn. In the diagram, entity-types are represented by rectangles, relationships by diamond shapes; and attributes are represented by ovals, key attributes underlined. Double lines indicate total participation of an entity set in a relationship. The entity set ***Coal seam*** represents all coal seams occurring in each of the coalfields in the Hwange area. The participation of the entity set ***Coal seam*** in the relationship *occurs in* between ***Coal seam*** and ***Coalfield*** is total. The relationship is a *many-to-one* because one coalfield can have many seams. The entity ***Coalfield*** represents all the areas where continuous coal seams can be traced.

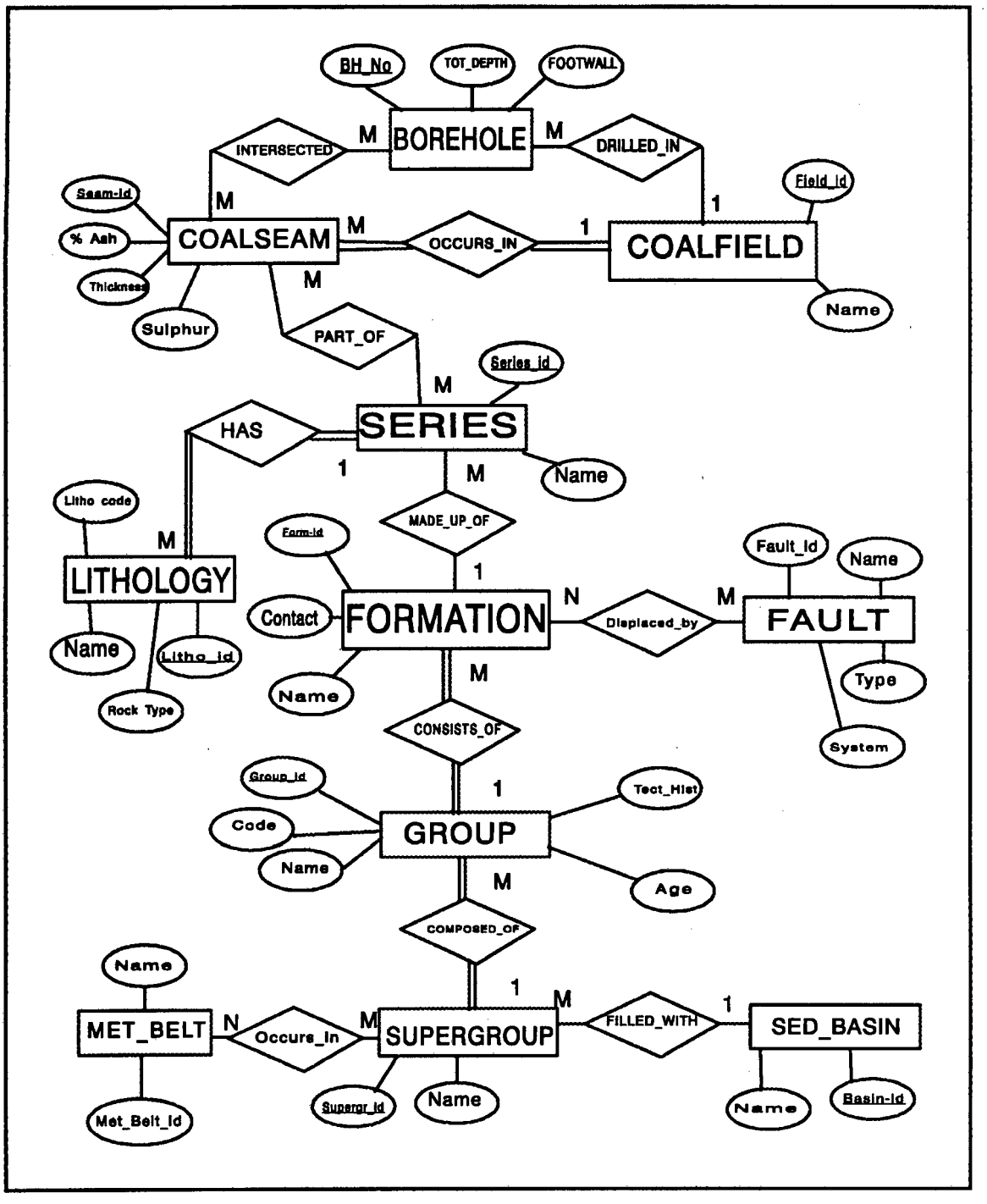

FIG 3.5: **Entity-Relationship representation of the Hwange geological and borehole data.**

M; N = many to many relationship, 1;M = one to many relationship, id = unique identifier.

The entity sets ***Coal seam*** and ***Series*** are related through the relationship type *part of.* A Series is a collection of sedimentary rock layers which may contain one or more coal seam or may not have any coal seams. The participation of coal seam in this *many-to-one* relationship is partial. The relationship *has* between ***Series*** and ***Lithology,*** was created to show that a series is composed of layers of different lithologies. The relationship is also a *many-to-one* because each series is composed of many lithological units. The participation of lithology in this relationship is total as no series can exist without lithological units.

The other *many-to one* relationships in the diagram are those between ***Formation*** and ***Group,*** ***Group*** and ***Supergroup***. These relationships indicate specialisation/generalisation. The *many-to-one* relationship between ***Formation*** and ***Group*** indicate the formations used to describe a specific Group in the database. Between ***Group*** and ***Supergroup*** the relationship shows the Groups that constitute a Supergroup.

The entity set ***Supergroup*** in the Hwange area represents all the different groups of rocks occurring in the sedimentary basins and metamorphic belts. The two entity sets, ***Sedimentary basin*** and ***Metamorphic belt*** are related to ***Supergroup*** via a *many-to-one* relationship and a *many-to-many* relationship, respectively. The ***Metamorphic belt*** entity-set refers to the different metamorphic epochs which took place in the area. There are two metamorphic provinces in the Hwange area, Zambezi Mobile Belt and the Magondi belt. Both contain rocks which have been affected by two metamorphic events. Thus the relationship between ***Metamorphic belt*** and ***Supergroup*** is a *many-to-many* relationship.

The other *many-to-many* relationships are the *displaced by* relationship between entity set ***Formation*** and ***Fault*** and *intersected* between ***Coal seam*** and ***Borehole***. Faults cut through different formations, (for example, the Entuba fault cut different formations). In some places the same faults displace one formation thus a single formation can also be cut by different faults. This gives a *many-to-many* relationship between ***Fault*** and ***Formation.*** Boreholes can intersect one or more coal seams. In the Hwange area, there are two seams, the Wankie main seam and the Madumabisa seam, boreholes can intersect one or all of them as well as

the seam can be intersected by more than one borehole. This gives the *many-to-many* relationship between ***Coal seam*** and ***Borehole.***

The entity sets mapped in the entity relationship diagram above give the geological entities of the Hwange Area which can be used for structural and geological evaluation. Depending upon the additional functionalities required, some of the entity sets can further be broken down or generalised to suit the processing requirements.

3.5. Transforming the Conceptual Schema (ER-Model) into the Relational Data Model.

The Relational data model was chosen for the implementation of the Hwange Geology database because the software ***(ARC/INFO, ARCVIEW)*** used in the investigation of the structure of the Hwange area uses the relational data model. The model also provides a conceptual arena for producing tabular subsets of geological entities which are easy to understand. This makes linkages between two or more tabular structures based on key attributes in specialised and generalised geological relationships more effective.

3.5.1 Transforming the Hwange geology conceptual schema into the Relational Data Model.

The Entity-Relationship (ER) conceptual schema shown in Figure 3.5 was mapped into the Relational data model. For each entity set in the ER diagram a relation/table was created with all the attributes of the entity set as fields or columns. The key attribute of each entity-set became the primary key in each relation and this was underlined and used to relate to other tables. The tables in Appendix 1 show relations created and corresponding to the following entity sets:

1. ***Coalseam***
2. ***Coalfield***
3. ***Series***
4. ***Lithology***
5. ***Formation***
6. ***Fault***
7. ***Subgroup***
8. ***Group***
9. ***Metamorphic Belt***
10. ***Sedimentary Basin.***
11. ***Borehole***
12. ***Farm***
13. ***Map Polygon***

Depending upon the participation constraints, the relationships between the entity sets were represented in different ways in the Relational data model. A binary, many-to-one relationship was implemented by including the primary key of the one (1) entity-type into each tuple of the many (M) entity-type. Using this principle, the primary key ***field_id*** of ***Coalfield*** relation was included in the relation ***Coal seam*** to implement the relationship "*occurs in*" between coal seam and coalfield. ***field_id*** appears as a *foreign key* in the relation coal seam to implement the relationship. Similarly the primary keys of the entity sets, ***Series, Formation, Subgroup, Group and Sedimentary Basin*** appear in the ***many*** entity relations of the *many-to-one* relationships they participate in.

The two *many-to-many* relationships in the diagram (Fig 3.5) between ***Formation*** and ***Fault*** and between ***Group*** and ***Met_Belt*** were implemented by creating a new table containing the primary keys of the two related entity sets. The relations *"displaced_by"* and *"occurs_in"* in Figure 3.6 represent the relationship sets, *"displaced_by"* and *"occurs_in"* in the entity relationship diagram (Fig 3.5). In the ***Fault-Formation*** relation, the new table created contains the primary keys of both ***Fault*** and ***Formation.*** In the ***Supergroup-Metamorphic_Belt*** relationship, the new table contains ***Supergroup_id*** and ***Met_Belt_id*** which are primary keys of the two entity sets.

Figure 3.6 below shows part of the transformation of the Hwange geology database conceptual schema into Relational model as well as the implementation of the relationships. The underlined attributes are the primary keys and the arrows show relational mapping using primary and foreign keys as explained in the previous sections. The direction of the arrow shows the transfer of a primary key of one entity to another as a foreign key to implement a relationship.

3.6 Database implementation and data retrieval from the Hwange Database

The design stages outlined in the previous sections allow efficient processing and retrieval of data from the database. Retrieval of data from the Hwange Database is by means of Structured Query Language (SQL), a relational query language. Generally a relational query is made up of three parts:

i. *a list of attributes to be displayed*
ii. list of source relations from which data are retrieved.
iii. search conditions.

The output is either a relation (table) in which each tuple is a collection of values of retrieved attributes or a portion of the map described by the chosen attributes.

To test the database design, a portion of the database was implemented using ***ARC/INFO*** and ***ARCVIEW*** software. Subsets of geological and land use data from the Hwange area were selected. Sample queries shown in later sections were formulated. The results of these queries were overlaid on Landsat TM data which allowed delineation of outlines based on spectral signatures and conditions of retrieval.

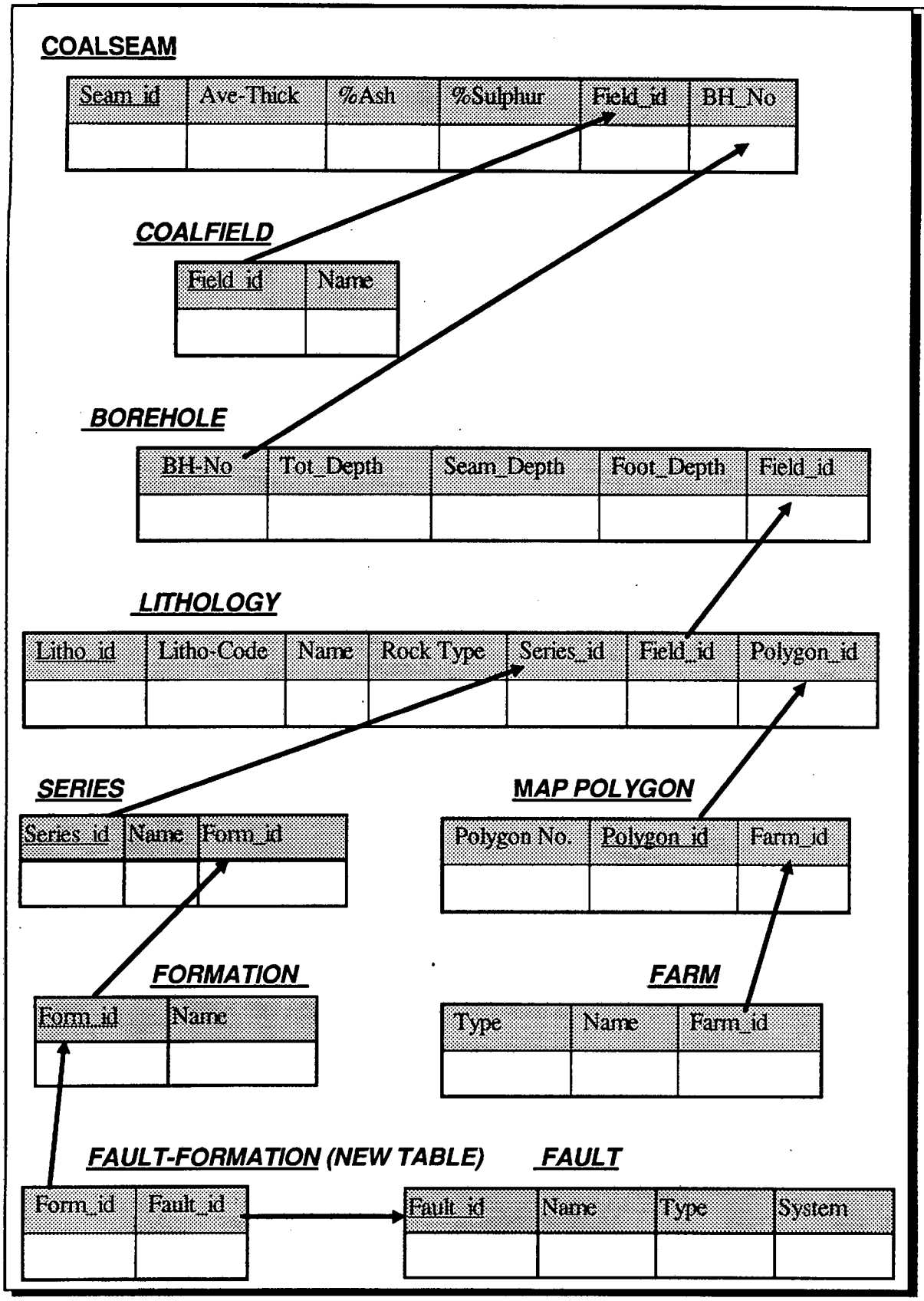

FIG 3.6: Transforming of the Hwange conceptual schema into Relational Model.

3.6.1 Querying The Hwange Database using Structured Query Language (SQL)

The structured query language (SQL) can be used to query the Hwange geology database. Information which can be retrieved from the Hwange database include structural, geological, topographic and coal seam properties. (A detailed account of data processing, manipulation and retrieval is given in Appendix 5).

Structured query language uses the statements ***SELECT, FROM*** and ***WHERE*** structured in the following way:

SELECT *(attributes)*
FROM *(relation where data is retrieved from)*
WHERE *(Condition)*
These statements can be used in conjunction with Boolean operators like **AND, OR, NOT,** and ***Relational operators*** such as, **=,<, >,** and ***Combinatory expressions*** **(UNION, INTERSECT** etc.).

To test the use of these statements in retrieving data from the Hwange Database, two sample queries used to locate areas affected by spontaneous combustion and faulted and areas with shallow coal seams occurring in a nature reserve are outlined below.

Query No1

Spontaneous combustion is associated with exposed and/or very shallow coal seams (Overburden thickness less than 10m), good quality coal. To find such areas say in the Entuba coalfield the query was structured in the following way using ***ARC/INFO:*** where ***reselect*** is used in place of the two expressions, ***FROM*** and ***WHERE.***

SELECT *"Coalfield"*
RESELECT **(WHERE)** *"Field_name 'cn' Entuba"*

AND SELECT "Lithology"

RESELECT (WHERE) *"Lithology 'cn' Burnt coal"*

INTERSECT

SELECT "Formation"

RESELECT "Contact 'cn' Faulted"

The results of this query are polygons and tables which describe the areas in the Entuba coalfield that have been affected by spontaneous combustion which are also faulted. The same result can be obtained by joining the different tables/relations and then formulating the queries.

Query No 2

The southern part of the study area falls in the Hwange National Park or Deka Safari Area. Being protected areas, the coalfields in the parks are of interest because any exploration activities would disturb the natural environment of the area. Thus the second query is concerned with delineating these areas.

To answer the question ***" Which areas (coalfields) with shallow good quality coal reserves (ash less than 15%, thickness greater than 5m and depth less than 100m) occur in a National Park or Safari Area?".***

Four tables containing information on coal quality (ash content, thickness etc), names of coalfields, depth to coal seam, names and the types of parks are joined.

The following expressions were used in ***ARCVIEW 2.1*** to retrieve the records which answer the above query:

([Seam_thickness] > 5) and ([Ash ,15%])

([Overburden] < 100) and ([Farm_type] = "national") or ([Farm_type] = "Safari Area")

These expressions resulted in a table showing areas with shallow good quality coal seams and occurring in the Hwange National Park and Deka Safari Area. Table 3.1 below shows a summary of the results of these two expressions.

TABLE 3.1: **Table showing areas with good quality coal occurring in a national park and safari area.**

Field_id	Coalfield Name	Seam Thickness (m)	%Ash	Overburden (in metres)	Farm_id	Farm_Type
1	W.Areas	6	14	50	1	National
1	W.Areas	6	14	50	3	Safari
2	Wankie	7	12	55	3	Safari
3	Chaba	8	13	74	3	Safari
5	Entuba	7.5	14	80	3	Safari

3.7 Discussion

The Hwange database was mainly designed for the purposes of integrating geological, structural and topographical data with Landsat TM data for analysis of lithological distribution and geological structures in the Hwange Area. Modifications of this design can be made depending upon additional functionalities required during data processing.

The Entity-Relationship model used as a conceptual model of the database allows flexibility and implementation of the same design using different models. The Relational model also allows the addition of derived entities which are usually added during the processing stage. This provides flexibility in the Hwange database. Extending the concept of entities to object class hierarchies would also allow implementation of this design in an Object-Oriented database package. Testing of the database design using data from the project area allows early assessment of the integrity of the database and a means of checking if the design satisfies all the requirements.

Chapter 4

The Structure of the Hwange Database

4.1. Introduction

The intended uses of a database determine its design and structure. The structure of a database refers to the data sets incorporated and their interrelationships. Structured design and organisation of data sets is crucial to the success of a GIS project because it governs the analysis and queries that can be raised with the database. Chapter 3 described the methodology used to design the geological part of the Hwange database and how lithology and geological structures data can be integrated and manipulated to find relationships between lithological distribution, coal seams and geological structures (faults, folds and shear zones). This chapter describes the organisation of data sets that comprise the Hwange database, data sources, accuracy, reliability and capturing methods used in constructing the Hwange database. Some of the attributes of the spatial data described in this chapter are given in Appendix 4.

4.2 The Hwange Database Structure

One of the main objectives of the project was to develop a database that can be integrated with remotely sensed (Landsat TM) data in order to analyse geological structures and lithological distributions in the Hwange area. Towards this end, subsets of lithological, structural, topographic, cadastral, land use and Landsat TM data covering the Hwange Area were selected and organised into layers (files). The following layers constitute the Hwange database constructed during this study:

LITHOLOGY (HWANGE)

FAULTS

RIVERS

SETTLEMENT

MINES

RELIEF

ROADS

BOUND (*BOUNDARY*)

POWER (*ELECTRICITY LINES*)

LANDSAT

BOREHOLE

Each of these layers is made up of two data sets, spatial and attribute data. The attribute data are managed in a relational data model as shown in Fig 4.1 and Appendix 4.

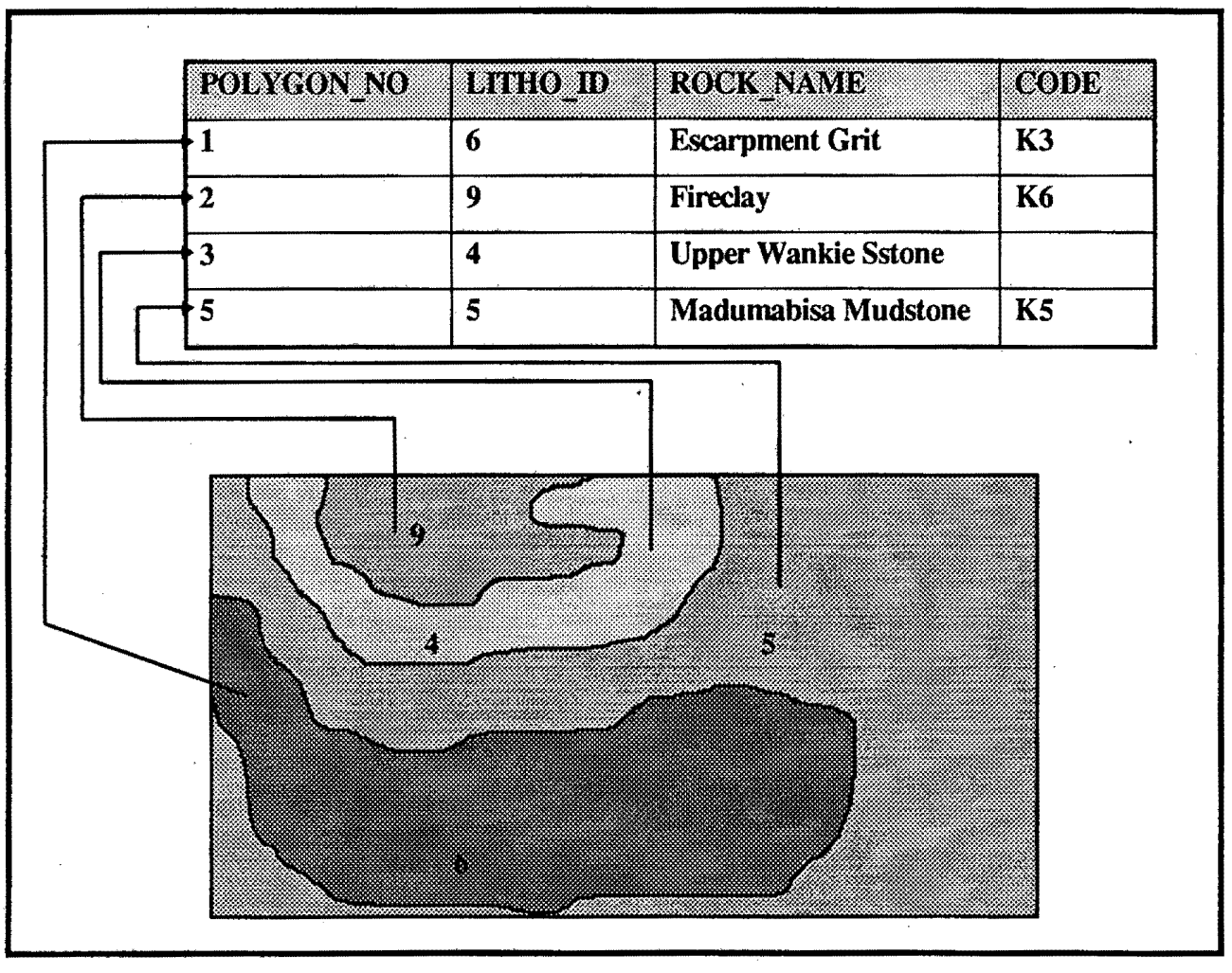

***FIG 4.1*: Diagram showing the attachment of attributes in a Relational database to spatial data.**

Combinations of these layers and integration of geophysics (magnetic) data can be done at any level of data processing. Table 4.1 shows grouping of these layers into four major storage layers namely, Geology, Topography, Cadastre and Image layers.

TABLE 4.1 : **Table showing the data sets comprising the Hwange Database**

LAYER	COVERAGES (FILE NAMES)	DESCRIPTION	FEATURE TYPE	AREA COVERAGE
GEOLOGY	LITHOLOGY	Lithological units boundaries	Polygon	Study Area
	FAULTS	Faults, Shear zones and Joints	Line	Study Area
	LINEAMENTS	Lineament map	Line	Study Area
	BOREHOLE	Coal exploration boreholes	Point	Coalfields
TOPOGRAPHY	RELIEF	Contour lines	Line	Coalfields
	SPOT HEIGHT	Spot heights and trig. beacons	Point	Coalfields
	RIVERS	Rivers and Streams	Point	Study Area
CADASTRAL	ROADS	Roads and Railways	Point	Study Area
	SETTLEMENT	Towns, Villages	Polygon	Study Area
	MINES	Mines,Claims, Shafts	Point	Study Area
	BOUNDARY	Administrative & Farm Boundaries	Line	Study Area
	POWER	Electricity lines	Line	Study Area
IMAGE	HWANGE1 - HWANGE 7	TM Bands1-7 ARC/INFO Grids	Grid Cell	Study Area

4.3 Geology Layer

The geological data set consists of a lithological and structural map (See Appendix 4).

4.3.1 Lithology

The lithology map was compiled using three 1:100 000 geological maps compiled by Watson (1960), Lockett (1979), Palloks (1984) and Landsat TM subscene covering Hwange area. Areas remapped and updated using Landsat TM data include part of the Dete Inlier, Western Areas coalfield and the northern half of the study area.

4.3.2 Geological Structures

The structural map (Figure 4.2) was compiled from interpretations of the study area using the Landsat TM subscene and correlated with phases of faulting and folding identified by Watson (1960), Stagman et al (1978) and Lockett (1979). The maps are composites of documented joints, faults, fold-axes and shear zones, and undocumented fractures mapped as lineaments on the Landsat TM image.

4.3.3 Boreholes (BHS)

Boreholes drilled for coal exploration were digitised from the maps compiled by Lockett (1979), Shell Developments (1981) and Palloks (1984, 1987). Borehole information shows the distribution of coal seams and their respective depths from the surface (See Appendix 4). This information is essential for targeting areas for further investigation.

4.3.4 Spatial Data

Lithological units were digitised in vector format from 1:100 000 geological maps by Watson (1960) and Lockett (1979) and from the Landsat TM subscene at 1:250 000 scale. The lithological units are represented by closed polygons which have topological relationships established during the data capturing process. Each polygon has a unique identifier used to attach attributes related to lithological units.

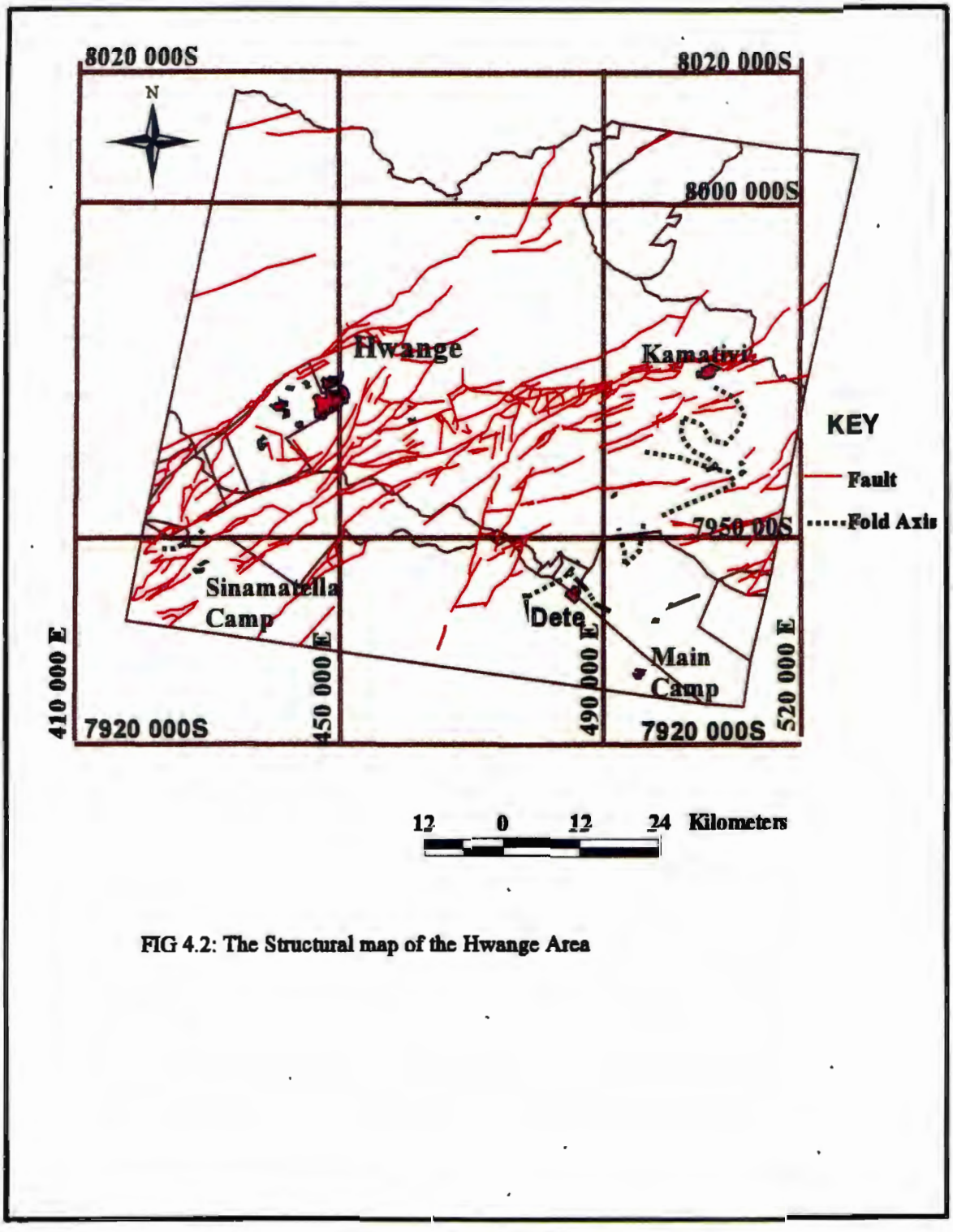

FIG 4.2: The Structural map of the Hwange Area

Geological structures (faults, joints, fold-axes) are stored in the database as lines. Each of the line segments belonging to one fault or joint set has a unique code which links it to descriptive data in attribute tables. Borehole positions are represented in the database as points with borehole numbers as unique identifiers.

4.3.5 Attribute Data

Digitised polygons (lithological units), linear features (geological structures) and borehole positions are linked to attribute data via unique identifiers. The concepts of key attribute and primary key have been discussed in Chapter 3. These together with other descriptive information are stored in relational tables. Descriptive data for lithological units and geological structures include names of lithostratigraphic units, formations, fault phases, coal seam thickness and quality. The entity relationship diagram (Fig 3.5) in the previous chapter and Tables 3.2-3.14 in Appendix 1 and Tables Ap 4.1- Ap 4.5 in Appendix 4 show some the attribute data of geological features. Borehole information include borehole numbers, depth, quality and thickness of seam intersected. The nomenclature used to describe the geological data is one used by Lockett (1979), Stagman (1978) and Lightfoot (1929).

4.4 Topographic Layer

4.4.1 Spatial Data

Topographic and drainage data contained in the Hwange data base were digitised from 1: 250 000 and 1:100 000 topographic maps acquired from the Surveyor General's office in Harare. The digitised contour map covers the area around the town of Hwange which encompasses the Entuba, Western Areas, Sinamatella, Wankie and Inyantue Coalfields. Spot heights and trigonometric beacons from the same area are also stored as points in the topographic layer of the database. These data sets together with fault and drainage data were used to create digital elevation models which were used for structural analysis. Large rivers, such as Lukosi, Deka, Inyantue and Gwayi rivers and dams are stored as polygons.

4.4.2 Attribute Data

Attribute data of the topographic layer of the Hwange database includes contour identity codes, which correspond to altitude, spot heights and beacon positions (x and y co-ordinates) and altitude. For each river and dam, numerical codes and names constitute the attribute data contained in relational tables.

4.5 Cadastral Layer

4.5.1 Spatial Data

The cadastral layer includes 1:100 000 maps showing road networks, railway lines, administrative boundaries, power lines, towns, villages, mines, and boundaries of the Deka Safari Area, Hwange National Park and Sikumi Forest Land.

4.5.2 Attribute Data

Attribute data contained in relational tables include road types and widths, power line voltages, mine names and minerals mined. Descriptive data for towns and other settlements include their names and functions as listed in Appendix 4.

4.6 Image Layer

4.6.1 Spatial Data

Cell-based spatial data sets consist of Landsat TM data. The Landsat TM5 scanner image is from the Zimbabwean winter season (20 June 1984), path 172 row 73. The subscene for the study area is 80 km by 120km. Image data are in two formats, ***ARC/INFO GRIDs*** and raster files made from band colour composites. The Landsat TM subscene consists of seven images taken by the Thematic Mapper scanner using seven spectral bands. The grids were stretched, georeferenced and classified.

RGB (Red,Green,Blue) and HSV (Hue,Saturation,Value) band composites of TM1,3,5 and TM1,4,7 are stored as single raster files.

The Landsat TM data were processed using edge enhancement, band ratioing, colour compositing and decorelation stretching techniques. Band images were used as composites with topographic, drainage and structural data to enhance three dimensional interpretation and visualisation of the study area. The images were classified and each region was given a unique identifier based on the range of pixel values in that class.

The TM scanner simultaneously collects data in seven narrow spectral bands with each pixel measuring 30 metres x 30 metres on the ground for the six non-thermal bands and 120m x 120m for the thermal band (TM band6). Table 4.2 below shows the characteristics of the seven bands recorded by the Thematic Mapper Scanner and responses of each TM band to various surface materials as described by Avery et al (1992) and Sabins (1978).

TABLE 4.2: **Characteristics of Landsat Thematic Mapper spectral bands.**

BAND	WAVELENGTH (MICROMETERS)	SPECTRAL LOCATION	RESPONSE TO SURFACE MATERIALS
1	0.45 - 0.56 (Blue-Green)	Visible	Penetrates water, Discrimination of rocks and soil from vegetation - reflected more by rocks and soil
2	0.52 -0.60 (Green)	Visible	Discriminate vegetation and cultural features
3	0.63 - 0.76 (Red)	Visible	Strong absorption by vegetation strongly reflected by soils- discriminates between soil and vegetation.
4	0.76 - 0.9 (Mid-Infrared)	Infrared	Strong absorption by water bodies and strong reflection from vegetation. Used mainly for vegetation mapping.
5	1.55 - 1.75 (Mid-Infrared)	Infrared	Sensitive to presence or absence of ferric iron/hematite, reflection increases with iron content increase.
6	10.5 -2.35	Thermal Infrared	Sensitive to thermal pollution, soil moisture, rock types .
7	2.08 - 2.35	Mid Infrared	Coincides with absorption band caused by hydrous minerals (clay, micas, oxides, sulphates.

4.6.2 Attribute Data

Processed and classified GRIDs have attributes stored in value attribute tables. The attributes were attached to a group of pixel values which represent land cover types. Fig 4.3 below shows the representation of attribute data attached to cell-based spatial data (Landsat TM data). Colour composites do not have attributes attached to them because they are not topologically represented in the database.

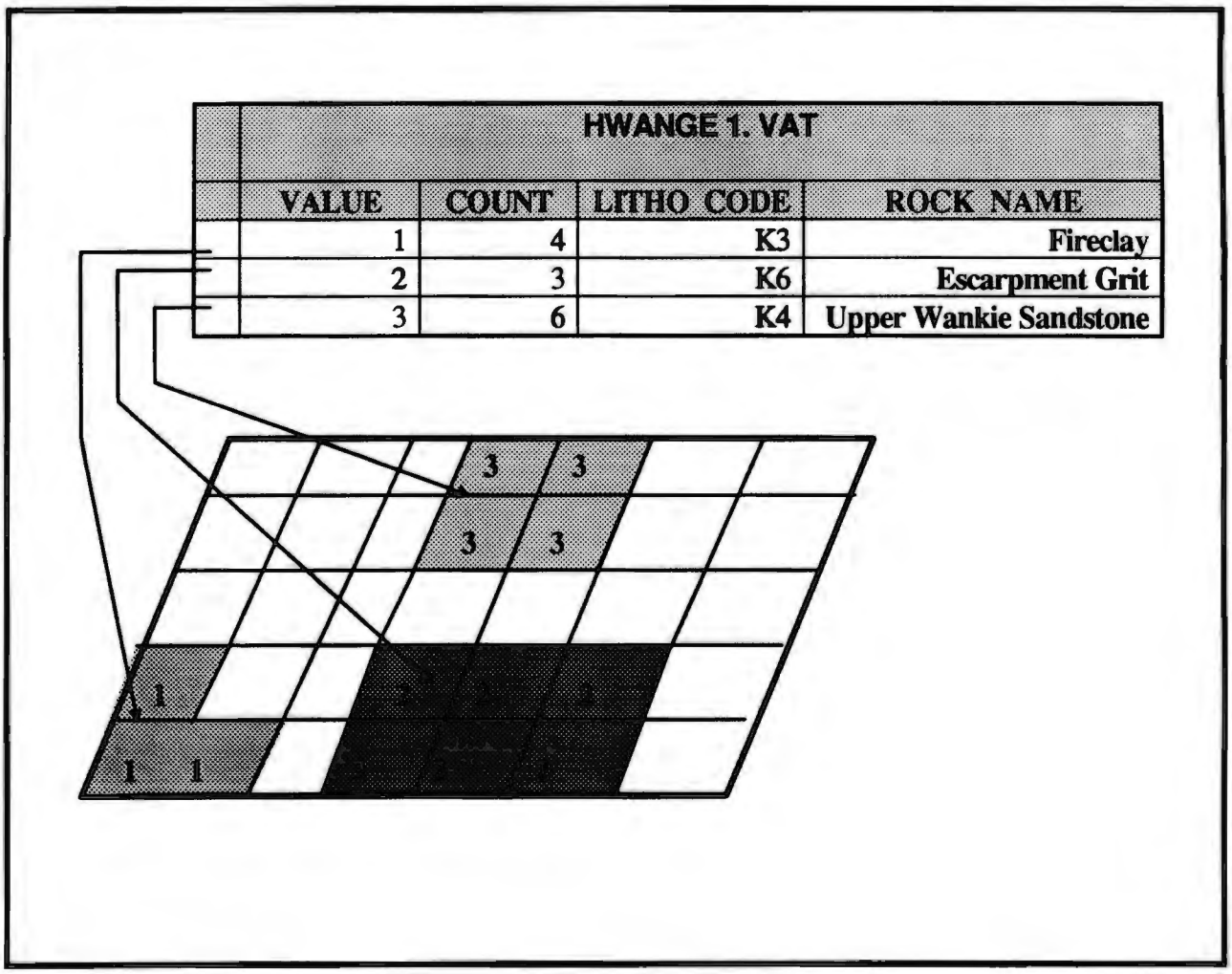

FIG 4.3: **Diagram showing attachment of attribute data to cell-based spatial data.**

4.7 Lineage

4.7.1 Data Sources

The largest proportion of map data used in the study came from the 1:100 000 geological map series accompanying Geological Survey Bulletins 48, 57 and 85 compiled by Watson (1960,1962) Lockett (1979) and Palloks (1984, 1987). Hard copy geological and topographic maps were

obtained from the Geological Survey Department in Zimbabwe. The maps were manually digitised and edited interactively using *ARC/INFO* software.

Topographic contours, spot heights and trigonometric beacons were converted from feet on hardcopy maps to metres upon digitisation. The hardcopy maps were compiled using the Universal Transverse Mercator grid and the same grid was adopted for all the data sets comprising the Hwange database.

The source of all raster data sets in the Hwange data base is the Landsat 5 TM subscene, path 172 row 73, quad 1 acquired on the 20 June 1984. Digital 1:100 000 topographic maps were used to register the image to real world co-ordinates. This allowed integration of image data with geological, topographic and cadastral data. Mapping of areas not covered by the digitised maps was done by screen digitising and vectorization of enhanced and classified Landsat TM images.
The Landsat TM data was acquired from *EOSAT* through Environment and Remote Sensing Institute (*ERSI*-Zimbabwe) on a computer compatible exabyte tape.

4.7.2 Probable Sources Of error in Hwange Database

The introduction of error in database creation is inevitable. Any representation of the earth is bound to contain error because the earth is round and the representations are planes. Also the actual nature of errors during data conversion are not precisely known. However, all the data sets used in this research were converted within the accepted root mean square (RMS) error ranges in the software used for conversions. Error in the database was introduced at different stages and these can be grouped in the following categories:

(i) **Geological map compilation**

Lithological boundaries on the ground are not as simple as represented on maps. Maps represent generalised boundaries, thus introducing error.

(ii) **Data conversion**

Topographic data was captured in feet. Conversion to metres resulted in errors as conversion factors are not absolute.

(iii) **Image registration**

Part of the database was constructed using georeferenced and processed Landsat TM band images. Ground control points used to register the images were taken from the southern and central portions of the study area where map data was available. Also, because of the limited number of control points (maximum of 60) that can be used in the software *(ARC/INFO)* and the scale of the maps used to register the images, accurate registration is only restricted to areas with more control points. This resulted in error propagating through any boundaries digitised from images.

(iv) **Digitising**

Manual digitising and paper stability also result in errors accumulating in the database. Paper maps shrink and stretch in response to change in humidity and storage conditions and folding.

(v) **Map Projections**

Co-ordinate transformation from one surface to another result in distortion. Maps and image co-ordinates were transformed from geographic co-ordinates to Universal Transverse Mercator grid, thus resulting in distortion.

(vi) **Data Processing**

Processing errors resulted from overlaying of vector data over raster data and interpretation of lithological data from Landsat TM images. Map data and image data were also at different scales, so overlaying the 1:250 000 image over 1:100 000 maps resulted in distortion of images to match the corresponding points on the map.

4.8 Discussion

The Hwange database consist of subsets of geological, topographic and land use data selected to develop a methodology for analysis of geological structures and lithological distribution in the Hwange area. These data sets as discussed earlier were obtained from two sources: hardcopy maps and digital satellite images. Combinations, manipulation and interpretation of the relationships between bedrock geology, geological structures and topography is possible. Integration of image data allows reconnaissance mapping of features not depicted on hardcopy maps and interpretation of the area at a regional scale.

The data sets can be converted to any format that supports ***ARC/INFO*** exchange files. The database structure is flexible and can be utilised together with other spatial databases without any database structure modifications. The attribute data are managed in a relational database but can also be implemented using object-oriented database concepts.

Chapter 5

Digital Image Processing and Interpretation

5.1 Introduction

The previous chapters described the information contained in the Hwange database and how the information can be used for geological and structural analysis of the Hwange area. This chapter is concerned with the digital image processing principles and techniques used to extract spatial data from the Landsat TM data of the Hwange area. It is also concerned with the determination of Landsat TM data products and combinations of products that best enable discrimination and mapping of lithological units and geological structures in the Hwange area.

The Landsat TM subscene was processed and analysed using various image processing techniques which include image restoration, image enhancement, edge detection and lineament analysis. These processes were performed to facilitate extraction of lithologic, structural and geomorphic information from the TM subscene and subsequent integration of the extracted spatial data with map data using ***ARC/INFO*** software.

In this study image restoration involved random noise correction and image registration. Image enhancement involved the use of techniques such as principal components analysis, decorelation stretching, edge enhancement and detection, single band contrast enhancement, RGB (red,green,blue) band colour compositing, band ratio and band difference colour compositing, hue saturation and value compositing and generation of vegetation index images (Finch 1990). Image interpretation was based on the available maps, field work and the results of image enhancement techniques performed using ***IDRISI, DISPLAY*** and ***ARC/INFO's GRID*** module.

5.2 Image Restoration

This is the correction of pixel locational errors and georeferencing of an image to real world co-ordinates. Georeferencing in this study was achieved by making use of ground control points. These are points that were identifiable on both the image and the digital geological maps such as road junctions, river confluences and electricity lines.

The correction of the Landsat TM scene was based on the Universal Transverse Mercator grid, to which all the map data used in this study were projected to. The cubic convolution algorithm (Avery et al 1992) was used to resample the pixel values during image registration to 30m by 30m resolution.

5.3 Image Enhancement

Image enhancement uses techniques/processes that improve the detectability of features or objects in a digital image for visual interpretation due to different colour contrasts (McCloy 1995). The Landsat TM image covering the Hwange area was enhanced to facilitate the detection of exposed coal measures, burning coal seams and rocks associated with shallow coal seams such as fireclay, carbonaceous shales, upper Wankie sandstone and also for identification of geological structures. The image was also enhanced for detection of iron oxide staining, silicification and detection of hydroxyl minerals which constitute some of the rocks in the Hwange area.

5.3.1 Principal Components Analysis (PCA)

Principal components analysis is the process by which highly correlated multichannel band image data can be compressed by calculating a new co-ordinate system. This condenses the scene variance in the original data into a new set of decorrelated image data (Mather 1989, Drury 1990)

Principal components analysis of the Landsat TM data for the Hwange area was applied on the five non-thermal TM bands (1,2,3,4,7). The correlation matrix of the Landsat TM reflected TM bands (1,2,3,4,7), shown in Table 5.1 shows that there is a strong correlation between the bands. TM

bands 2 and 4 have least correlation with other bands thus TM band 4 was chosen for geobotanical analysis. Details of other matrices and eigen vectors are given in Appendix 2.

Table 5.1 Correlation Matrix

	Band 1	**Band 2**	**Band 3**	**Band 4**	**Band 7**
Band 1	1.000000	0.959593	0.991242	0.991242	0.875529
Band 2	0.959593	1.000000	0.931862	0.991242	0.719356
Band 3	0.991242	0.931862	1.000000	0.991242	0.823324
Band 4	0.991242	0.991242	0.991242	1.000000	0.875529
Band 7	0.875529	0.719356	0.823324	0.875529	1.000000

A set of three band principal components colour composites was created. This resulted in images with a higher spectral discrimination capability among the Lower Karoo sediments, Upper Karoo sediments and the surrounding basaltic and metamorphic rocks.

The principal components results indicated that the composites containing the first three components was able to discriminate most of the rocks (see component loading summary in Appendix 2). The most informative PCA composite was the one with PC1= red, PC2 = green and PC3 = blue. In this composite the Karoo basalts in the western portion of the study area are displayed in grey and red shades, the ripple-marked flags and Escarpment grits in bright red colours. Burnt coal areas and mine dumps display a characteristic deep blue colour and the same colour is also displayed by the exposed carbonaceous shales. The composite also discriminates upper Wankie sandstone and lower Wankie sandstones in shades of pale blue. The Madumabisa mudstone shows a bright green colour and the surrounding granites and gneiss are discriminated in different shades of purple, brown and maroon. Fireclay is also distinctive on this image in light green colour. The Proterozoic schists belts are poorly discriminated on the PCA colour composite.

5.3.2 Decorelation stretching

This is another technique which uses the same principle as principal components analysis. The technique also emphasises spectral information in correlated Landsat TM band images. Decorelation stretching enables exaggeration of colour differences of both raw images and colour composites. In this study, decorelation stretching was applied to the most informative reflected TM bands, 1, 4, 5 and 7 which were also used to produce false colour composite images.

5.3.2.1 Decorelation Stretch band colour composite (DSCC)

Figure 5.1 below is a Red-Green-Blue (RGB) equal area decorrelation stretching colour composite image of part of the Hwange area produced using TM bands 4,5 and 7. The green hues displayed in the western corner show the extent of the Karoo basalt. Fireclay around the Wankie Collieries and in the south-western parts of the study area is easily identifiable in bright yellow tones. The upper Wankie sandstone is clearly discriminated in maroon shades whereas carbonaceous shales and exposed coal seams are displayed in dark blue tones. Mine dumps are also distinctive on this band composite as they are the only areas displayed in different shades of black and dark grey. The sporadic bright green colour occurring throughout the image shows the distribution of active vegetation and the deep brown shades show areas with burnt coal.

The gneiss along the Entuba fault zone, granites and graphitic schists to the east of the study area are displayed in shades ranging from pink to purple. The graphitic schists are discernible from the sheared gneiss by their strong SW-NE trending fabric and the granites by their purple granular texture. This colour composite together with the contrast stretched colour composite and band difference colour composites were used to construct the lithological map (Fig 2.5) and structural map (Fig 4.2) of the Hwange area.

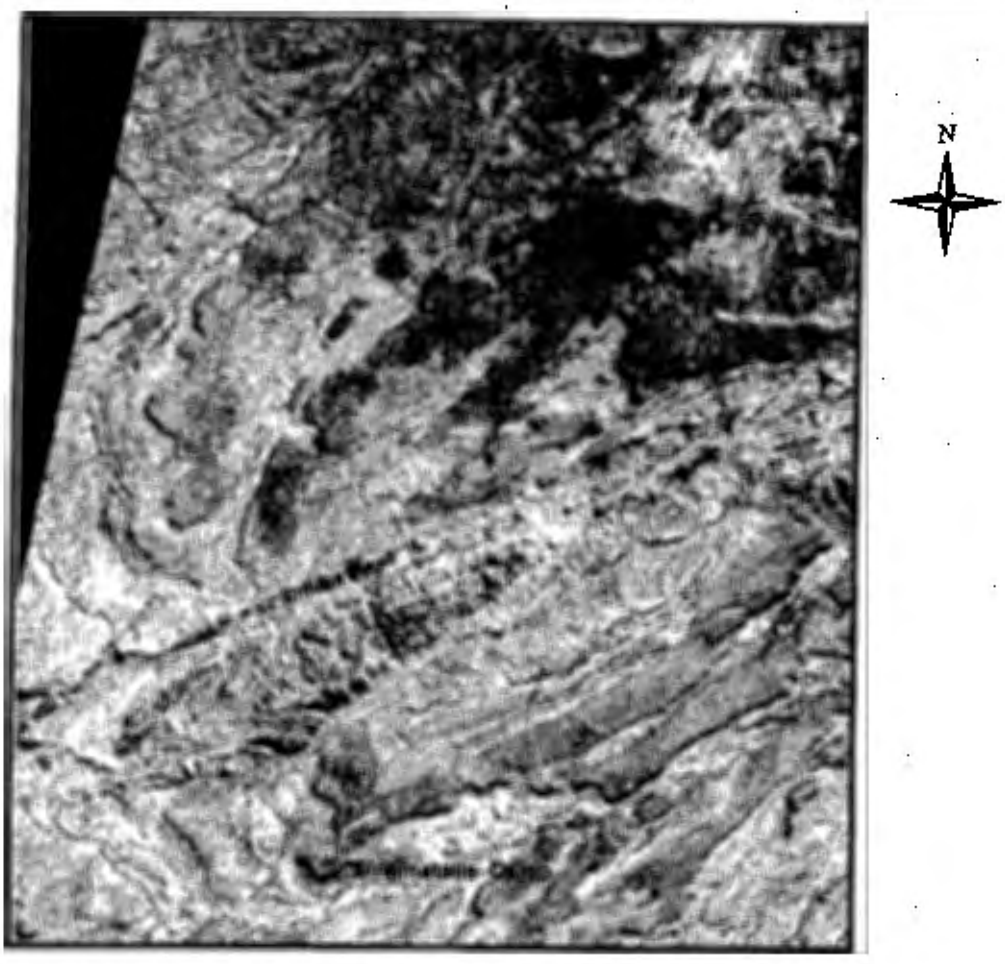

FIG 5.1: TM bands 4,5,7 Decorrelation stretch colour composite of the western part of the Hwange Area

5.3.3 Contrast Stretched Band Colour Composites (RGB)

These were produced by assigning one of the primary colours (red, green,blue) to each spectral band and then combining the bands to produce a false colour image. Contrast stretched three band colour composites proved to be the most useful products for lithological mapping in the Hwange area.

Choosing the best band combinations was done empirically by visually assessing all the 20 possible three band combinations. Visual examination based on spectral parameters and luminosity contrast of the different colour composites was used to determine the most informative band sets. Similar to other researchers such as Moore (1990) and Davis (1989), the colour allocation and band choice for presentation was found to have a big influence on the value of the colour composite images for

lithological interpretation. Visual assessment of the colour composites showed that, for the Hwange area's, sedimentary, basaltic and metamorphic terrains, the most useful colour composite images are RGB equal area contrast stretched composites. In decreasing order, the best discriminative sets are composites of TM bands 4;5;7, 1;4;7, 2;5;7, 1;3;7, 2;4;5, 3;4;5, and 3;4;7.

5.3.3.1 TM Band 4,5,7 (RGB) False Colour Composite

Figures 5.2 and 5.3 show RGB TM 4,5,7 colour composites. The image displays Lower Karoo sediments and basement rocks effectively. Fireclay is displayed in yellow, upper Wankie sandstone in orange and Madumabisa mudstone in dark blue. The Dwyka sediments and the lower Wankie sandstone are very distinctive in pink. The iron oxide rich Escarpment grits are displayed on the image in deep greens, but there is poor discrimination of the Kalahari sands and alluvial sediments which are both shown as pale green.

The Batoka basalt in the western portion show characteristic grey colours which enhance their contact with brightly coloured lower Karoo sediments. Burnt coal areas are also clearly distinguishable in shades of dark brown to deep red and these tend to be noticeable even in areas with dense vegetation cover.

This band composite also shows most of the rocks of the Dete-Kamativi inlier. The three schists belts (Tshontanda, Inyantue and Kamativi) cannot be distinguished based on colour alone but on the differences in structural fabric which is stronger in the Tshontanda and Kamativi Belts than Inyantue Belt.

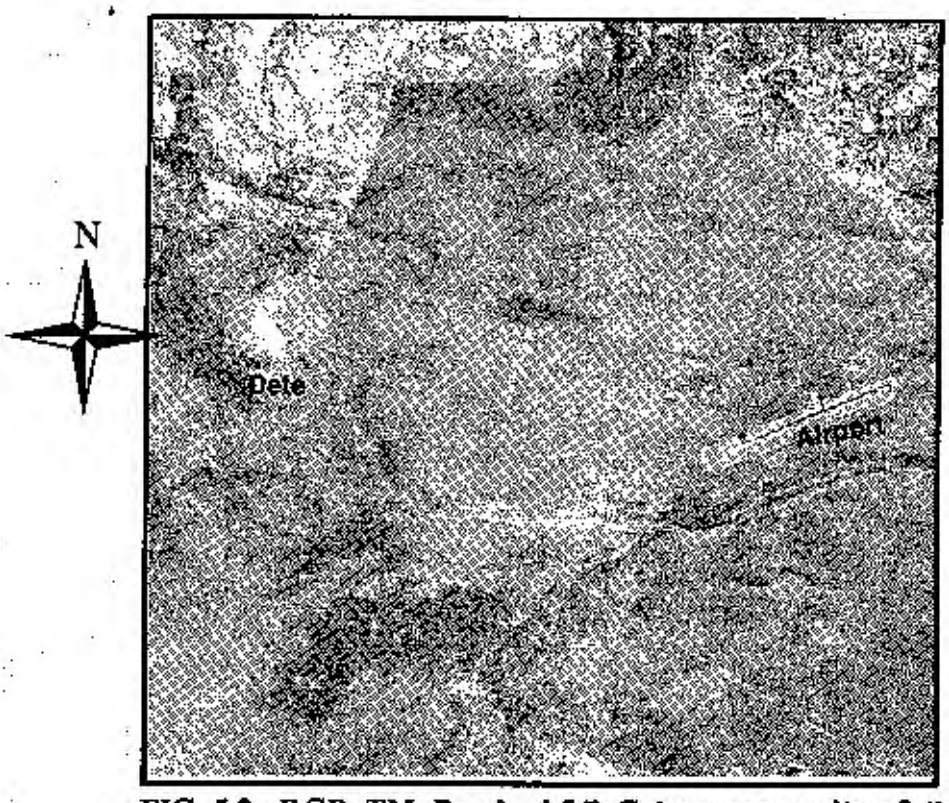

FIG 5.2: RGB TM Bands 4,5,7 Colour composite of the eastern part of the Hwange Area

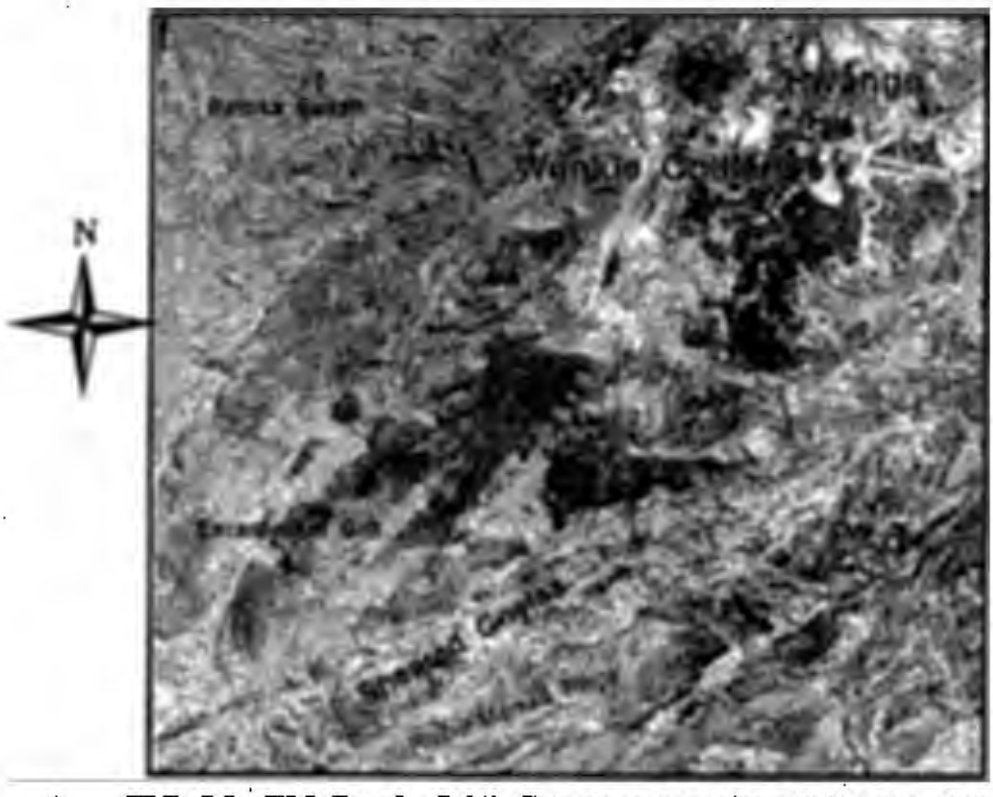

FIG 5.3: TM Bands 5,4,7 Colour composite of the western part of the Hwange Area

The amphibolites covering the eastern part of the study area are shown in dark blues which discriminate them from folded quartzite shown in pale browns. The Proterozoic granites are displayed in maroon shades and show a characteristic granular texture depicting the numerous castle kopjes dominating the granitic terrain. The sheared gneiss can be distinguished from granites by their lighter shades of brown and pink and a strong NE-SW trending fabric. The metapelites of the Malaputese group in the eastern part are poorly discernible from the pink paragneisses although in some parts they display very sharp contacts.

5.3.3.2 TM 7,4,1 RGB False Colour Composite

This composite is the most suitable general image for lithological, soil and vegetation mapping. In this image all the clay-rich rocks can easily be distinguished in different shades of blue. Fireclay is the most distinctive of all in pale blue, exposed coal measures, carbonaceous mudstone and mine dumps in deep blues. The Madumabisa mudstone shown as a purple colour whereas the basalt is displayed in blue-green hues. The Sijarira sediments are distinctive on this image and are displayed in yellow which distinguish them from the orange colour showing the lower Wankie sandstone and the Dwyka sediments and red colour showing the Escarpment grits.

The colour composite also discriminates between different schists belts of the Inyantue, Tshontanda and Kamativi formations. The metamorphic and structural fabric prevalent in the schists belt is highly enhanced in this band composite. The garnet schists, which dominate the Inyantue Formation, are displayed in light orange and the graphitic schists in all the three belts are in dark greys. The veined schists of the Kamativi and Tshontanda Formations are displayed in bright orange and contact aureoles between these rocks and the intrusive granites are also identifiable.

Similar to the TM 4,5,7 band composite, the mafic amphibolites, quartzite and the pink gneiss of the Malaputese group can also be identified, although the different gneisses cannot be discriminated from one another.

5.3.3.3 TM 2,4,7 RGB False Colour Composite

This composite was also very effective in mapping rock units particularly for mudstone, fireclay, burnt coal areas and carbonaceous shales. Besides discriminating all the other rocks identified on the previous two composites, the composite clearly shows burnt coal areas and carbonaceous shales in shades of maroon and black.

5.3.3.4 TM 2,5,7 RGB False Colour Composite

Dolerite dykes and other linear features such as shear zones and graphitic schist bands are clearly identifiable on this image in red and black shades respectively. Of all the band composites, this is the only combination that uniquely identify the dolerite dykes. The Karoo basalt, Escarpment grits, fireclay and Madumabisa mudstone are also discernible, but not in any better way than done by the previously described images.

5.3.3.5 TM 1,3,7 RGB False Colour Composite

This band colour composite is the most appropriate for mapping burnt coal areas, mine dumps and strongly sheared gneiss. The image displays burnt coal areas in deep reds and clearly discriminate these areas even where they are covered with dense vegetation. The image also enhances geological structures such as faults and shear zones, thus was useful for mapping strongly sheared gneiss such as the one along the Entuba fault zone.

5.3.3.6 TM 2,4,5 RGB False Colour Composite

This image is similar to the above composites but this composite distinguishes granites, gneiss and alluvium from the Kalahari sands. The granites are displayed in shades of deep red and the strong east-west fabric and purples define the gneiss from the granites. Alluvium along river valleys is shown in bright reds as opposed to the blue of the Kalahari sands.

5.3.3 7 TM 3,4,7 False Colour Composite

This composite, besides being good for mapping vegetation and clay minerals, was used to map silicified rocks along the Entuba fault zone. This is the only band composite on which quartz veins were detected in shades of yellow.

5.3.4 Band Difference Images

Differential reflectance of soil, rocks and vegetation can be used to highlight certain rock types, mineral types and vegetation (Moore 1990). Band difference images were produced by subtraction of one band digital number values from another and displayed as both monochrome and colour composite images. Band difference images were used in this study to show rocks with hydrated minerals (fireclay, mudstone, weathered basalt) iron oxides (grits and amphibolites) and distribution of active vegetation. Four band difference images were generated by subtracting the following band pairs from each other, TM5 - TM7, TM4 - TM3, TM4 - TM2, TM7 - TM4.

5.3.4.1 TM Band 5 - TM Band 7

TM band 5 corresponds to the wavelength range of maximum rock and mineral reflectance and TM band 7 coincides with the strong absorption features for clays and micas (Avery et al 1992). The band difference image of these two bands in the Hwange area, therefore, highlights clays which are the major components of fireclay, mudstone and the weathering products of the basalt and amphibolites. This band difference image displayed as a monochrome image enabled discrimination of several lithologies. The most distinctive lithologies are carbonaceous shales, Dwyka sediments, burnt coal areas, graphitic schists and fireclay.

5.3.4.2 TM Band 3 - TM Band 1

The image is the red minus blue. It enhanced the structural features but shows very poor distinction between individual lithologies.

5.3.4.3 TM Band 4 - TM Band 3

This image enhances edges and areas with active vegetation. Most of the prominent structural features such as faults and shear zones which support dense vegetation can easily be mapped using this band difference image. Fig 5.4 shows the TM4 - TM3 image; Pale tones show areas with active vegetation, that is main rivers, fractured areas and other areas with subsurface water.

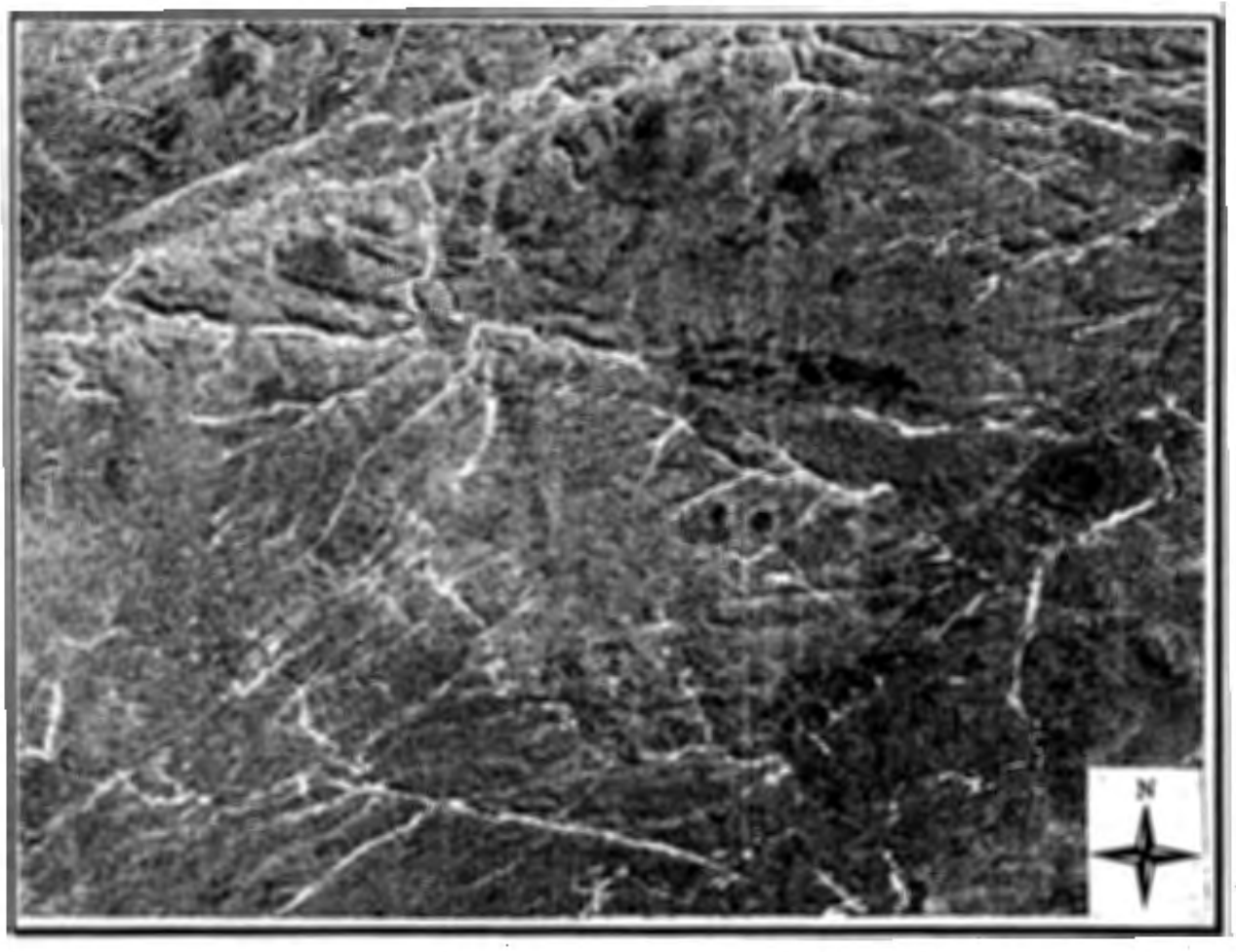

***FIG 5.4*: TM4 - TM3 image. Light tones show areas with active vegetation.**

5.3.4.4 TM band 7 - TM band 4

The image distinguishes clays and oxidised rocks such as the amphibolites, graphitic schists, basalt and grits. It also shows some of the rocks in areas where they are covered with vegetation as subtraction of TM band 4 removes the effect of vegetation cover.

5.3.5 False Colour Band Difference Composites

Colour composite images made by combinations of the three band difference images were used to emphasise the colour differences between lithologies. False colour composites of three sets of band difference images, TM5 - TM7, TM4 - TM2, TM4 - TM3, TM4 - TM3, TM4 - TM2, TM7 - TM4 and TM - TM7; TM4 - TM3; TM7 - TM4 proved very effective in mapping lithological units.

5.3.5.1 TM 5-7, 4-3, 4-2, RGB Colour Composite

The image is effective in mapping the lower Karoo sediments. Fireclay and Madumabisa mudstone are displayed in shades of red, basalt in green and upper Wankie sandstone in red. The band composite is also effective in discriminating vegetation activity associated with geological structures and major rivers. These are displayed in shades of green.

5.3.5.2 TM5-TM7; TM4-TM3; TM7-TM4 RGB False Colour Composite

This image discriminates most of the lithologies discernible on previous images. It is very effective in distinguishing the ripple marked flags and upper Wankie sandstone which are not apparent on any other band combinations.

5.3.5.3 TM4-TM3; TM4-TM2; TM7-TM4 RGB False Colour Composite

The colour composite was selected as the best image for mapping the Precambrian rocks. All the Precambrian rocks, both mafic and silicate rocks are distinctive and different gneiss are easily identifiable in shades of pink, maroon and red. The clay rich rocks such as amphibolites, mudstone and weathered basalt are displayed in shades of blue and green. This image together with the BCC TM1,4,7 and TM 4,5,7 and the decorelation stretching image were used to construct the geological and structural maps shown in Figs 2.5 and 4.2.

5.3.6 Band Ratio Images

The interband ratioing of multispectral images enhances spectral-reflectance or colour differences between surface materials that are often difficult to detect on standard band composite images. Interband ratioing is effective in normalising spectral data by removing brightness contrasts and emphasising colour content of the data (Mather, 1989, Avery 1992). By so doing the shadow effects are minimised because a new data set is created.

Band ratioing was accomplished in this study by taking band ratios of the most informative band pairs of the six nonthermal bands. The most informative band ratios were found to be TM 5/4, TM 7/5, TM 3/1, and TM 3/2. The resultant images showed very little contrast so they were displayed as colour composites.

The TM 3/1 (red/blue) and TM 3/2 (red/green) ratios are important for delineating ferric iron rich rocks (light tones) such as iron oxide cemented grits and ferric iron poor rocks (dark tones) such as mudstone and silicate rocks.

The TM 5/7 ratio was useful for delineating clay rich rocks (pale tones on grey images) such as mudstone, fireclay and basalt and the TM 4/3 ratio uniquely defines the distribution of vegetation. However because of the poor tonal differences, the images were not as effective as band difference images. Poor tonal differences in colour composites was removed by incorporating one of the original images in the composites, a technique also used by Goertz (1989).

5.3.6.1 TM 5/4; TM 7/5; TM 3/1 False Colour Composite

This interband ratio colour composite was very effective in distinguishing between the Karoo sediments. The composite discriminates among the lower and upper Wankie sandstones which are difficult to distinguish on other colour images. Fireclay, burnt coal and Madumabisa mudstone can also be identified easily on the image.

5.3.6.2 TM 3/1;TM 3/2; TM 1 False Colour Composite

The content of this image is more or less the same as the one above, but the inclusion of one original image improved the contrast and hence improving the display colours of ferric iron rich rocks such as grit, amphibolite and basaltic rocks .

5.3.7 Hue Saturation Value (HSV) Colour Composites

Hue colour composition is another image enhancement method which has been found particularly suitable for rock and soil image display. The system involves representation of the colour of any pixel by three criteria: *hue* (indicating the dominant wavelength of colour given in a numeric system where 0 represents red, with the number increasing to 255 along the visible spectrum), *saturation* (representing the purity of colour): and *value/intensity* (representing the brightness value)(Berger 1994). The HSV composites of the Landsat TM data covering the Hwange area were made by displaying one band as hue, a second as saturation band and a third as value band after contrast stretching of the band images.

The HSV colour composites were not as effective as the (RGB) false colour composites. The only HSV composite used was the one made using band difference images TM 5-7, TM 4-3,TM 7-4. The composite was very effective in delineating mine dumps around Wankie Collieries and delineating carbonaceous shale outcrops which are displayed in shades of brown and orange. Despite the success of this method in many sedimentary basins (Berger 1994) the method was found not to be very effective in mapping the Lower Karoo sediments and the surrounding basaltic and metamorphic rocks in the Hwange area because of very little colour differences shown by these rocks on HSV colour composites.

5.4 Fracture Detection

Fracture detection involved identification of linear features on edge enhanced images and Normalised Vegetation Index images. These were used to construct the structural map of the

Hwange area. Fig 5.5 is a flow diagram showing the steps followed in detecting different types of fractures and their subsequent use in construction of the structural model of the Hwange area.

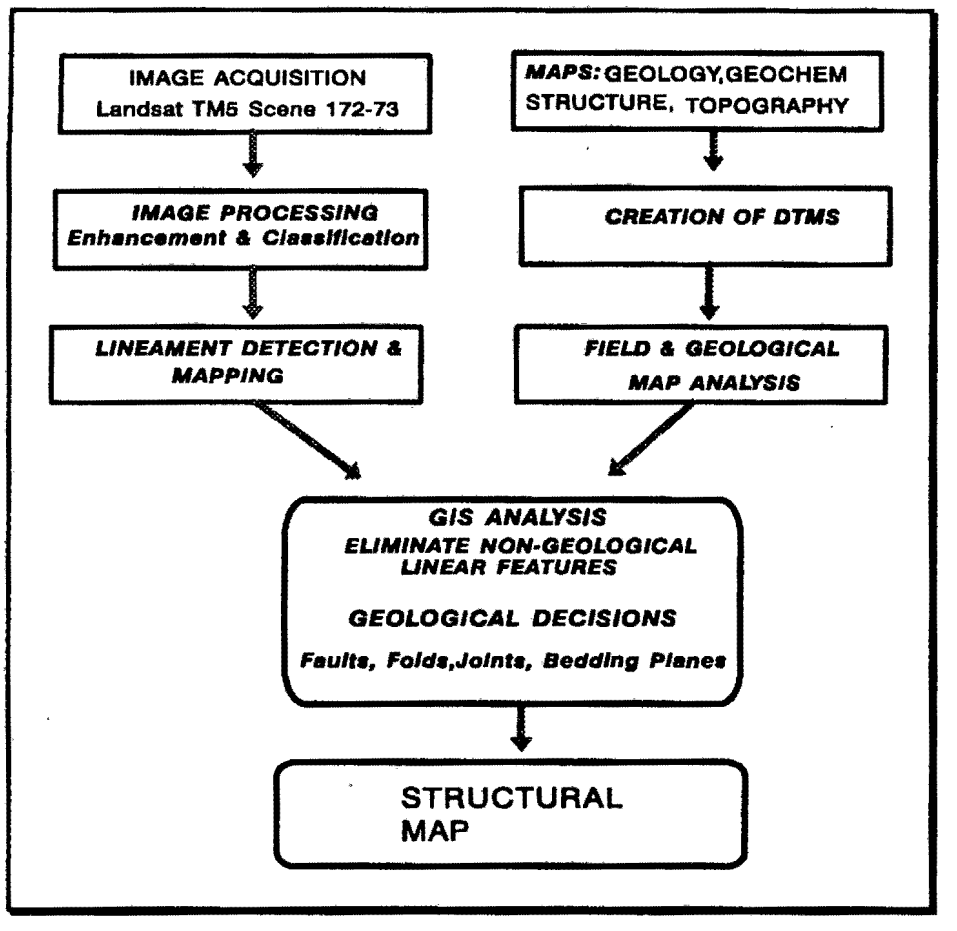

FIG 5.5: **Flow Diagram showing steps followed in fracture detection and mapping.**

5.4.1 Edge Enhancement

Edges are very abrupt changes in pixel values which represent high spatial frequencies (Avery et al 1992). The edge enhancement algorithms are designed to emphasise rapid changes in the digital number levels of an image from one pixel to another, thus allowing detection of geological features such as faults, joints, shear zones and lithological boundaries.

In this study edge enhancement was achieved by high-pass filtering of TM bands 4, 5 and 7 images using a convolution operation by a 3 x 3 pixel window to increase lineament contrast. A high pass

filter is a kernel or window passed through a digital image to enhance the high frequency data (Avery 1992). Laplacian filters were passed in different directions and the image multiplied by a factor of 2 to increase the contrast. The original images were also added with the filtered images and linearly stretched to produce edge enhanced images and colour composites.

5.4.2 Normalised Difference Vegetation Index (NDVI)

The reflection characteristics of vegetation during the dry season of a semi arid environment have been used to suggest areas where ground water may be more abundant or near the surface (Finch 1990). In the Hwange area, field studies have shown that most of the ground water reserves occur along faults and joints and vegetation growth tends to continue along these during the dry season. Using this idea, vegetation activity during the winter season can be used to locate fractures. Ratio combinations in the wavelength ranges of 0.7 to 1.1um (nearIR) to those in the 0.6 to 0.7um (red) range developed for vegetation monitoring (Avery et al 1992) were used in the semi-arid region of Hwange to detect lineaments, some of which are not apparent on filtered images. During the winter season (which is the season the image was acquired) deciduous vegetation along major rivers and fractures remain active. The Normalised Difference Vegetation Index (NDVI) was used to analyse these areas with active vegetation. The index is defined using TM bands 4 and 3 as given in the following formula:

$$\mathbf{NDVI} = \frac{\textbf{Near IR (4) - Red Band (3)}}{\textbf{Near IR (4) + Red Band (3)}}$$

Fig 5.6 shows the NDVI image of part of the Hwange area. Light tones with preferred orientation shows rivers and fractures (lineaments). The lineaments were visually inspected and input to a GIS for integration with other data sets. Most of the lineaments with active vegetation were found to have little relationships with river systems and settlement patterns but a strong relationship to the mapped faults.

FIG 5.6: NDVI Image of the western part of the Hwange Area

5.5 Lineament Mapping

The filtered images and normalised difference vegetation index *(NDVI)* images and colour composites of the Hwange area show different types of linear features. These features were formed due to a number of processes which include erosion along joints, faults, bedding planes and sub-surface geological processes. The lineaments were identified by visual inspection and digitised as straight lines and incorporated into the Hwange database.

Fig 5.7 below shows a remotely sensed lineament map of 749 lineaments constructed using the filtered images, colour composites, and the vegetation index image. Two attributes of lineaments were considered during the identification of linear features:

(i) Orientation/azimuth

(ii) Length of the lineament.

These two attributes were also measured on the mapped faults in the area, thus giving a quantitative and graphical method of comparing the relationships between lineaments and mapped faults. The significance of these interpreted lineaments and their relationships to mapped faults were analysed using histograms and also overlay techniques in a GIS. Details of these analyses are discussed in Chapter 6. Digital spatial analysis of the lineaments and integration with mapped faults was performed using ***ARC/INFO*** and ***ARCVIEW*** software.

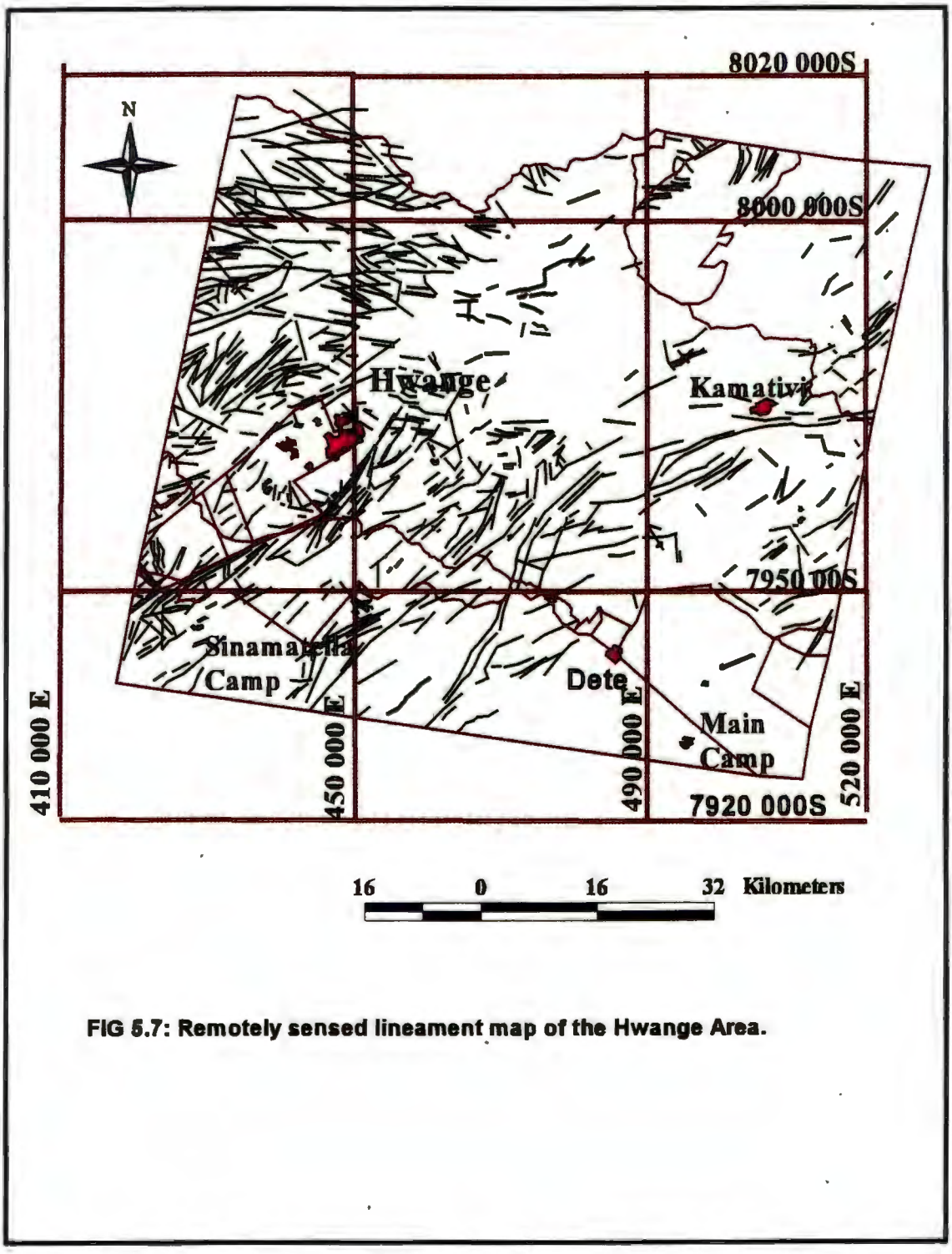

FIG 5.7: Remotely sensed lineament map of the Hwange Area.

The lineament map (Fig 5.7), shows a number of concentrations of lineaments with the NE-SW and ENE-WSW orientation.

The ***Mean Area Length parameter*** for these lineaments was also calculated using the formula adapted from Newton (1987) which involve both length and frequency of lineaments. The parameter is given by

$$\frac{Ls}{Fs}$$

where: **Ls** = Total length in mapped area (Hwange area)

Fs = Total number in mapped area

This parameter gives the density of fractures in the mapped area and so aids understanding of the distribution of fractures in different parts of the mapped area. The ***mean area length parameter*** also shows concentrations of lineaments in three main zones, in the Inyantue valley, along the Entuba zone and on the Karoo basalts in the north-west sector of the study area. This suggests the influence of the major fault zones passing through these areas and the joints on the Karoo basalts on the development of lineament patterns as discussed in later sections..

5.6 Discrimination of Karoo and basement rocks using Landsat TM data

This section briefly discusses the TM discrimination of rock units in the Hwange area and the summary of TM products that uniquely distinguish Karoo rocks and other rocks in the area. No single colour composite image provides discrimination for all rocks but generally, the best distinction is given by the decorelation stretch colour composite (DSCC), followed by the ordinary RGB band colour Composite (BCC) of TM bands 1,4,7 and 4,5,7 and the Band Difference Composites (BDC). A few rocks are clearly discernible on the Band Ratio Colour composites (BRC).

The Kalahari sands (red) on BCC and blue on DSCC are easily distinguished from upper and lower Wankie sandstones (orange) on BCC and DSCC. Discrimination is also enhanced by the dense vegetation cover over the sands.

The Escarpment grit is best noticeable on the BCC image where the grit displays bright blue colours. On this image all the areas covered with Escarpment grits are easily discriminated from other areas covered with coarse grained sandstones and weathered granites probably because of the elevated reflectance values for TM bands 5 and 7 resulting from iron oxide cementing the grits.

The Batoka basalt are distinguished from the lower and upper Karoo sediments by the deep blue colour to deep green colour on the BCC, BRC and BDC involving band 7. This can also be accounted for by the presence of iron oxide and clays which occur as weathering products of these basalts (Drury 1990).

The ripple-marked flags and the other upper Karoo sandstone units are best distinguished in the BDC of TM5-7,TM4-3,TM7-4 where they display deep orange colour as opposed to pale blue colour shown by grits and upper Wankie sandstone in yellow and green shades.

Madumabisa mudstone is represented by a pale blue colour in BDC, deep blue in BRC and purple in BCC. These colours distinguish the mudstone from the sandstones, fireclay and carbonaceous varieties of mudstone. Detection of the Madumabisa mudstone was done in composites including TM bands 5 and 7.

The upper and lower Wankie sandstones are very difficult to distinguish from each other in any of the colour composites because of their similarity in composition and occurrence. The two sandstone units are easily discriminated from the glacial sediments and the Sijarira sediments on the BRC and BDC images where they appear in shades of red and orange respectively as compared to the pale pink colour of glacial beds in both images. On the BRC image (TM5/7), the lower Wankie sandstone can be identified in shades of bright orange, probably because of the calcite cement causing absorption in the wavelength region represented by TM band 7 (Hunt 1977)

Fireclay is clearly shown in all composites that include TM band 7. On the DSCC, BCC and BRC it is distinguished from other clayey rocks by a bright yellow colour and on the BDC composed of TM 7-5, 4-3, 3-1 by a pale blue colour.

Burnt coal areas are easily discernible on all band composites in shades of maroon and deep red. Generally the BCC of any band combination gives the best discrimination and it is the one on which unmapped burnt coal areas around Pongora siding south-east of Hwange were detected.

Carbonaceous shales and coal are distinguished from burnt coal areas and mine dumps by characteristic bright blue colours on the BCC image with TM bands 7,4,2. Mine dumps in all the composites display black colours with a lot of haze where there is a lot of smoke as found in the Wankie Colliery No2 Opencast mine.

The Dwyka sediments are not uniquely distinguished in any of the colour composites. In most of the band composites they display colours similar to the Wankie sandstones but in the band difference image of TM band 5 - TM band 7 and band difference composite including the TM band 5 - TM band 7 image, they appear in pale blue colour as opposed to the deep blue colour displayed by the upper and lower Wankie sandstones in similar images.

The remainder of the lithologic units constitute the Precambrian rocks. These units are easily distinguishable from Karoo rocks and other sedimentary rocks on the BCC and BDC images. The Sijarira Group constitutes the only sedimentary unit of the Precambrian rocks. This is represented by a deep yellow to green colour on the BCC (TM bands 7,4,1). The rest of the Precambrian rocks are metamorphic and igneous rocks showing different degrees of metamorphism.

Granites and gneisses of the Dete-Kamativi and Entuba inliers are clearly distinguished on the BCC in shades of brown and characteristic granular texture given by numerous castle kopjes and inselbergs covering the granitic terrain. Yellow bands in the granite-gneiss terrain represent quartz veins and other silicified rocks.

The BCC (TM7,4,1) also discriminates most of the metamorphic rocks. Graphitic schists (black), Inyantue formation schists in yellow, amphibolites red, and the pink paragneisses appear in shades of pink and orange and metapelites in shades of green. Dolerite dykes are only distinguishable on the BDC image where they appear as maroon and brown elongated features.

5.7 Discussion

The analysis and interpretation of Landsat TM data described above shows that rocks react differently to the seven TM bands. No single colour composite of these bands can permit unambiguous discrimination among the rocks in the Hwange Area. Some band combinations such as TM bands 1,4,7; 2,5,7; and 4,5,7, however, distinguish most of the Karoo rocks in the Hwange Area and so can be used to locate areas with a higher potential for coal.

Edge enhancement techniques allowed detection of lineaments associated with different lithologic units and major fracture zones such as Deka Fault, Entuba Fault and Magondi Belt. Lineament attributes analysed are length and orientation both of which can give relationships between lineaments density and different sedimentary, tectonic and igneous activities identified in the area.

The TM data enabled identification of 90% of the previously mapped lithologic units and about 85% of the mapped faults. These were input into a GIS to test their relationships with major geological structures. However the data was found not to be effective in distinguishing between rocks with minor differences in composition such as granitic gneiss and granite.

Chapter 6

Data Integration and Analysis: *Interpretation of lithologic patterns, geological structures and coal seam characteristics.*

6.1 Introduction

One of the main objectives of this study is to provide information on lithologic units, coal seam characteristics, fault patterns and displacement in the Hwange area so as to prioritise coal exploration and understanding of the structural features controlling the overall structures of the coalfields. The Hwange GIS provides a platform to combine, process, analyse, manipulate and interpret the relationships between the geological and structural data sets stored in the Hwange database. It also allows modelling of the data to predict outcomes, for instance modelling of fault characteristics to predict areas that are heavily faulted or faulted by certain fault types. Details of the interpretations of the data sets from remote sensing are discussed in this section and retrieval of the modelled parameters in a GIS is illustrated in Appendix 5.

6.2 Interpretation of Landsat TM images

The techniques used to process the Landsat TM images covering the Hwange area and subsequent extraction of geological features revealed previously unrecognised major structures. It also revealed continuity of some lithological units which had not been observed during field mapping. The use of colour images as described in the previous chapter enhanced the gross variation of surface geology, lineaments, vegetation and detection of regional geological structures. Discrimination of lithologic units was effected by the sensitivity of different minerals to the seven Landsat TM bands. Although no single colour composite image was able to discriminate all the rocks, several combinations of Landsat TM reflective bands managed to map geological features in the Hwange coalfields and the surrounding areas.

6.2.1 Lower Karoo rocks

The most easily discernible rocks of the Karoo group are those associated with spontaneous combustion. These were easily identified on the decorrelation stretched images, false colour composites and band difference images in shades of deep red to maroon. In the grey scale images they are relatively dark as compared to other sedimentary rocks of the Karoo group. This distinct characteristic facilitated detection of the burnt coal areas around the Pongora siding, south-east of the town of Hwange. The area was previously mapped as lower Wankie sandstone and glacial sediments. Discrimination of these areas using TM bands 3 and 4 (on which they display dark colours) suggests that the material produced during combustion, probably rich in silica show high absorbance of these reflective TM bands. Burnt coal areas only occur in areas where the coal seam has been exposed such as in the Entuba, Wankie and Lukosi coalfields. Fig 6.1 below shows areas affected by spontaneous combustion in the Entuba, Lukosi and Wankie Concession areas. These areas are displayed in dark tones on the six reflective TM band images.

The only area with coal seams currently burning are those in the Wankie Concession where the coal seam has been exposed as a result of open cast mining. These areas also show pale tones on the TM band 6 image and bright colours on band composites including TM band 6 image because of the heat generated from the burning coal seams.

There does not any appear clear relationship between the degree of localised fracturing and areas affected by spontaneous ignition although most of the burnt coal seams are bound by faults in shallow areas along the margins of the Entuba and Inyantue fault zones. Movement along these faults could have resulted in tilting of areas around these faults thereby causing exposure of fractured coal seams to the atmosphere. The Dwyka sediments are difficult to discriminate from the lower and upper Wankie sandstones. This is partly because of their limited exposure to the south-east and south-west of Hwange in the Lukosi and Western Areas coalfields, respectively. The only image that distinguishes the glacial sediments clearly is the grey scale image of band difference image of TM band 5 - TM band 7.

FIG 6.1: Image showing the distribution of areas affected by spontaneous combustion in the Entuba, Wankie and Inyantue Coalfields
B = Burnt Coal

This image gives brighter signatures in areas covered with glacial beds, probably because of the high reflectance of the TM band 5 by the alteration products of the glacial beds.

The carbonaceous shales and coal also have limited exposure, but where they have been exposed they are easily discriminated from mine dumps on colour composites including TM bands 7, 4 and 2. The main component of the carbonaceous shales are clays and organic materials. Clays, sulphur and carbonate materials have been found to show low reflectance at 2.1um to 2.5um corresponding to the wavelength of TM band 7 (Beaumont and Forster 1992), thus the carbonaceous shales were detected on TM band composites involving TM band 7.

Fireclay was easily discriminated on TM colour composites involving bands 5 and 7 on false colour normal composites and decorrelation stretch colour composites. Clay minerals such as kaolinite and montmorillonite constitute the bulk of minerals forming fireclay. These have OH- ions in the mineral structure which cause rapid decrease in reflectance between 1.6um and 2.5um, thus poor reflection of TM bands 5 and 7 (Asrar 1989). This together with the absence of iron oxides in the rock could have allowed discrimination of fireclay in the Wankie Concession, Western Areas coalfield, Sinamatella field, Lukosi and Inyantue fields. The reaction of fireclay to TM band 7 is similar to that of hydrothermal alteration zones, thus could also support the origin of fireclay as an alteration product of mudstones (Watson 1960).

The upper and lower Wankie sandstones detected in all the coalfields are rich in silicates such as quartz, plagioclase and k-feldspars. These tend to reflect bands with a higher wavelength such as TM bands 5 and 7 and tend to show high absorption of TM bands 1-3 (Woldai 1995). The pale tones shown by these lithologies on black and white images of TM bands 5 and 7 and bright red and pink colours in colour composites with TM bands 5 and 7 could be a function of this behaviour. Clear distinction of these sandstones is hindered by a thick layer of sand covering the sandstones.

The Madumabisa mudstone is clearly distinguished in the band ratio image, band difference and the normal false colour composites of TM bands 5 and TM 5/7. Madumabisa mudstone contain alumino-silicates, carbonates and minerals containing hydroxyl ions which have been found to have

a narrow and distinctive absorption bands in the 2.1um to 2.5um region (Hunt 1977). Carbonates such as calcite and siderite constitute a considerable portion of the Madumabisa mudstone together with clays such as kaolinite and montmorillonite. These rocks, therefore, have a very strong absorption in TM band 7, showing deep purple, red and blue colours in the normal false colour and decorrelation stretch composites involving TM bands 5 and 7.

6.2.2 *Upper Karoo Rocks*

The Escarpment grits consist of very coarse sandstone with iron oxide cement. The grit has been altered as a result of weathering to gosaneous ironstone and the surface is characterised by red iron stained soils. Laboratory results have shown that weathered iron show intense absorption at short wavelengths (Forster and Beaumont 1992) and very weak reflectance in the blue region of the electromagnetic spectrum corresponding to TM bands 1 and 2. Iron oxide rich rocks show very strong reflectance in the red region (TM band 3) and increase in ferric iron also increases reflectance of TM band 5. Because of this, band ratio images involving TM band 3 and band 1 has very high values for the iron stained areas (Avery et al 1992). This could account for the discrimination of the escarpment grits on the TM1,3,5 and TM1,3,7 and band ratio images of TM 3/1, 3/5 and 5/7. The grey scale images of TM bands 3 and 5 show light tones for areas covered by grits. Grey scale images of TM bands 1,4 and 7 show dark tones for these areas thus showing strong absorbance of these bands by the grits. This rock unit can easily be discriminated on image composites with TM band 3, band 1 and band 5.

The Batoka basalt forms the only volcanic unit of the Karoo group in the Hwange area. The basaltic rocks are rich in iron bearing alumino-silicates. The iron rich alumino-silicates are altered to clay and iron rich/hematitic soils upon weathering. This increases the composition of ferric iron and clays in the rocks. Iron stained montmorillonitic and kaolinitic clays form the bulk of the clays produced as weathering products of the basalts. The presence of both iron oxide and clay minerals result in strong absorption of TM bands 1 and 7 and strong reflection of the intermediate TM bands 3 and 5 thus help to detect these rocks in the colour composites involving TM bands 1, 3, and 7 and TM bands 4,5 and 7.

The abundance of clays and carbonates such as calcite tend to shift

the absorption spectrum of these rocks also to a higher wavelength around 2.1um (Woldai 1995), therefore allowing detection of carbonate rich portions of the Batoka basalts.

The ripple-marked flags form the topmost layer of the Karoo sediments detected in the Hwange area. These are only distinguished on the band ratio images of TM band 3, 4, 5 and 7. This could be because of the abundance of altered alumino-silicates as well as iron oxides which give a strong reflection of TM band 5 and strong absorption of TM band 7.

6.2.3 Tertiary and Recent Sediments

The Kalahari sands constitute the Tertiary sediments occurring in the Hwange area. Discrimination of the Kalahari sands is best achieved on the normal false colour composite and decorrelation colour composites involving TM bands 2,4 and 5. This could be partly because of high reflectance of band 4 by the dense active vegetation covering the Kalahari sands. The major component of these sands is silica which show high reflectance in bands 2-7 (Curran 1985) thus suggesting light tones in the grey scale images and bright colours in colour composites.

The clear boundaries of mine dumps around the Wankie collieries are best seen on the TM band 1 and TM band 6 grey scale image and band composites involving TM band 6 and TM band 7. Most of the mine dumps are burning due to pyrite oxidation. Because of strong heat absorption of coal and heat generated from spontaneous ignition, the absorption spectrum of the dumps to 8um-14um thermal infrared region (Asrar 1989), thus allowing mapping of areas where coal has been mined using TM band 6 image. TM band 1 is very sensitive to smoke, thus identification of burning areas was also facilitated by the inclusion of TM band 1 images in the colour composites. Smoke plumes from the burning mine dumps in the Wankie Collieries on the band colour composite made from TM bands 2, 1 and 6 are clearly highlighted in shades of grey to pale blue.

6.2.4 Precambrian Rocks

The Sijarira meta-sediments are difficult to discriminate from the Wankie sandstones and the ripple-marked flags on enhanced images because of their similarity in composition to the Wankie

sandstones. The rocks were only discriminated based on their locations as mapped by Watson (1960) and intersected by boreholes drilled in some of the coalfields.

The granites and gneisses of the Entuba zone and the Dete-Kamativi inlier were discriminated on almost all the colour composites. This is because of the characteristic linear fabric and probably because of the high reflectance of silicate minerals of all the TM bands. The gneisses are discriminated from the Proterozoic granites by means of their strong foliation (which define regional metamorphism) and the granites by the granular texture defined by castle kopjes and inselbergs. These two show more or less the same colours on colour composites because of their similarity in composition.

The dolerite dykes, biotite schists, amphibolites and mafic granulites are clearly distinguished in normal false colour composites and decorrelation stretch composites involving TM bands 3, 5, and 7 and TM 4, 5, 7. The reason for discrimination on these bands could be the response of the weathering products of iron- and magnesium-rich minerals forming the bulk of these rocks (Lockett 1979). The amphibolites are covered with red hematitic clayey soils and are also altered to tremolite and chlorite schists. The garnetiferous schists with iron-stained and silica-rich soils. Because iron-bearing minerals (goethite and hematite) have a distinctive broad absorption bands centred in the ultraviolet, visible and infrared portions of the electromagnetic spectrum, the amphibolites and the mafic granulites show strong reflection of TM bands 3 and 4, and 5 thus their clear distinction in TM 1,4,7 and 3,4 and 5 band composites. The reaction to TM band 7 is also given by the clays and micas which are also alteration products of the mafic granulites and amphibolites.

The graphitic schists and ferruginous slates of the Piriwiri Group are easily discriminated on most of the grey scale band images because of the high absorption of all the bands by graphite. The Inyantue and Kamativi schist zones are clearly distinguished on TM band 5 and TM band 7 grey scale images. This could be a result of strong reflection of TM band 5 by ferruginous cherts and slates and strong absorption of TM band 7 by micas such as biotite and muscovite that constitute the bulk of the schists. The other schists are only discriminated from the gneisses by the very strong foliation. TM band 7 is the most effective in discriminating the Piriwiri schists probably because of the presence of alteration minerals.

6.3 Geological Structures Mapping

Mapping of geological structures was done through the analysis of linear features such as foliation traces, faults, shear zones, joints and fold axes detected on the Landsat TM image of the Hwange area overlaid on previously mapped structures. Most of the linear features were found to be related to the episodes of faulting and folding identified by Watson (1960), Lockett (1979), and others not previously known.

6.3.1 Folds

Folds were easily identified because of the well expressed fold structures and steep plunge of the strata. Folds were identified on all the TM band images. The most spectacular folds are those affecting the Malaputese Group towards the east of the study area. These can be traced towards the south beneath the Kalahari sands on which they give a surface imprint, particularly in the area around Dete (See Fig 6.2A). The most striking fold detected in this study which was previously not known is along the Entuba inlier. The fold is easily traced on the Landsat TM band images but was not mapped during field work nor does it appear on any existing maps. The fold is made up of a synformal feature with minor parasitic folds. The limbs are cut on both sides by the Entuba shear zones. Fig 6.2B shows the Entuba synform west of Sinamatella camp.

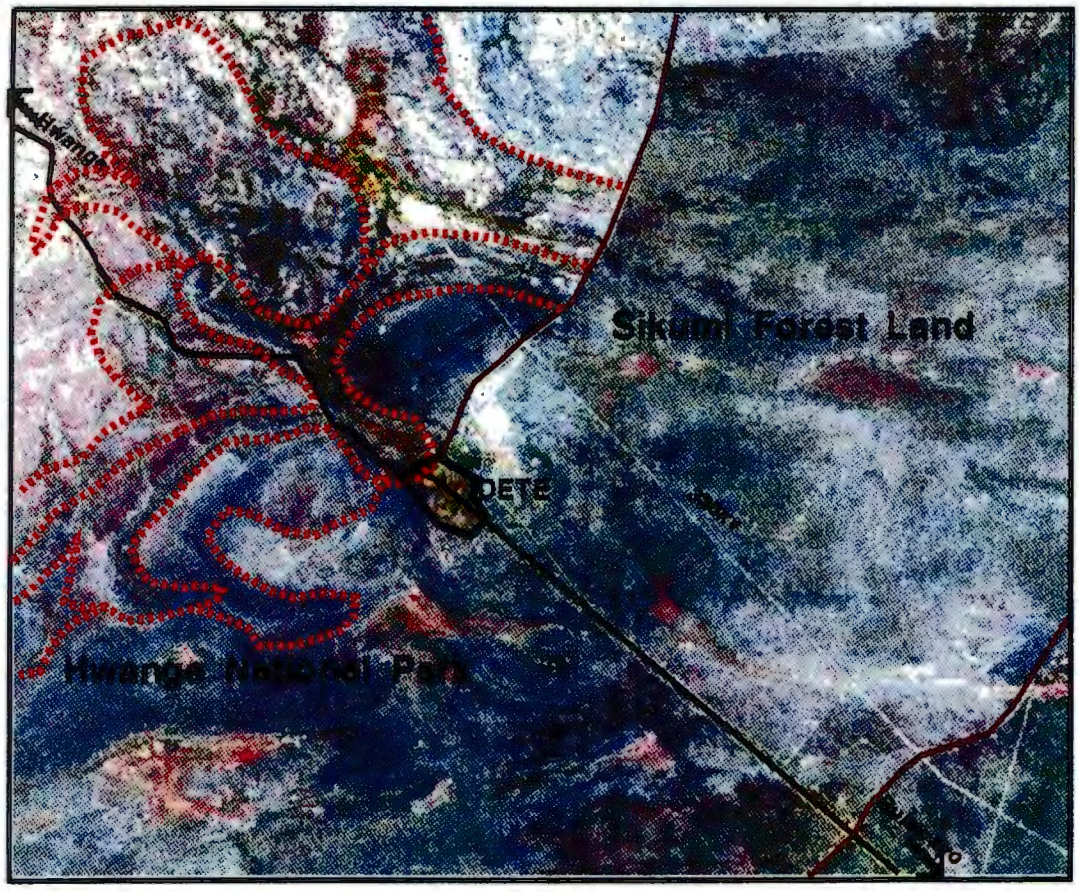

N

FIG 6.2A: Band colour composite showing folds around the village of Dete

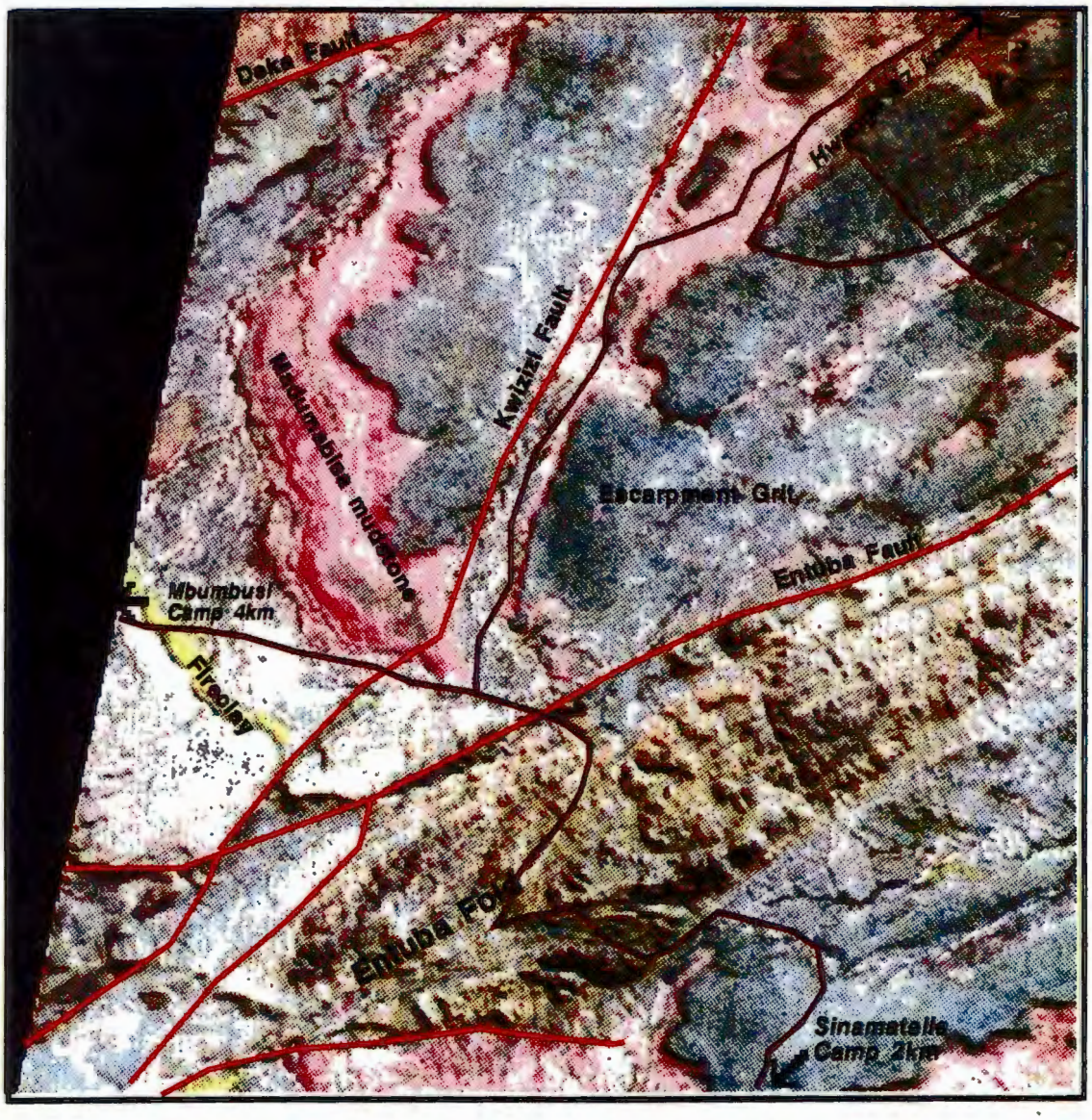

FIG 6.2B: Image showing the Entuba Fold

6.3.2 *Lineament Analysis and Fault Tectonics*

Lineament analysis performed in this study was an attempt to better constrain the geological structures (faults, joints and shear zones) to improve understanding of the development of the Hwange Coalfields and the associated fault zones. As stated earlier, lineament analysis of the Landsat TM data of the Hwange area also attempted to map the extent of the western extension of the Zambezi Rift faults and analyse the variations in displacement of the main coal seam in some of the coalfields such as the Entuba field. Two attributes of the lineaments and faults were considered in the analysis, viz. their orientation and length. These attributes were analysed using histograms shown in Figures 6.3A to 6.4B, as well as overlaying the lineament map on the lithology and fault maps in a GIS. Figures 6.3A and 6.3B show percentage occurrence of lineaments and faults plotted against orientation. Figures 6.4A and 6.4B show percentage occurrence of lineaments and faults versus length, and Figure 6.5 is a histogram of lineament lengths plotted against azimuth (orientation).

The azimuth frequency and total length histograms (Figs 6.3A and 6.4A) indicate that there are five major groups of lineaments in the Hwange area. These groups comprise lineaments trending between 30^0- 45^0, 46^0- 60^0, 61^0- 75^0, 76^0 - 90^0, 91^0-105^0. The first three groups (30^0-75^0) are mainly concentrated in the central part of the study area, the 76^0-90^0 trending group is evenly distributed throughout the map except in the north-west corner where the 91^0-105^0 trending lineaments dominate. The three middle groups of lineaments, 46^0-90^0 constitute the majority of the lineaments in the Hwange area. The percentage orientation histogram (Fig 6.3A) has its mode at 75^0 (ENE).

Comparison of the azimuth frequency histogram of lineaments (Fig 6.3A) and azimuth frequency histogram of faults (Fig 6.3B) shows that they both have modes at 75^0 and a lesser mode at 60^0. This suggests a strong relationship between the orientations of mapped faults and lineaments, although some of the lineaments identified as faults were not previously mapped. The length frequency histogram of lineaments and that of faults show modes at different lengths. The lineament length frequency histogram shows a mode at 3km - 5km length and the fault length histogram at 1-

3km. This shows that the lineaments mapped were longer than the mapped faults. Overlaying of the lineament map on the fault map however, shows a good correspondence of the lineaments and

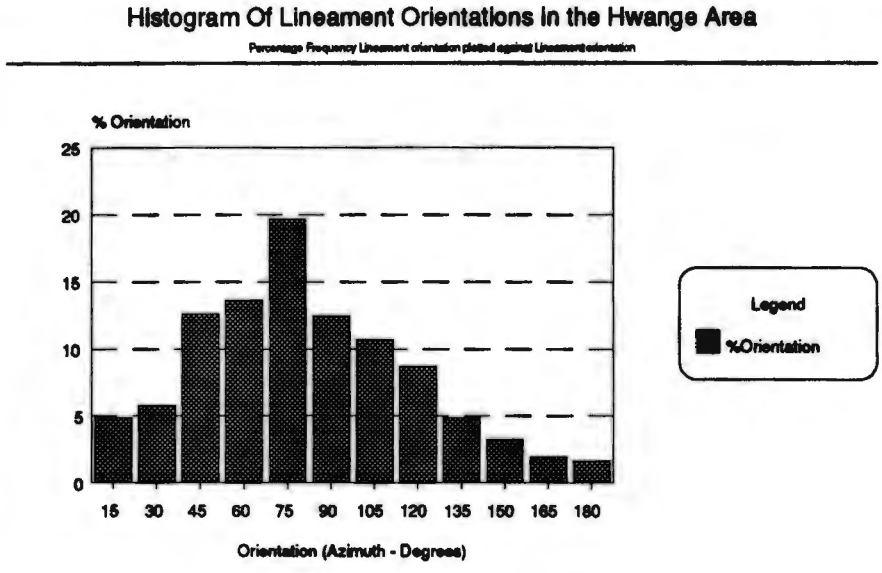

Fig 6.3A

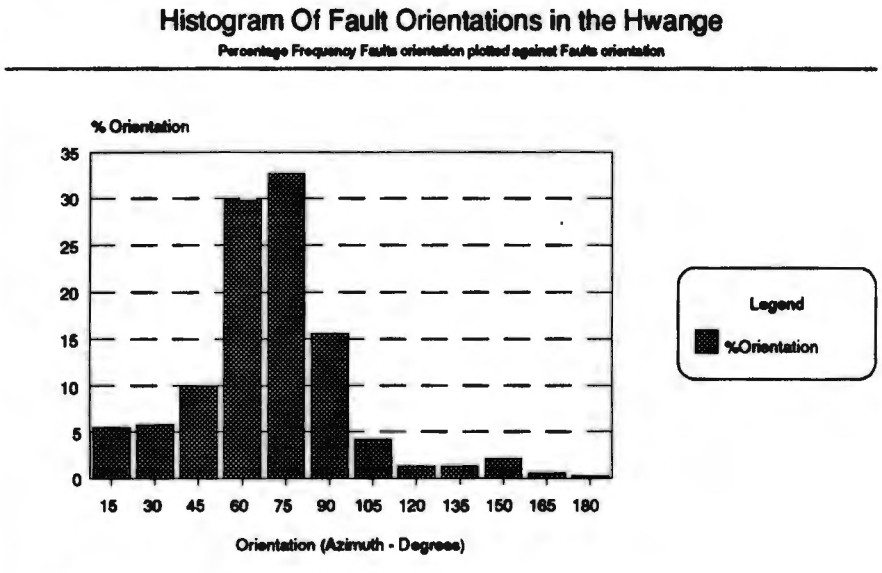

Fig 6.3B

***FIG 6.3 A and 6.3B*: Histograms showing Lineament and Fault orientations in the Hwange Area**

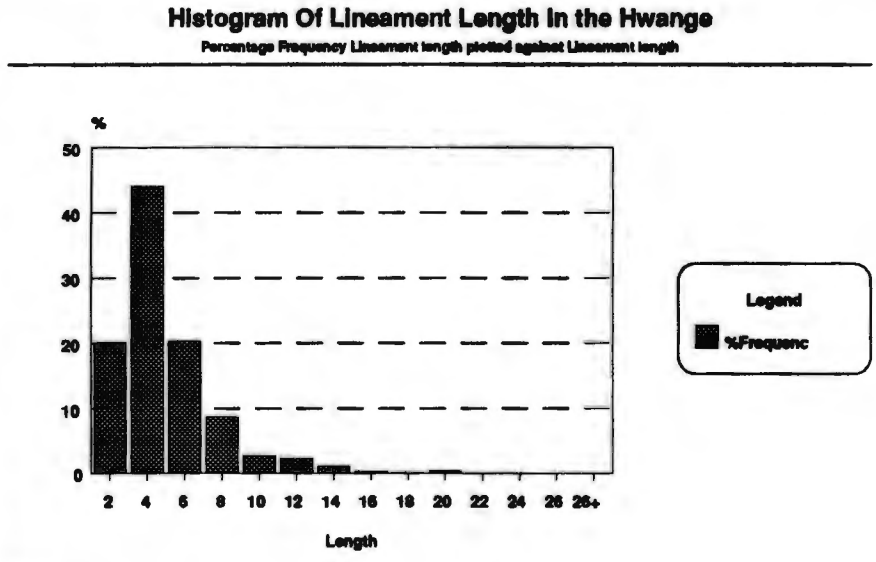

Fig 6.4A

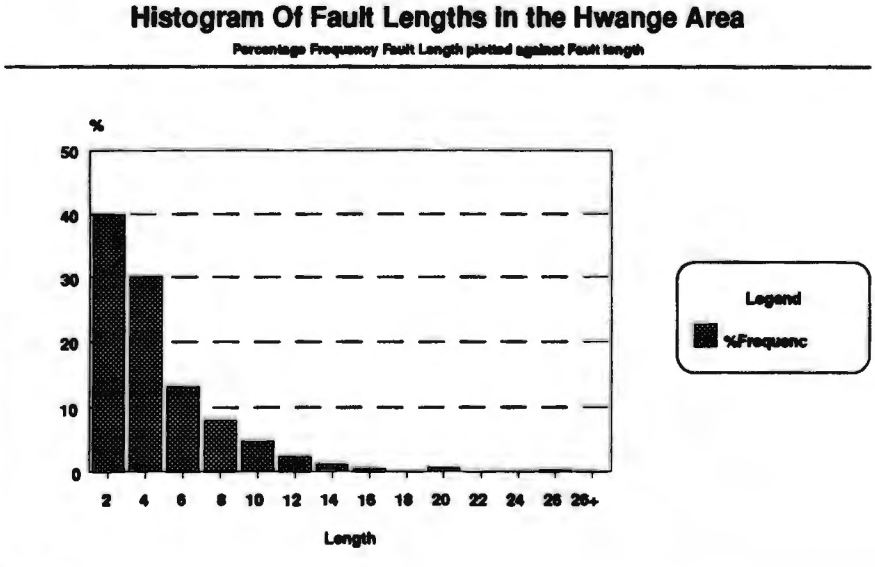

Fig 6.4B

FIGS 6.4A and 6.4B: **Histograms showing Lineament and Fault lengths in the Hwange Area**

mapped faults. In some cases the locations of lineaments coincide with that of mapped faults although the lineaments extend beyond where the faults were not traced. This may be because the full length of a lineament or fault can be more easily determined on an image than in the field. It is difficult to locate faults where they are covered with superficial sediments in the field, but may be less difficult on a satellite image. Fig 6.5 shows a histogram of lineament length versus azimuth. The lineaments trending 61^0-75^0 have a greater offset and length. This also suggests that lineaments with this trend have bigger effects in this area as they affect larger areas than other groups.

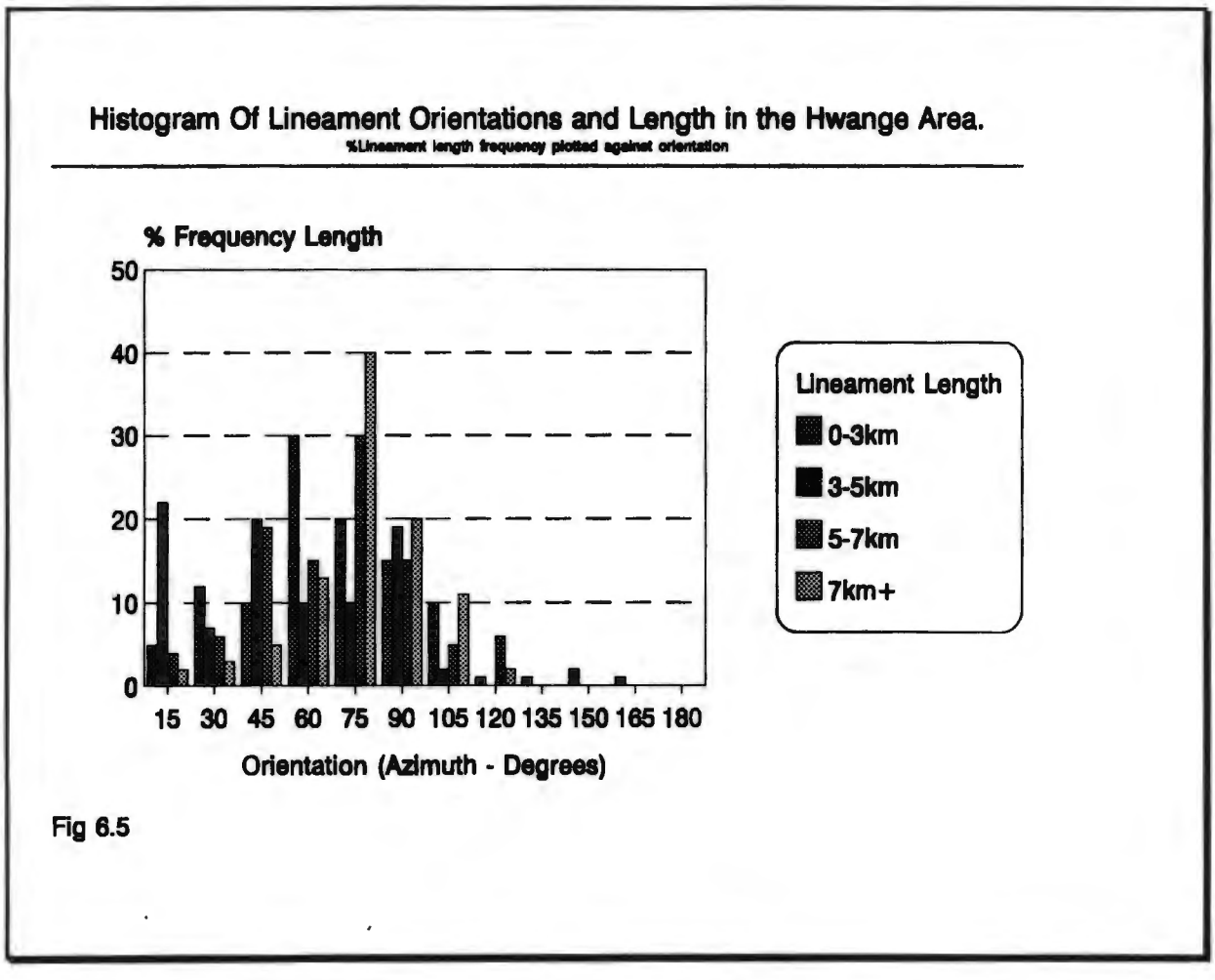

Fig 6.5

***FIG 6.5*: Histogram showing lineament length and orientations.**

Overlaying of the lineament map (Fig 5.7) and the lithology map showed that the 30^0-45^0, 46^0-60^0 and 61^0-75^0 trending lineament groups mainly occur in the Karoo sediments close to the basement - Karoo contact. The 75^0-90^0 trending lineaments occur mainly on the Karoo basalt covering the north-west and western parts of the study area. The last major group of lineaments (90^0-105^0) occur in almost every part of the Hwange area. In the Karoo sediments some of these lineaments define compositional layering of the sedimentary rocks.

Proximity analysis of the lineament map and fault map showed that most of the lineaments originate from the three mapped fault zones, the Deka fault, Entuba fault and the Inyantue fault zones. The only exception are the lineaments in the basalt (north-west) which appear not to be related to any fault zone but rather define joint sets possibly developed during cooling of the basalt.

Fig 6.6 shows the number of lineaments within a distance of five kilometres from major fault zones. The histogram shows that the Entuba and Inyantue fault zones are associated with most of the lineaments in the Hwange area followed by the Deka, Sinamatella and Lukosi fault zones. About 242 of the 749 lineaments occur within 5km of the Entuba fault and most coalfields also occur within this distance from this fault, therefore suggesting the influence of this fault on the development of faults and distribution of Karoo units in the shallow coalfields.

The NNE-NE (30^0- 45^0) lineaments are considered to be the oldest set of conjugate faults and foliations developed during the Zambezi and Magondi metamorphic events because these are cut by all the other lineaments, particularly the ENE, NE and E-W trending faults. The NE to E trending lineaments are more dominant than other groups with greater size and larger offsets and a much more persistent lineament length of over 7 kilometres than all the other lineaments. This together with overlay analysis performed in a GIS proved that the NE direction is the main fault direction corresponding to the Zambezi Rift system in the Hwange area and is the major fault set responsible for fracturing in the Wankie, Chaba, Entuba, Sinamatella and parts of the Western Areas coalfield. Fig 6.7 shows a lineament map overlaid on a fault map. The map shows that most of the lineaments are associated with the major fault zones.

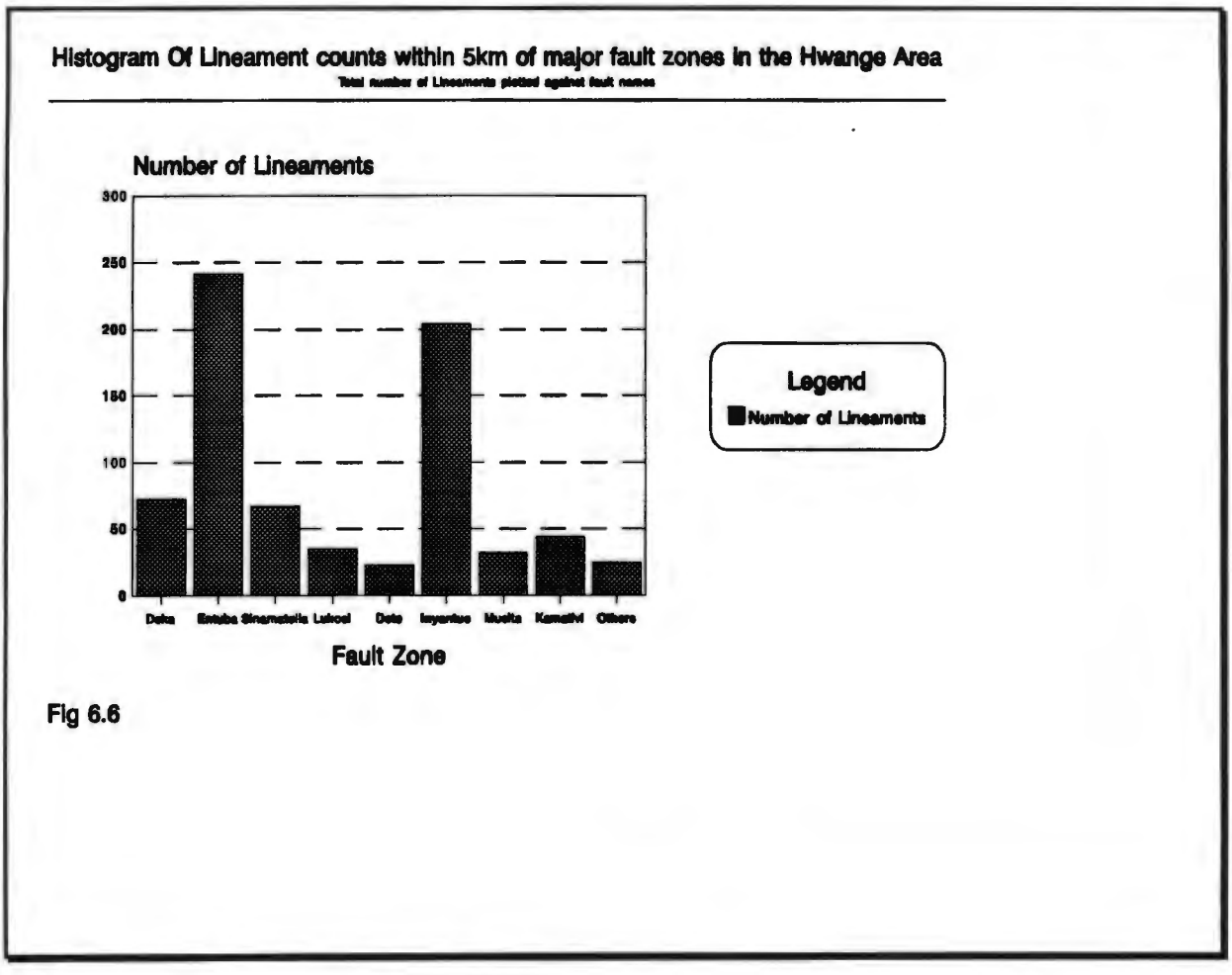

Fig 6.6

FIG 6.6: **Histogram showing the density of lineaments within 5km of major fault zones in the Hwange Area**

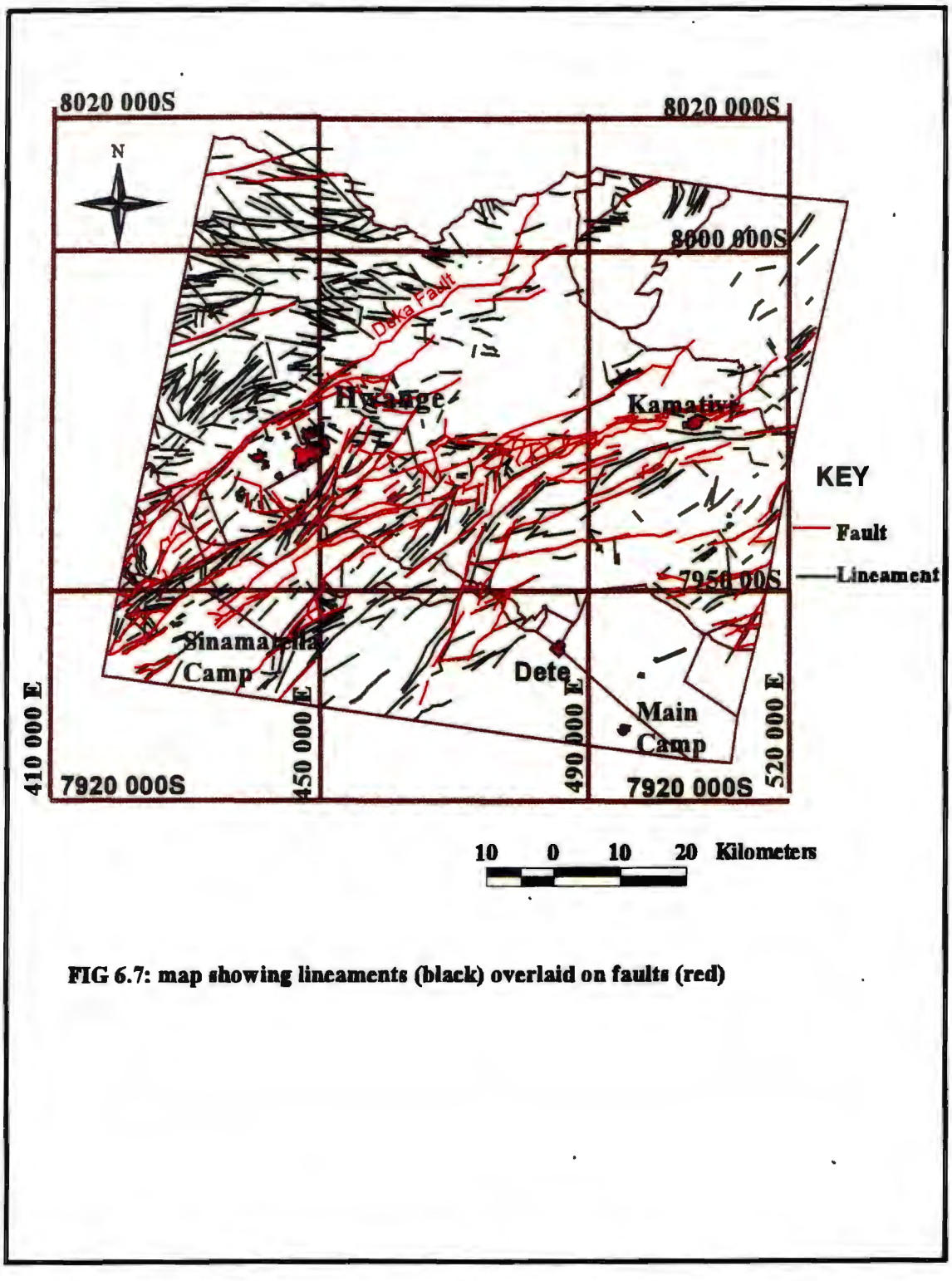

FIG 6.7: map showing lineaments (black) overlaid on faults (red)

Another striking feature about the lineaments identified as faults in this area is that they are generally characterised by the alignments of present day river channels. Inspection of the Landsat TM image of the area shows that, the Lukosi river, to the south-east of Hwange is dominantly controlled by a series of NE-SW and ENE-WSW faults. The Kamandama south of Hwange is controlled by the Entuba fault, the Chambumo river by the Chambumo fault, the Deka river by the Deka fault, Lukunguni and Matetsi rivers follow major joints on the Batoka basalts and the Kwizizi and Guyo rivers are controlled by the Kwizizi fault. Faults therefore are responsible for the linear topography of the area made up of elongated ridges prevalent in the Hwange area and thus control the shapes of the coalfields. Fig 6.8 shows a fault map overlaid on drainage map of the central and western parts of the Hwange area. The map shows that some of the river segments have a NNE to ENE trend which correspond to the dominant orientation of lineaments defining joints and major faults in the area although the direction of water flow is controlled by the general northward tilt of the Mid-Zambezi basin.

6.3.3 Fault tectonics and Distribution of Karoo units

Exposure of the lower Karoo units such as Dwyka sediments, carbonaceous shales and coal, fireclay and upper and lower Wankie sandstones are mainly restricted to the vicinity of the Entuba, Inyantue and Sinamatella fault zones, except around the coal mining town of Hwange. Most of these areas are within a distance of less than five kilometres from these major faults. In most of these areas such as the Chaba, Entuba, Sinamatella and Western Areas, the main seam is well developed (composed of mainly coking coal) and burnt where it has been exposed. This could suggest coalification at greater depths and uplifting during coal formation or after the coal seams had been formed as a result of post-depositional faulting. Lockett (1979) and Duguid (1986) suggests the exposure of the Lower Karoo units and lack of proper development of the main coal seam close to faults as a result of reactivation of old faults during deposition but in the Chaba and Entuba fields the seam is well developed, therefore suggesting post depositional tilting.

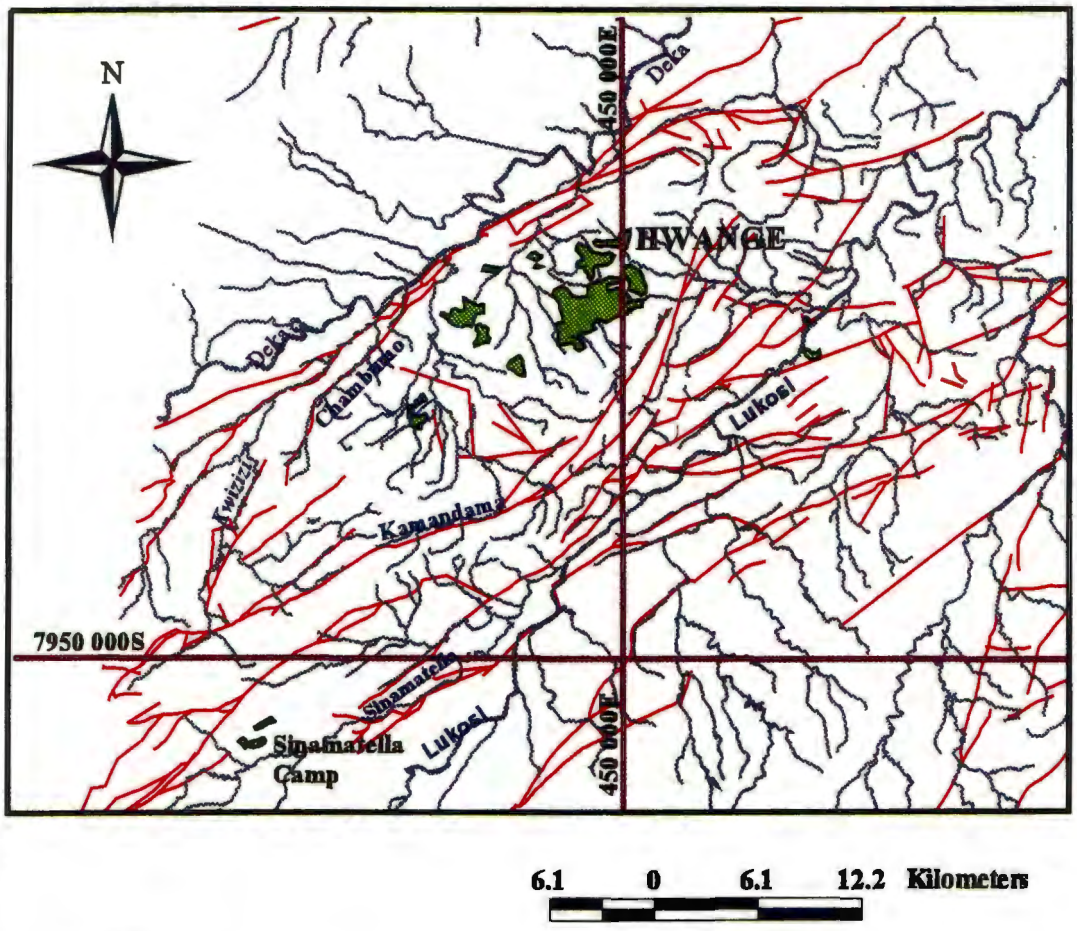

FIG 6.8: Map showing the orientations of river segments and faults in the central and western parts of the Hwange Area

Several features on Landsat TM images and in the field suggest uplift of some of these shallow areas in the Hwange coalfields. There are remnants of upper Karoo sediments on high ground and wherever the lower Karoo sediments are exposed in the Wankie, Chaba and Entuba fields, they are bound by faults. The biggest exposure of the lower units of the Lower Karoo is around Hwange town. The greater part of the coal seam is burnt in this area and is bound to the south by two faults (Chaba faults) which branch from the Entuba fault in the Chaba field. The faults down-faulted the Madumabisa mudstone south of the Wankie Opencast Mine. Movement along these faults and along the main Entuba fault could have resulted in localised uplift around Hwange town resulting in erosion of the Madumabisa mudstone sequence exposing the relatively flat lying lower Karoo units which appear as a circular feature cut to the east and south by faults.

6.3.4 The Entuba Fault Zone

Field mapping and analysis of Landsat TM data suggests strike-slip movement coupled with dipslip along the Entuba fault zone. Strike-slip character is apparent, with most of the lineaments branching into coalfields identified as faults. The strike-slip movement along the Entuba fault is also supported by the well developed breccia zones and slickensided shear surfaces found along the fault zone. Fig 6.9 is a photograph taken at a place about 6km south-east of Hwange along the Entuba fault zone. The photograph show well developed shear surfaces with sub-horizontal lineations and sigma porphyroblasts representing dextral movement and cut by a small dextral fault.

Several geomorphic indicators identified along the Entuba zone on the Landsat TM images overlaid on lithology map also support strike-slip movement coupled with dipslip. The fault zone displays nearly straight and smoothly curving traces as opposed to the zigzag nature of the Deka fault which is a normal fault. Prost (1989) found that most strike-slip faults are associated with such fault traces. Structural and topographic discontinuities, linear ridges with sheared rocks such as the Ingagula, Surichenji, Lukosi and Mbumbusi ridges are all characteristic ridges associated with lateral movement along faults. Truncation of the Escarpment grit ridges in the Western Areas, Wankie and Sinamatella fields also displays lateral movement along the Entuba fault zone.

***FIG 6.9*: Brecciated and slickensided shear surfaces along the Entuba Fault cut by smaller dextral faults.**

The dipslip movement which produced fault scarps to the south of Hwange also down faulted the Karoo rocks. Correlation of the lower Karoo units such as fireclay (yellow on the image) and carbonaceous mudstones in the Western Areas and Sinamatella fields show that the area to the north-west of the Entuba zone was moved to the right (See Fig 6.10) thus suggesting right lateral strike slip movement for the Entuba fault. Fig 6.10 is a colour composite showing the Entuba fault zone and truncation of Escarpment grit ridges in the Western Areas and Wankie coalfields.

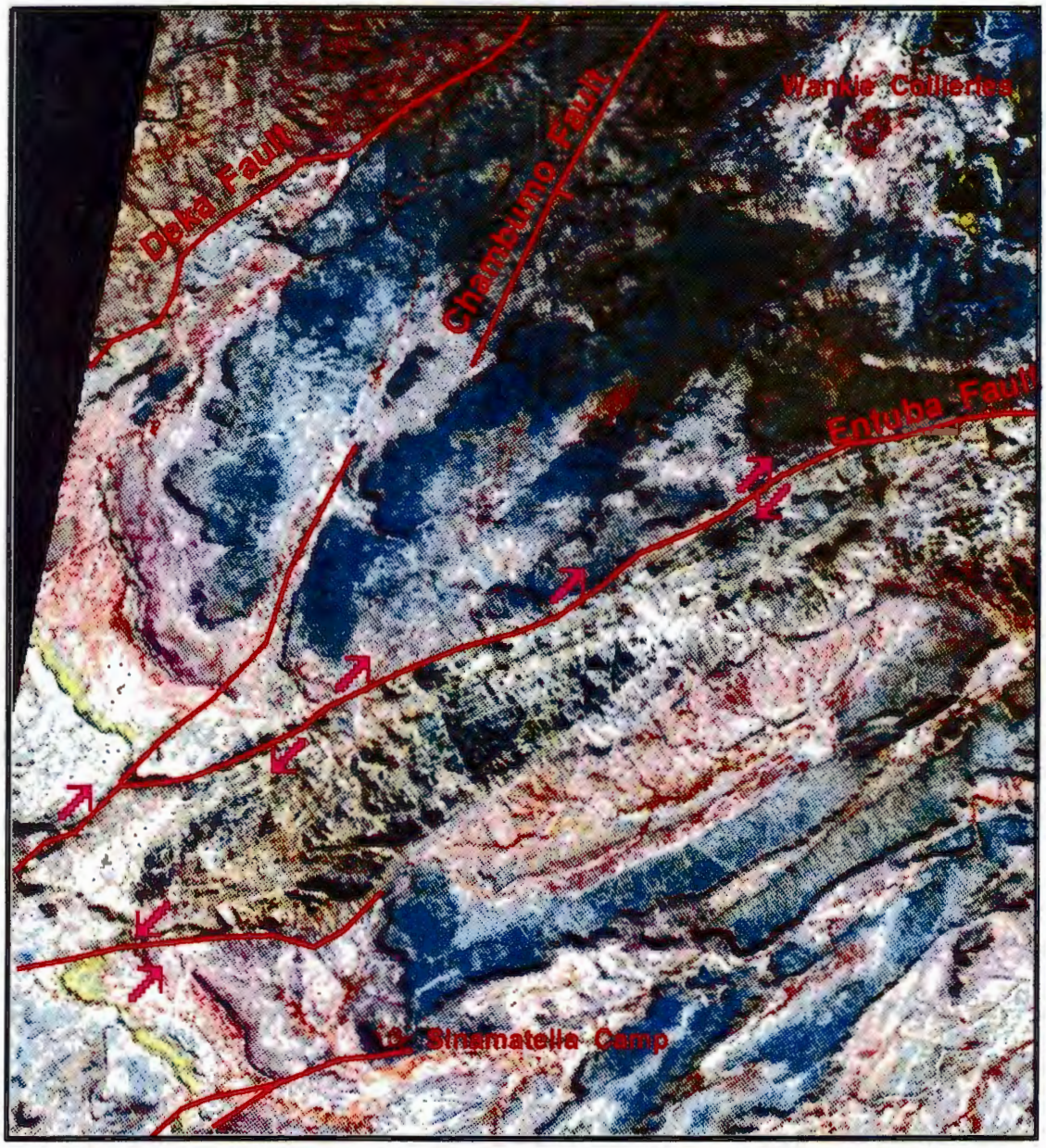

FIG 6.10: Colour Composite showing the Entuba Fault and truncation of sedimentary units along the fault Arrows show interpreted direction of movement

6.3.5 Fault Tectonics and Coal Seam Displacement

Proximity analysis involving coalfields and borehole data revealed more lineaments in the Entuba, Western Areas and Chaba coalfields to be faults. Analysis of depths to footwall of boreholes on either sides of these faults in the heavily fractured coalfields (Entuba, Western Areas and Chaba) revealed that variations in seam depth can partly be explained by variations in displacements along the post-depositional faults of the Zambezi Rift System. In the Entuba field, for example, depths to the top of a coal seam vary over distances of less than 500m from 80m to about 520m. Analysis of most boreholes in the coalfield within distances of 200m from faults showed that the faults are mainly responsible for this variations, Wherever the lineaments have been identified as faults, depths to the top of coal seam were compared on either side of the fault and the same results were found, where there is considerable vertical displacement along the fault. The variations also show block faulting within the Entuba and Lukosi coalfields with displacement increasing towards the east.

The same situation was found in the south-western part of the Western Areas coalfield in which Palloks (1984) attributed local vertical variations of depth to coal seam to the undulating nature of the pre-Karoo floor. In other coalfields such as Lukosi, Sinamatella and Inyantue, lack of borehole information hampered the analysis of vertical variations of coal seam depths in relation to fault patterns.

The Entuba and Lukosi faults and their splays in particular, were found to be responsible for the displacement of seams in the Entuba, Western Areas and Sinamatella coalfields. These are defined by lineaments trending NE to E. Therefore in the Hwange area, the most important fault sets are the NE, ENE and E trending fractures which show maximum displacement of the Karoo rocks. Fig 6.11 is a cross section drawn across the Entuba field and Fig 6.12 is a map of the Entuba coalfield showing variations in seam depth across several faults mapped in the area. The map shows that there is considerable vertical displacement of the seam intersected by boreholes on either sides of faults and displacement along the block faults increases towards the east and south-east.

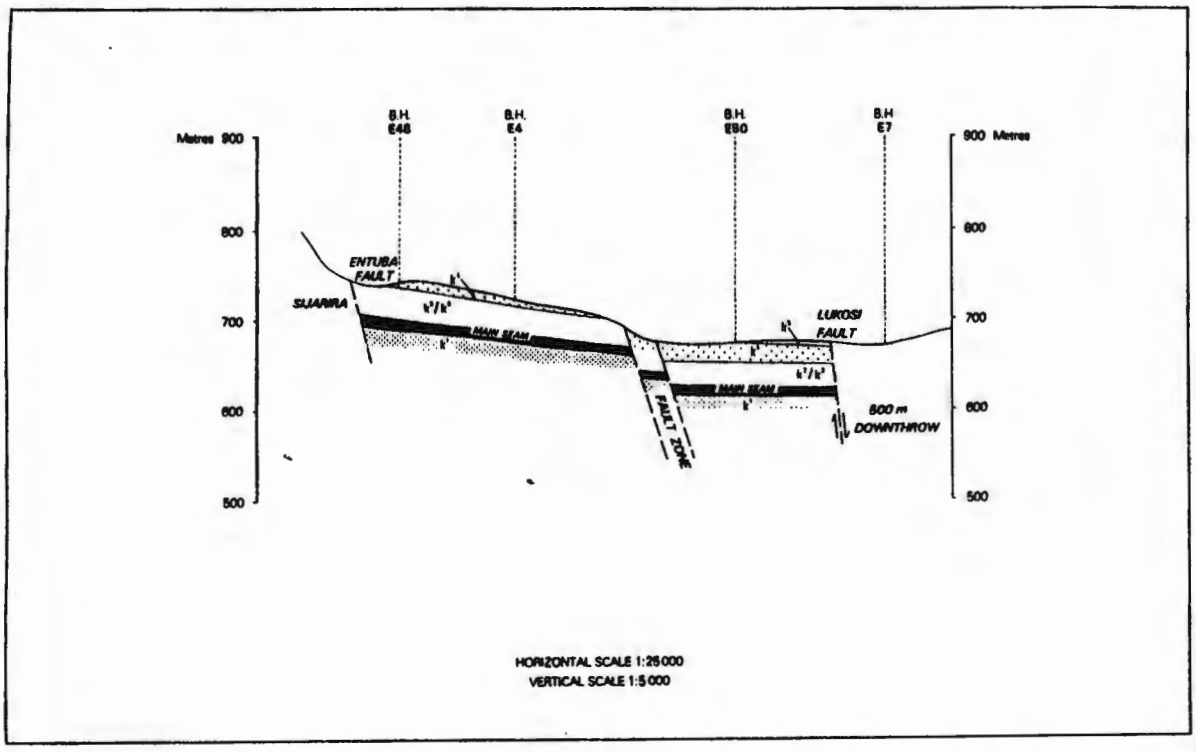

FIG 6.11: Cross section across the central part of the Entuba Coalfield showing vertical displacement of coal seams.

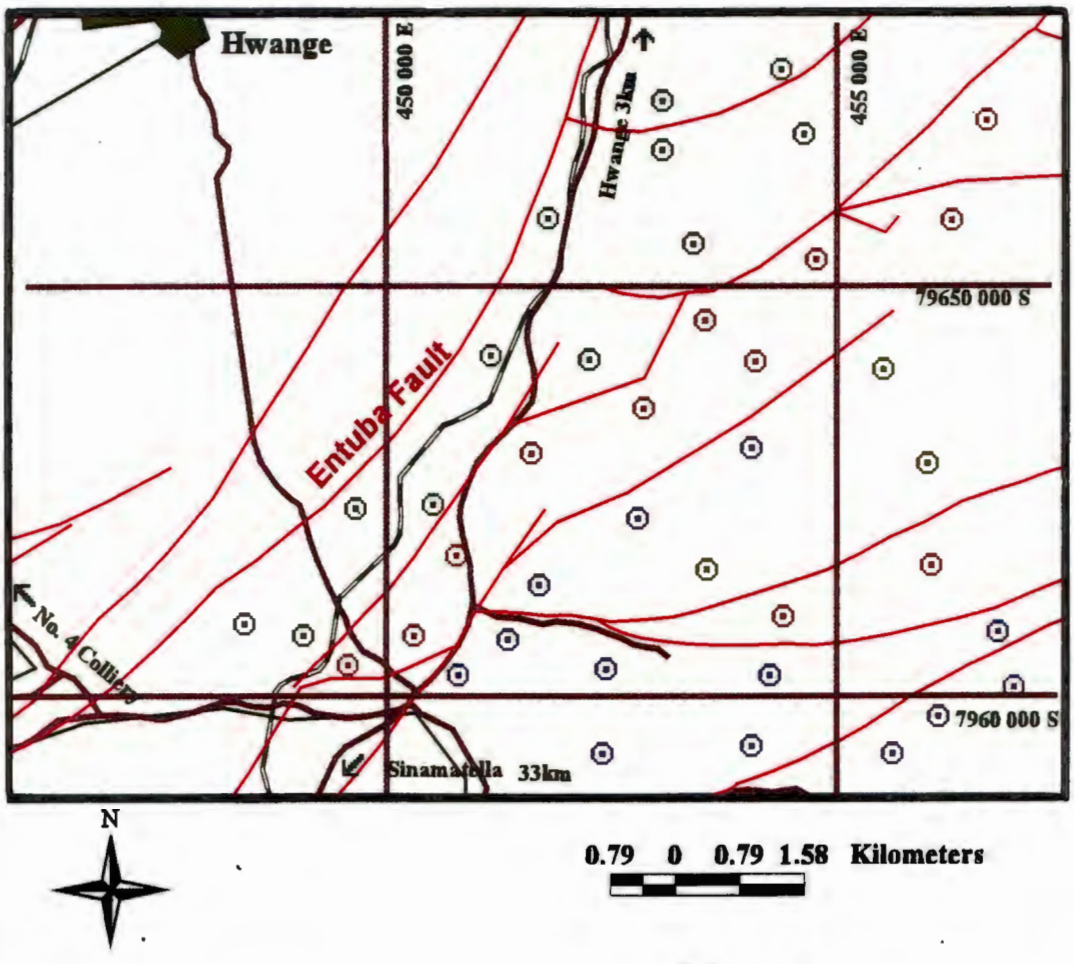

FIG 6.12: Map showing the distribution of exploration boreholes and faults in the Entuba Coalfield

6.4 Discussion

The interpretation of the structures and field relationships of the rocks in the Hwange area was facilitated by manipulation of the geological data in a GIS. This allowed complex relationships between the geological structures and lithologic units to be determined which were not apparent in the field. The relationships between fault patterns and the depth of coal seams in the Entuba coalfield is one such relationship determined after integrating exploration data with geological structures mapped on satellite images. Quantitative measurements such as measurements of lineament orientations, lineament lengths, fault orientations and river segments orientations also allowed interpretation of the relationships between fault patterns, joints, folds and the development of landforms and drainage patterns in the Hwange area. These relationships were used to interpret and propose structural models of the areas like the Wankie coalfield, Entuba coalfield and the Entuba inlier given in this chapter.

Chapter 7

Conclusions and Recommendations

7.1 Conclusions

The research in this thesis has addressed realistic coal-industry problems of the Hwange area in terms of fault patterns, distribution of coal seams and mapping of lithologic units. The Hwange area is of interest because it is the only current source of bituminous coal in Zimbabwe. The area consists of a wide spectrum of rocks ranging from old gneisses, amphibolites, granulites and granites, surrounding the coal bearing Karoo sediments of the Mid Zambezi basin.

To address some of the geological problems of the Hwange area, remotely-sensed data, together with map data were integrated in a spatial database to allow modelling of the different parameters. The spatial database includes geological and non-geological information such as land use, drainage, communication networks and settlement patterns. Geological data included in the database include lithological units, topography, structural features (faults, joints and shear zones), coal seam characteristics and exploration drillhole information. To allow incorporation of these data sets together with geological data, a structured design of the database was adopted. The Entity Relationship (ER) model was used as a conceptual model and the Relational model as the implementation model.

Landsat TM data acquired on 20 June 1984 was used to update the existing maps and for mapping other areas and structures not shown on existing maps. Several image processing techniques were tested and the enhancement methods that gave maximum information were used for discriminating lithologic units and geological structures which form the most important part of the Hwange database. The image enhancement techniques found to be very effective for mapping in the Hwange area include, decorrelation stretching, normal false colour compositing, band difference, band ratio, principal components analysis and vegetation index images.

The colour composites made using any combinations of TM bands 1, 3, 4, 5 and 7 were very effective in discriminating the Karoo and cratonic rocks. TM bands 3 and 5 grey scale images and composites were effective in discriminating the Karoo basalts and the Escarpment grits mainly because of their high iron oxide content. TM band 7, because of its sensitivity to clay and other hydrous minerals such as micas, allowed distinction of most of the Karoo rocks which are dominated by mudstones, shales and clays. These rocks show very strong absorbance of band 7.

Colour composites, ratio and band difference images involving TM band 4 were used to detect faults associated with healthy vegetation during the winter. Water is usually trapped along the fractures in this semi-arid region and so is available to vegetation during the winter. Detection of these linear vegetated areas allowed detection of faults not apparent in the field nor discernible on other images.

Fracture detection was accomplished through image filtering and digitising of all lineaments detected on the filtered images. Two attributes of the lineaments were considered, orientation and length of the lineaments. Analysis of the lineaments using a GIS and histograms showed that modes of both orientations and length correspond to the faults previously mapped by Lockett (1979) and Watson (1960). Some of the faults detected were previously unknown.

Four major trends of lineaments and faults were found in the Hwange area. These are NNE-SSW, NE-SW, E-W and NW-SE . The NNE-SSW trending lineaments constitute 24% of the total lineaments and correspond to foliation traces and faults along the Magondi and Zambezi Mobile belts, the NE-SW and ENE-WSW trending lineaments (47 % of the total lineaments) correspond to the Zambezi Rift system and some joint sets in the Karoo basalt. The E-W (25% of the total lineament count) correspond to joints in the Karoo basalt and the NW-SE trending which forms the remaining 4% of the lineaments mapped, to the bedding planes in the Karoo sediments and some faults branching from the NE-SW trending faults.

The Entuba shear zone, the Lukosi and Deka faults are the master faults affecting the Hwange coalfields. Other faults affecting the Wankie Concession, Chaba, Entuba, Lukosi and some parts of

the Western Areas and Sinamatella coalfields are secondary splays of the Entuba shear zone, Deka and Lukosi faults which extend for distances of over 50 km in the area.

Interpretation of the Landsat TM data overlaid on mapped geological structures showed that the southern part of the Entuba inlier consists of a synformal fold plunging towards the south and cut on both limbs by strike-slip faults. Correlation of the Karoo strata such as positions of fireclay and carbonaceous shales in the Sinamatella and Western Areas coalfields, and the assessment of geomorphic indicators such as truncation of ridges, and occurrence of fault scarps, shows that movement along the Entuba fault was right lateral strike-slip coupled with dipslip movement. This suggests that the Western Areas and Wankie fields moved to the right and the Sinamatella and Entuba fields to the left.

Comparison of exploration drill hole depths to the top and bottom of the main coal seam on either sides of the major faults in the Entuba, Western Areas, Chaba and Sinamatella coalfields showed that vertical variations of coal seam is a function of vertical displacement along faults. Variations of seam depth from one field to another are primarily a function of the structure of the pre-Karoo floor and post-depositional faulting. The overall shapes of the coalfields can also be attributed to the effects of post-depositional faulting. Integration of interpreted geological features with map data in a GIS allowed selection of exploration targets and retrieval of certain lithologic units by means of formulating queries. Using the Structured Query Language and Relational algebra, the general information on lithologic units, faults, coal seams and land use can be accessed by setting conditions of retrieval.

Using the analytical tools in a GIS, areas with shallow coal seams were identified as exploration targets in the Western Areas coalfield (along the Mbumbusi road), in the Sinamatella field (north-west of Mandavu Dam), and the western part of the Entuba coalfield. These areas are also surrounded by deeper coal seams which can be mined using underground methods. The selected areas have a total of more than 1.48 billion tonnes of probable opencastable coal reserves and about 4 billion tonnes of probable underground coal reserves based on the borehole spacing of less than 3km and the average coal seam thicknesses intersected by boreholes in these areas and specific gravity of 1.5t/m^3.

This study therefore showed that integration of remotely sensed data and map data in a *2D GIS* can aid understanding of the geological structures and mineral distribution. Although information from a sedimentary basin was used in this study, the study has established a rationale for collection of geological data from remote sensing and existing maps, storage, retrieval and manipulation of the data to establish spatial relationships between geological phenomena.

7.2 Recommendations

Interpretations of geological structures and lithologic patterns for the southern part of the study area were supported by geological maps and field work. For the northern part of the study area, geological maps at the scale of the image were not available; interpretations, therefore, were mainly based on structures detected on the Landsat TM scene. To effectively interpret the subsurface geology of this area, diamond core drilling together with gravity and magnetic survey needs to be carried out to support geological structures detected in this study.

For the exploration targets identified in the Entuba, Sinamatella, Lukosi and Western Areas coalfields, gravity and magnetic survey also needs to be carried out together with diamond drilling. The data can be integrated with satellite imagery in a spatially referenced database as illustrated in this research to determine local variations of coal seams, fracture patterns and visualisation of the coalfields subsurface geology. Integration of these data sets in a GIS for each coalfield can give an insight into the lithological and structural relationships in each coalfield and so, help to minimise risks during mining.

9.0 References

Armstrong M.P. Densham P.J., 1990. Database Organization Strategies For Spatial decision Support Systems *Int.Journal of Geographic Information Systems, **Vol 4,*** pp 3-20.

Asabere R.K., 1992. Environmental assessment in the Mining Industry Using GIS, *Mapping Awareness and GIS in Europe, **Vol 6. No 9,*** Nov 1992, pp 41-44.

Asrar G., 1989. Theory and applications of Optical Remote Sensing, John Wiley, New York.

Avery T.E. Berlin G.L., 1992. Fundamentals of Remote sensing and Airphoto Interpretation, Macmillan, New York.

Barrett B.S. Curtis L.F., 1992. Introduction to Environmental Remote Sensing, Chapman and Hall, London.

Beaumont E.A. Foster N.H., 1992. Remote Sensing, Treatise of Petroleum Geology, Reprint Series 19, *The American Association of Petroleum Geologists*, Tulsa Oklahoma.

Berger Z., 1994. Satellite Hydrocarbon Exploration, Interpretation and Integration on Techniques, Springer-Verlag, Berlin.

Bonham-Carter G.F., 1994. Geographic Information Systems for Geoscientists: Modelling with GIS, Pergamon, Ontario.

Bosworth W., 1989. Basin and Range style Tectonics in East Africa, *Journal of African Earth Sciences, **Vol.8, Nos 2/3/4***, pp. 191-201.

Broderick T.J. Palloks H-H., 1982. The Western Areas Coalfield, *Records of Zimbabwe Coalfields **No.9,*** Zimbabwe Geological Survey, Harare.

Buhmann D. Lepper J., 1990. Significant mineral variations in the Lower Karoo deposits of the Mid-Zambezi Basin, Zimbabwe and their palaeoenvironmental implications. *South African Journal of Geology, **Vol.93, No. 5/6,*** Dec 1990, pp 744-753.

Burrough P.A., 1986. Principles of Geographic Information Systems for Land Resource Management, Clarendon Press, London.

Calkins H.W. Marble D.F., 1987. The Transition to Automated Production Cartography: Design of the Master Database, *The American Cartographer, **Vol.14.***

Chorowicz J., 1989. Transfer and transform fault zones in continental rifts: examples in the Afro-Arabian Rift System. Implications of Crust breaking. *Journal of African Earth Sciences, **Vol 8. No. 2/3/4,*** pp. 203-214.

Curran P.J., 1985. Principles of Remote Sensing, Longman, London.

Haris R., 1987. Satellite Remote Sensing, Routledge and Kegan Paul, London.

Hunt G.R., 1977. Spectral signatures of particulate minerals in the visible and near infrared, *Geophysics*, **Vol 41**, pp 501-513.

Date C.J., 1981. An Introduction to Database Systems, Addison- Wesley, Massachusetts.

Davis P.A. Berlin G.L., 1989. Rock discrimanation in the complex geologic environment of Jabal Salma, Saudi Arabia, Using Landsat Thematic Mapper data, *Photogrammetry Engineering and Remote Sensing, **Vol 55,*** August 1989, pp 1147-1160.

Davis P.A. Berlin G.L., Chavez P.S.,1987. Descrimination of Altered Basaltic Rocks in Southwestern United States by Analysis of Landsat Thematic Mapper Data: *Photogrammetry Engineering and Remote Sensing, **Vol 53, No.1,*** Jan 1987, pp 45-55.

Drury S.A., 1990. A Guide to Remote Sensing: Interpreting the Images of the Earth, Oxford University Press, Oxford.

Duguid K.B., 1986. Coal resources of Zimbabwe, *Mineral Resources of Southern Africa, **Vol 2,*** pp 2091-2098, Geological Society of South Africa, Johannesburg.

Duguid K.B., 1986. The coalfields of Zimbabwe, *Mineral Resources of Southern Africa, **Vol 2,*** pp 2087 - 2089, Geological Society of South Africa, Johannesburg.

Elmasri R. Navathe S.B., 1989. Fundamentals of Database Systems, Cummings, Redwood, Canada.

Fernandez R.N. Rusinkiewicz M.,1993. A conceptual design of a soil database for a Geographical Information System: *Int. J.Geographic Information Systems **Vol. 7, No. 6,*** pp 525 - 539.

Finch J.W.,1990. Location of high-yielding groundwater sites in Zimbabwe by use of remotely sensed data: In Remote Sensing: An operational technology for Mining and Petroleum Industries, Institute of Mining and Metallurgy, London.

Frostick L.E. Reid I., 1990. Structural control of sedimentation patterns and implications for economic potential of the East African Rift Basins. *Journal of African Earth Sciences, **Vol. 10. No. 1/2*** pp. 307-318.

Goertz A.F.H., 1989. Spectral Remote Sensing in Geology, In Asrar G., Theory and Applications of Optical Remote Sensing, John Wiley, New York, pp 491-523.

Gutmanis J.C. Lee H.M.H., 1990. New understanding of geological structure based on a remote sensing study at a geothermal field in southern California, U.S.A. In Remote Sensing: An operational technology for the Mining and Petroleum Industries, Institute of Mining and Metallurgy, London.

Haughton S.H., 1969. Geological history of Southern Africa, Geological Society of South Africa, Cape Town.

Kogbe C.A. Burollet P.F. 1990. A review of Continental Sediments. *Journal of Arican Earth Sciences, **Vol. 10, No. 1/2*** , pp 1-25.

Lambaise J.J., 1989. The Framework of African Rifting During Phanerozoic. *Journal of African Earth Sciences, **Vol. 8, Nos.2/3/4*** pp. 183-190.

Laurini R. Thompson D.,1992. Fundamentals of Spatial Information Systems, Academic Press, London.

Leyshon P.R. Tennick F.P., 1988. The Proterozoic Magondi Mobile belt, A review: *South African Journal Of Geology, **Vol 91, No1,*** pp 114-131.

Lightfoot B., 1929. The Geology of the Central Part of the Wankie Coalfield, *Zimbabwe Geological Survey Bulletin **No.15,*** Harare.

Lockett N.H., 1979. The Geology of the Country around Dett, *Zimbabwe Geological Survey Bulletin **No. 85***, Harare.pp 198.

Mah A. Taylor G.R. Lennox P. Balia L., 1995. Lineament analyses of Landsat Thematic Mapper Images, Northern Territory, Australia: *Photogrammetry Engineering and Remote Sensing, **Volume LXI, Number 6,*** pp 761-773.

Marble D.F., 1988. Approaches to the efficient design of spatial databases at a global scale: Building databases for global science, Taylor and Francis, London.

Mather P.M.,1989. Computer Processing of Remotely Sensed Images, An Introduction, John Wiley, New York.

Maufe H.B., 1931. A Geological Traverse down the Lower Inyantue Valley, Wankie District, Short Report ***26,*** Zimbabwe Geological Survey, Harare.

McCloy K.R., 1995. Resource Management Information Systems, Taylor and Francis, London.

Moore J.M. Guo L.J., 1990. Image enhancement of epithermal gold deposit alteration zones in Southeast Spain, Institute of Mining and Metallurgy, London.

Morris K., 1990. Automatic Detection of three-dimensional geological features from remotely sensed imagery and digital terrain models, In Remote Sensing: An operational technology for the Mining and Petroleum Industries, Institute of Mining and Metallurgy, London.

Mubu M.S., 1995. Aeromagnetic mapping and Interpretation of mafic Dykes in Southern Africa, Unpubl. Msc thesis, Department of Earth Resources Survey, ITC, Delft.

Navathe S. Schkolink M., 1978. View Representation in Logical database design, *In Proceedings of ACM-SIGMOID International Conference on Management of data.* Austin TX, ACM Press, pp 144-156.

Newton A.R., 1987. The fracture pattern around the Sutherland diatreme, Cape Province, from remote sensing, *South African Journal of Geology,* ***Vol.90, No.2,*** June 1987, pp 99-106.

Newton A.R., 1989. New data from Landsat image interpretation in the Richtersveld, *South African Journal of Geology, **Vol.92, No.2,*** June 1989, pp 125-133.

Nyerges T.L., 1989. Schema Integration analysis for the development of GIS databases *Int.Journal of Geographical Information Systems, **Vol.3, No.2*** pp 153-183.

Orpen J.L. Swain C.J. Nugent C. Zhou P.P., 1989. Wrench-fault and half graben tectonics in the development of the Palaeeozoic Zambezi Karoo basins in Zimbabwe-the "Lower Zambezi" and "Mid-Zambezi" basins respectively- and regional implications. *Journal of African Earth Sciences*, **Vol.8 Nos. 2/3/4** pp. 215-229.

Osterlen P.M., 1990. A new Occurrence of Dwyka Formation in Western Zimbabwe, *South African Journal of Geology, **Vol 93, No.2,*** pp 382-388.

Pallöks H-H., 1984. An assessment of some of the coal deposits in Northwest Zimbabwe, *Mineral Resources Series **No.19,*** Zimbabwe Geological Survey, Harare.

Palloks H-H., 1987. The Wankie Concession Area, *Records of Zimbabwe Coalfields **No.5,*** Zimbabwe Geological Survey, Harare.

Pardo O.H., 1995. Visualisation of Hidden geology in a 2D GIS with support from interpretation of potential field anomalies, Unpubl. MSC thesis, Department of Earth Resources Surveys, ITC, Delft.

Petters S.W., 1991. Regional geology of Africa, *Lecture Notes in Earth sciences **40,*** Springer-Verlag, Berlin.pp 169-172; 355-356; 508-525.

Praat P.J. Adamski J.J., 1994. Database Systems Management and Design, Boyd and Fraser, Massachusetts.

Prost G.L., 1989. Recognizing thrust faults on remote sensing images, *World Oil, Vol 211, No.3,* pp 39-45.

Qari M.Y.H.T., 1991. Application of Landsat TM Data to Geological studies, Al-Khabt Area, Southern Arabia, *Photogrammetry Engineering and Remote Sensing, Vol. 57, No. 4,* April 1991, pp 421- 429.

Rowan L.C. Bowers T.L., 1995. Analysis of Linear Features Mapped in Landsat Thematic mapper and side-looking Airborne Radar Images of the 1° by 1° Quadrangle, Nevada and California: Implications for Mineral Resource Studies, *Photogrammetry Engineering and Remote Sensing, Vol LXI, N0.6 June 1995,* pp 749-759.

Sabins F.F., 1978. Remote Sensing: Principles and Applications, Freeman, San Francisco.

Schowengerdt R.A., 1983. Techniques For Image processing and Classification in Remote Sensing, Academic Press, New York.

Shell Developments Zimbabwe (Pvt) Limited, 1981. Report on the Work carried out on the Entuba and Western Areas Coalfields of North west Zimbabwe, Unpublished, Zimbabwe Geological Survey Technical files.

Siegal B.S., 1980. Remote Sensing in Geology, John Wiley, New York.

Smith R.M.H. Eriksson P.G. Botha W.J., 1993. A review of the stratigraphy and sedimentary environments of the Karoo-aged basins of Southern Africa. *Journal of African Earth Sciences, Vol.16, No.1/2,* pp. 143-169.

Stagman J.G. Broderick T.J., 1978. An Outline of the Geology of Rhodesia, Zimbabwe Geological Survey Bulletin **80,** Harare pp 126.

Stowe C.W., 1989. Discussion on The Proterozoic Magondi Belt in Zimbabwe, *South African Journal of Geology, **Vol. 92, No.1*** March 1989, pp 69-71.

Thompson A.O. Broderick T.J. Palloks H-H., 1982. The Entuba Coalfield, Zimbabwe Geological Survey, *Records of Zimbabwe Coalfields* , **No.9.**

Tiercelin J.J., 1990. Rift-basin sedimentation: responses to climate, tectonism and volcanism. Examples from East African Rift. *Journal of African Earth Sciences, **Vol.10, Nos 1/2*** pp 283-305.

Ward C.R., 1984. Coal geology and coal technology, Blackwell, Melbourne.

Watson R.L.A., 1960. The Geology and Coal Resources of the Country around Wankie, Southern Rhodesia, *Zimbabwe Geological Survey Bulletin **48,*** Harare.pp 52.

Watson R.L.A., 1962. The Geology of the Kamativi and Lubimbi Areas, Zimbabwe Geological Survey Bulletin **57**, Harare, pp 42.

White G., 1990. Database Concepts 1, *NCGIA Unit 43.*

Wilsher W. Naicker I. Wullschleger N. Herbert R. De Wit M.J. Vitali E., 1993. Towards Intelligent Spatial Computing for Earth Sciences in South Africa: *S. Africa Journal of Science, **Vol 89** pp 315-323, July 1993.*

Woldai T., 1995. Lithologic and Structural mapping in a Vegetated low relief terrain using multiple source remotely sensed data: A case study of the Calanas area in Southwest Spain, *ITC Journal* **1995-2,** Eschede.

Yemane K. Kelts K., 1990. A short review of palaeoenvironments for Lower Beaufort (Upper Permian) Karoo sequences from southern to central Africa: A major Gondwana Lacustrine episode. *Journal of African Earth Sciences, **Vol.10, No.1/2*** pp.170-185.

Yesou H. Besnus Y. Rolet J., 1993. Extraction of spectral information from Landsat TM data and merger with SPOT panchromatic imagery - a contribution to the study of geological structures, *ISPRS Journal of Photogrammetry and Remote Sensing, **Vol48, No 5,*** pp 23-35.

Appendix 1

Tables of Entities

Table 3.2: **Coal seam**

No.	*Seam_id*	*Average Thickness*	*%Ash*	*%Sulphur*

Table 3.3: **Coalfield**

No.	*Field_id*	*Coalfield_Name*

Table 3.4: **Map Polygon**

Polygon_No.	*Polygon_id*

Table 3.5: **Series**

Series_id	*Series_Name*

Table 3.6 **Lithology**

No.	*Litho_id*	*Litho code*	*Name*	*Rock Type*	*Economic Minerals*

Table 3.7: **Formation**

Formation_id	*Formation Name*	*Contact with surrounding rocks*

Table 3.8: Group

Group id	*Group code*	*Tectonic history*	*Name*	*Age*

Table 3.9: Supergroup

Supergroup id	*Name*

Table 3.10 : Metamorphic Belt

Met-Belt id	*Name*

Table 3.11 : Sedimentary Basin

Basin id	*Name*

Table 3.12: Fault

Fault id	*Name*	*Type*	*System*

Table 3.13: Borehole

BH No	*X Coord*	*Y Coord*	*Z (Elev)*	*Total Depth*	*Seam Depth*	*Overburden Thickness*	*Footwall depth*

Table 3.14: Farm

Farm id	*Name*	*Type*

Appendix 2

Covariance Matrix

	Band 1	Band 2	Band 3	Band 4	Band 5
Band 1	3.75	2.36	3.44	3.44	1.73
Band 2	2.36	7.01	7.01	7.01	5.64
Band 3	3.44	7.01	13.10	13.10	7.77
Band 4	3.44	7.01	13.10	13.10	7.77
Band 7	1.73	5.64	7.77	7.77	25.75

Correlation Matrix

	Band 1	Band 2	Band 3	Band 4	Band 7
Band 1	1.000000	0.959593	0.891242	0.991242	0.875529
Band 2	0.959593	1.000000	0.931862	0.931862	0.719356
Band 3	0.891242	0.931862	1.000000	1.000000	0.823324
Band 4	0.991242	0.931862	1.000000	1.000000	0.8233324
Band 7	0.875529	0.719356	0.823324	0.823324	1.0000000

Component Summary

Component	C1	C2	C3	C4	C5
%Variance	64.85	16.56	11.68	6.90	0.00
Eigenvalue	3.24	0.83	0.58	0.35	0.00

Component Loading Summary

	C1	C2	C3	C4	C5
Band 1	0.633893	-0.546422	-0.545253	0.048035	0.0000
Band 2	0.853553	0.006380	0.097948	-0.511678	0.0000
Band 3	0.946368	-0.037131	0.253782	0.196475	0.0000
Band 4	0.946368	-0.037131	0.253782	0.196475	0.0000
Band 7	0.566517	0.725850	-0.385364	0.060759	0.0000

Appendix 3

Table AP 3.1 : Fault orientations in the Hwange Area

Azimuth (degrees)	Frequency	%Orientation
0-15	21	5.53
15-30	22	5.79
30-45	38	10
45-60	79	20.79
60-75	124	32.63
75-90	59	15.53
90-105	16	4.21
105-120	5	1.32
120-135	5	1.32
135-150	8	2.10
150-165	2	0.53
165-180	1	0.26

Table AP 3.2 : Lineament orientations in the Hwange area

Azimuth	Frequency	%Orientation
0-15	37	4.88
15-30	43	5.77
30-45	94	12.57
45-60	102	13.61
60-75	147	19.67
75-90	93	12.43
90-105	80	10.65
105-120	65	8.73
120-135	37	4.88
135-150	24	3.25
150-165	15	1.92
165-180	12	1.64

Table AP 3.3: Fault lengths in the Hwange Area

Length (metres)	Count	%Frequency	Total length
0-2000	165	39.91	181392.76
2000-4000	128	30.19	363441.61
4000-6000	56	13.21	270109.16
6000-8000	34	8.02	237481.94
8000-10000	20	4.72	178165.82
10000-12000	10	2.36	108211.80
12000-14000	5	1.18	63154.85
14000-16000	2	0.47	29327.51
16000-18000	0	0	0
18000-20000	3	0.71	57956.51
20000-22000	0	0	0
22000-24000	0	0	0
24000-26000	1	0.23	25587.13
26000+	0	0	0

Table AP 3.4: Lineament lengths

Length (metres)	Frequency/Count	%Frequency	Total Length
0-2000	151	20.16	208424.71
2000-4000	330	44.06	982040.15
4000-6000	152	20.29	735762.46
6000-8000	65	8.68	449766.14
8000-10000	20	2.68	178846.94
10000-12000	17	2.27	180785.87
12000-14000	8	1.07	104295.75
14000-16000	2	0.28	30564.71
16000-18000	1	0.13	16107.98
18000-20000	3	0.40	56668.89
20000-22000	0	0	0
22000-24000	0	0	0
24000-26000	0	0	0
26000+	0	0	0

Table AP 3.5: Azimuth and Lengths of lineaments

Azimuth (degrees)	%Frequency 0-3km	%Frequency 3-5km	%Frequency 5-7km	%Frequency 7km+
0-15	5	22	4	2
15-30	6	3	6	3
30-45	10	20	19	5
45-60	30	10	15	13
60-75	32	28	30	40
75-90	15	15	15	20
90-105	4	2	5	11
105-120	11	0	6	2
120-135	21	0	0	0
135-150	12	0	0	0
150-165	1	0	0	0
165-180	0	0	0	0

Appendix 4

Table AP 4.1: Attributes of lithological Units

AREA	PERIMET-ER	HWANGE_	HWANGE_ID	LITHO_ID	LITHO_CODE	LITHO_NAME
66031820	37838.3	2	825	6	k	Escarpment grit
74352480	55152.12	3	819	2	r	Kalahari sand
6982626	12876.96	4	848	2	r	Kalahari sand
3192596	8029.774	5	827	4	k7	Ripple marked flags
31673220	59319.58	6	828	34	Fb	Fault breccia
66462140	33967.55	7	817	4	k7	Ripple marked flags
1748227	6746.699	8	847	2	r	Kalahari sand
12791590	14289.59	9	849	2	r	Kalahari sand
21192010	37782.31	10	830	2	r	Kalahari sand
10485580	22870.34	11	845	2	r	Kalahari sand
22110260	26257.85	12	833	2	r	Kalahari sand
28258070	33495.21	13	823	3	B	Batoka basalt
3988976	11212.26	14	831	2	r	Kalahari sand
726407.1	4746.448	15	846	2	r	Kalahari sand
1043107	6173.485	16	832	2	r	Kalahari sand
7659795	22329.35	17	815	7	k5	Madumabisa mudstone
739265.8	4767.769	18	850	2	r	Kalahari sand

9804307	13572.31	19	822	6	k6	Escarpment grit
95245120	72934.13	20	834	34	Fb	Fault breccia
1087474	5625.962	21	829	3	B	Batoka basalt
14480910	29002.32	22	816	7	k5	Madumabis a mudstone
4753972	12435.62	23	813	7	k5	Madumabis a mudstone
32566630	48527.41	24	142	4	k7	Ripple marked flags
1035540	9434.84	25	810	7	k5	Madumabis a mudstone
480589.1	5645.136	26	811	7	k5	Madumabis a mudstone
17496300	39225.79	27	115	7	k5	Madumabis a Mudstone
5645595	19924.38	28	77	6	k6	Escarpment grit
559882.3	8067.12	29	812	7	k5	Madumabis a mudstone
32023980	62805.61	30	59	6	k6	Escarpment grit
1032639	5227.897	31	117	7	k5	Madumabis a Mudstone
641330	4045.761	32	118	7	k5	Madumabis a Mudstone
495622.3	3988.63	33	116	7	k5	Madumabis a Mudstone
14781020	29090.11	34	836	1	Al	Alluvium
1509472	9958.72	35	119	7	k5	Madumabis a Mudstone
1170440	6222.898	36	143	4	k7	Ripple marked flags
5132757	9774.316	37	617	20	Gb	Biotite Gneiss and Migmatites
684803.6	3586.152	38	8	10	k2	Carbonaceous Shale
2331109	9204.386	39	85	12	k1	Lower Wankie Sandstone

539337.1	3397.312	40	60	6	k6	Escarpment grit
5746171	19371.98	41	223	7	k5	Madumabis a Mudstone
105395	1215.571	42	150	22	G	Massive granite
151665.4	1658.592	43	240	1	Al	Alluvium
1889408	13160.17	44	239	1	Al	Alluvium
42976.84	1033.269	45	336	15	Tp	Tourmaline -garnet pegmatite
417314.5	2546.657	46	743	6	k6	Escarpment grit
442996.6	3153.9	47	225	6	k6	Escarpment grit
1421347	8569.023	48	330	24	km kms kmb	Veined tourmaline-garnet schists
146565.9	2140.401	49	331	15	Tp	Tourmaline -garnet pegmatite
93113.7	1980.682	50	332	15	Tp	Tourmaline -garnet pegmatite
262847.8	1922.75	51	222	7	k5	Madumabis a Mudstone
77706.81	1502.764	52	333	15	Tp	Tourmaline -garnet pegmatite
189885.1	2106.13	53	250	8	k4	Upper Wankie sandstone
562232.8	3845.15	54	283	12	k1	Lower Wankie Sandstone
21415110	30653.45	55	65	6	k6	Escarpment grit
437691.3	6028.02	56	337	15	Tp	Tourmaline -garnet pegmatite
161219.9	1901.732	57	341	19	Gp	Porphyritic granite
1204079	9940.468	58	129	7	k5	Madumabis a Mudstone

103134.5	1865.135	59	335	15	Tp	Tourmaline -garnet pegmatite
34570.2	754.41	60	334	15	Tp	Tourmaline -garnet pegmatite
7217556	21208.66	61	597	21	Gn	Strongly foliated gneiss
318287.1	4814.249	62	338	15	Tp	Tourmaline -garnet pegmatite
315923.8	3992.532	63	216	7	k5	Madumabis a Mudstone
1983337	12848.26	64	130	7	k5	Madumabis a Mudstone
694988.5	4925.342	65	66	6	k6	Escarpment grit
307867.4	2774.417	66	220	7	k5	Madumabis a Mudstone
1116624	5425.022	67	879	6	k6	Escarpment grit
1281017	5562.599	68	227	6	k6	Escarpment grit
102076.2	2576.751	69	537	32	mq,mqf,mq g	Quartzite
8645079	22504.76	70	595	21	Gn	Strongly foliated gneiss
5693303	29344.79	71	301	26	im	Garnet-Biotite Gneiss
360138.9	4355.621	72	277	12	k1	Lower Wankie Sandstone
150443300	183674.6	73	596	21	Gn	Strongly foliated gneiss
340192.4	5177.259	74	300	10	k2	Carbonaceo us Shale
635248.5	10835.78	75	278	12	k1	Lower Wankie Sandstone
149362.7	3041.055	76	339	15	Tp	Tourmaline -garnet pegmatite

246954.9	4963.227	77	505	7	k5	Madumabis a Mudstone
192040.1	2774:857	78	215	7	k5	Madumabis a Mudstone
411322.3	4472.607	79	344	19	Gp	Porphyritic granite
4448908	23347.16	80	279	12	k1	Lower Wankie Sandstone
681564.8	11833.46	81	538	32	mq,mqf,mq g	Quartzite
154563.4	2409.849	82	718	12	k1	Lower Wankie Sandstone
962143.3	13140.64	83	503	7	k5	Madumabis a Mudstone
1910964	10333.19	84	473	31	m,mc,mq,m b	metapelites
445266.9	6132.873	85	674	16	D	Dolerite Dyke
335436.2	3109.384	86	67	6	k6	Escarpment grit
479283.9	6085.524	87	719	12	k1	Lower Wankie Sandstone
1884320	9007.58	88	10	10	k2	Carbonaceo us Shale
13767960	60114.35	89	343	19	Gp	Porphyritic granite
337355.9	3494.683	90	282	12	k1	Lower Wankie Sandstone
668845	7589.597	91	342	19	Gp	Porphyritic granite
11664610	45393.23	92	472	31	m,mc,mq,m b	metapelites
2005164	13839.27	93	598	21	Gn	Strongly foliated gneiss
375880.4	5007.918	94	745	25	km,kms	Veined tourmaline garnet schist
981597.2	7487.601	95	6	10	k2	Carbonaceo us Shale

320853.3	11266.16	96	676	16	D	Dolerite Dyke
111366.2	2836.227	97	650	32	mq	Quartzite
633020.4	3704.673	98	56	6	k6	Escarpment grit
298451.4	4699.802	99	380	19	Gp	Porphyritic granite
2189067	6816.792	100	839	6	k6	Madumabis a mudstone
1801009	12361.25	101	251	8	k4	Upper Wankie sandstone
831104.8	7535.271	102	507	7	k5	Madumabis a Mudstone
177100.6	3098.025	103	652	31	m,mc	Sillimanite gneiss
24381500	31895.81	104	230	6	k6	Escarpment grit
1008944	7928.949	105	276	12	k1	Lower Wankie Sandstone
273558.8	2406.674	106	511	7	k5	Madumabis a mudstone
307052.2	6501.886	107	685	16	D	Dolerite Dyke
220179.4	4437.982	108	281	12	k1	Lower Wankie Sandstone
2671187	22100.27	109	296	10	k2	Carbonaceo us Shale
920157.3	6790.491	110	599	21	Gn	Strongly foliated gneiss
383492.3	3565.74	111	345	19	Gp	Porphyritic granite
167235.2	1726.748	112	94	8	k4	Upper Wankie sandstone
2108353	11081.96	113	275	12	k1	Lower Wankie Sandstone
48317.05	1031.555	114	50	9	k3	Fireclay
367228.1	7897.879	115	539	32	mq,mqf,mq g	Quartzite
2330605	11991.35	116	128	7	k5	Madumabis

						a Mudstone
46161.45	797.488	117	57	6	k6	Escarpment grit
5076379	12873.99	118	156	22	G	Massive granite
343935.2	3061.356	119	153	22	G	Massive granite
14598270	60895.12	120	747	20	Gb	Biotite Gneiss and Migmatites
947568.9	8156.564	121	600	21	Gn	Strongly foliated gneiss
33307.25	685.8786	122	219	7	k5	Madumabis a Mudstone
172694.5	5657.119	123	686	16	D	Dolerite Dyke
406049.5	10692.88	124	675	16	D	Dolerite Dyke
24031.58	585.7365	125	50	9	k3	Fireclay
1501246	6131.241	126	536	32	mq,mqf,mqg	Quartzite
181535.8	2857.981	127	601	21	Gn	Strongly foliated gneiss
30162750	48151.63	128	406	29	mBh,mcc	Mafic and calcareous amphibolites
21579.03	558.0399	129	50	9	k3	Fireclay
639351.8	17503.9	130	678	16	D	Dolerite Dyke
1059947	7545.546	131	252	8	k4	Upper Wankie sandstone
408520.1	4801.411	132	477	31	m,mc,mq,mb	metapelites
414771	5375.762	133	242	1	Al	Alluvium
78373.98	1027.034	134	50	9	k3	Fireclay
32943.97	727.9759	135	218	7	k5	Madumabis a Mudstone
145890.2	2233.961	136	475	31	m,mc,mq,mb	metapelites
58392.11	931.7195	137	50	9	k3	Fireclay
1280789	13362.31	138	476	31	m,mc,mq,m	metapelites

					b	
838268.4	5006.691	139	869	8	k4	Upper Wankie sandstone
498663	3106.791	140	295	10	k2	Carbonaceous Shale
104073.3	1578.067	141	340	15	Tp	Tourmaline-garnet pegmatite
465940.3	4709.149	142	541	32	mq,mqf,mqg	Quartzite
151751.4	2134.133	143	840	14	sj	Sijarira sediments
70683.17	2458.965	144	651	16	D	Dolerite Dyke
689493.6	6933.585	145	264	9	k3	Fireclay
956228.1	14892.41	146	542	32	mq,mqf,mqg	Quartzite
3839050	29811.15	147	540	32	mq,mqf,mqg	Quartzite
178028.2	2794.505	148	474	31	m,mc,mq,mb	metapelites
271204.2	6456.342	149	683	16	D	Dolerite Dyke
119326.5	2567.531	150	680	31	m,mc,mq	Sillimanite Gneiss
2838276	9785.238	151	764	7	k5	Madumabisa mudstone
2290660	14439.96	152	274	12	k1	Lower Wankie Sandstone
210160.2	2662.454	153	165	16	D	Dolerite Dyke
1952016	11704.7	154	293	10	k2	Carbonaceous Shale
337005.4	3768.379	155	163	22	G	Massive granite and Nebulitic gneiss
1929192	12524.54	156	253	8	k4	Upper Wankie sandstone
85971.75	1321.685	157	164	22	G	Massive granite and Nebulitic

						gneiss
2039936	10575.61	158	292	10	k2	Carbonaceous Shale
86500.02	1357.933	159	506	7	k5	Madumabisa Mudstone
19951.25	666.9185	160	46	9	k3	Fireclay
549388.8	5204.165	161	238	1	Al	Alluvium
423848.7	4031.652	162	259	8	k4	Upper Wankie sandstone
60612.69	976.7606	163	52	6	k6	Escarpment grit
191100.4	3284.886	164	681	31	m,mc,mq	Sillimanite Gneiss
134148.2	1955.761	165	294	10	k2	Carbonaceous Shale
196026.3	2712.953	166	24	12	k1	Lower Wankie Sandstone
96420.98	1997.12	167	687	31	m,mc,mq	Sillimanite gneiss
53909.38	976.5909	168	870	10	k2	Carbonaceous Shale
3624912	23682.39	169	671	32	mq,mqf	Quartzite
436185.6	3094.536	170	291	10	k2	Carbonaceous Shale
2575498	23539.31	171	479	31	m,mc,mq,mb	metapelites
119442.5	1311.179	172	50	9	k3	Fireclay
588267.8	4199.044	173	679	20	Gb	Biotite Gneiss and Migmatites
37052	1031.411	174	166	16	D	Dolerite Dyke
415126.3	4550.798	175	221	7	k5	Madumabisa Mudstone
1934761	30321.75	176	684	16	D	Dolerite Dyke
640853	5483.438	177	237	1	Al	Alluvium
37651.33	792.5598	178	266	9	k3	Fireclay
33575580	79041.1	179	644	22	G	Massive Granite and Nebulitic Gneiss
179118.3	5533.784	180	682	16	D	Dolerite

						Dyke
806907	7990.498	181	302	26	im	Garnet-Biotite Gneiss
38285980	187705.2	182	494	31	m,mc,mq,mb	metapelites
714164.3	8561.185	183	255	8	k4	Upper Wankie sandstone
417710	4112.477	184	290	10	k2	Carbonaceous Shale
134772.5	1615.099	185	748	21	Gn	Strongly foliated gneiss
61917.2	1567.844	186	508	7	k5	Madumabisa mudstone
2362803	23407.9	187	672	31	m,mc,mq	Andalusite Gneiss
12082830	36637.8	188	404	29	mB, mBh	Amphibolites
135953.9	1899.788	189	478	31	m,mc,mq,mb	metapelites
166227.8	3699.283	190	549	32	mq,mqf,mqg	Quartzite
72274.05	1460.416	191	688	32	mq, mqf	Quartzite
33260.47	935.952	192	677	31	m,mc.mq	Sillimanite gneiss
1684907	7683.37	193	53	6	k6	Escarpment grit
358371.4	3925.992	194	254	8	k4	Upper Wankie sandstone
95015.38	1801.655	195	510	12	k1	Lower Wankie Sandstone
241493.4	5124.914	196	716	16	D	Dolerite Dyke
3531361	13660.27	197	544	32	mq,mqf,mqg	Quartzite
3743021	27602.91	198	407	29	mBh,mcc	Mafic and calcareous amphibolites
33624050	43304.29	199	535	32	mq,mqf,mqg	Quartzite

Table AP 4.2 : Attributes of Mines

AREA	PERIMETER	MINES_	MINES_ID	NAME	TYPE	STATUS	MINERAL
0	0	1	1	Kamativi	ug+oc	closed	tin,tantalum
0	0	2	2	Kalinda	ug	closed	tin,tantalum
0	0	3	3	Ringals	claim	surrendered	copper
0	0	4	4	Chiwawa	claim	surrendered	copper
0	0	5	5	Python	claim	surrendered	copper
0	0	6	6	Sinyanga	claim	surrendered	copper
0	0	7	7	Regina	oc	closed	tin
0	0	8	8	Lutope	ug	closed	tin
0	0	9	9	San	oc	closed	tin
0	0	10	10	Kapata	oc	closed	tin
0	0	11	11	Marion	ug	closed	Flourite
0	0	12	12	First_Claims	oc	closed	Flourite
0	0	13	13	Lukosi_Shafts	ug	closed	coal
0	0	14	14	Labrynth	ug	closed	Flourite
0	0	15	15	Entuba Shaft	ug	closed	coal
0	0	16	16	Entuba	oc	closed	Flourite
0	0	17	17	Wankie_No1	ug	closed	coal
0	0	18	18	Wankie_No2	ug	closed	coal
0	0	19	19	Wankie_No3	ug	open	coal
0	0	20	20	Wankie_No4	ug	closed	coal
0	0	21	21	Lupote	claim	surrendered	copper
0	0	22	22	Gwayi_River	ug	closed	copper
0	0	23	23	Betlyn	oc	closed	Flourite
0	0	24	24	Lulu	oc	closed	Lead-Zinc
0	0	25	25	Luso_Spar	oc	closed	Flourite
0	0	26	26	Anglo	ug	closed	copper

0	0	27	27	Tung	oc	closed	Tungsten
0	0	28	28	Kwala	oc	closed	Mica
0	0	29	29	Luca	oc	closed	copper
0	0	30	30	Ubique	oc	closed	Mica
0	0	31	31	Gem_South	oc	closed	Mica
0	0	32	32	RHA	ug	closed	Tungsten
0	0	33	33	Eden	oc	closed	Mica
0	0	34	34	Penrose	oc	closed	Mica
0	0	35	35	Inyantue	ug+oc	closed	coal,graphite
0	0	36	36	Elbas	oc	closed	Lead-Zinc
0	0	37	37	Donga	oc	closed	tin, lead-zinc
0	0	38	38	Kapami	oc	closed	tin,granite
0	0	39	39	JJ	oc	closed	Mica
0	0	40	40	Kamalala	oc	closed	tin
0	0	41	41	Paola	oc	closed	Mica
0	0	42	42	Evvans	claim	surrendered	copper
0	0	43	43	Fin	ug	closed	copper
0	0	44	44	Five_Aces	claim	surrendered	copper
0	0	45	45	Copper_Rock	ug	closed	copper
0	0	46	46	Cobra	oc	closed	copper
0	0	47	47	Adder	ug	closed	copper
0	0	48	48	Gaboon_Viper	ug	closed	copper
0	0	49	49	Python	ug	closed	copper
0	0	50	50	Chiwawa	claim	surrendered	copper
0	0	51	51	Joeys	oc	closed	copper
0	0	52	52	Jans	oc	closed	copper
0	0	53	53	Fly	oc	closed	tantalum
0	0	54	55	Wallys	ug	closed	copper
0	0	55	56	Larrys	ug	closed	copper
0	0	56	57	Nola	oc	closed	limestone
0	0	57	58	Diary	oc	closed	copper
0	0	58	59	Gurambira	oc	closed	copper
0	0	59	60	Rona	claim	surrendered	nickel
0	0	60	61	Mpofu	claim	surrendered	silica
0	0	61	62	Rhuwesa	o/c	closed	Mica

0	0	62	63	GBM	oc	closed	limestone
0	0	63	64	Evvan_Shaft	ug	closed	copper
0	0	64	65	Copra	oc	closed	copper
0	0	65	66	Joeval	oc	closed	copper
0	0	66	68	Zang	oc	closed	copper
0	0	67	69	Wankie Opencast	oc	open	coal

Table AP 4.3: Attributes of Boreholes

AREA	PERIMETER	BHS_	BH_NO	TOTALDEPTH	SEAM_DEPTH	FIELD_ID	FOOTWDEPTH	ASH	SEAM_THICK
0	0	1	1	62.48	50.9	3	62.18	15.5	11.28
0	0	2	2	71.93	61.26	3	71.32	17.2	10.06
0	0	3	3	481.58	475.79	6	480.67	33.1	4.88
0	0	4	4	393.8	0	6	0	0	0
0	0	5	5	155.45	0	6	0	0	0
0	0	6	6	645.57	641.3	6	642.82	24.1	1.52
0	0	7	7	457.2	0	6	0	0	0
0	0	8	8	374.9	368.5	6	370.02	29.7	1.52
0	0	9	9	314.35	0	6	0	0	0
0	0	10	10	263.65	0	6	0	0	0
0	0	11	11	21.34	14.63	6	17.37	23.25	2.74
0	0	12	12	11.58	0	6	0	0	0
0	0	13	13	170.99	0	6	0	0	0
0	0	14	14	166.12	153.92	3	164.29	17.1	10.36
0	0	15	15	182.88	119.48	3	132.89	21.9	13.41
0	0	16	16	231.34	219.76	3	230.73	17.7	9.45
0	0	17	17	240.79	228.9	3	238.05	17.1	9.14
0	0	18	18	306.32	298.09	3	304.8	23.3	6.71
0	0	19	19	33.53	0	3	0	0	0
0	0	20	21	292.61	282.24	3	290.47	22.1	8.23
0	0	21	23	182.88	0	5	0	0	0
0	0	22	24	81.69	0	5	0	0	0
0	0	23	25	124.97	0	5	0	0	0
0	0	24	26	23.77	0	5	0	0	0
0	0	25	27	22.55	0	5	0	0	0
0	0	26	28	25.91	0	5	0	0	0
0	0	27	30	107.59	0	6	0	0	0
0	0	28	31	490.42	0	3	0	0	0
0	0	29	32	507.49	495.3	3	500.18	17.2	4.88

0	0	30	33	432.21	0	5	0	0	0
0	0	31	34	392.58	384.05	4	389.84	16.6	5.79
0	0	32	35	252.98	226.77	4	231.95	23	5.18
0	0	33	36	59.44	50	4	59	23.74	3.05
0	0	34	37	725.42	0	3	0	0	0
0	0	35	38	242.32	231.34	4	236.22	21.7	4.9
0	0	36	39	70.1	59.13	3	69.18	14.5	11.28
0	0	37	20	60.96	48.68	3	60.65	15.5	10.97
0	0	38	22	76.12	0	3	0	0	0
0	0	39	29	487.2	0	3	0	0	0
0	0	40	40	280.72	0	3	0	0	0
0	0	41	41	56.46	38.89	3	47.39	15.6	12.5
0	0	42	42	46.63	33	3	43.38	13.4	10.38
0	0	43	43	46.33	33.7	3	44.53	11.2	10.83
0	0	44	44	51.51	35.25	3	46.18	8.9	10.93
0	0	45	45	63.4	49.68	3	61.77	8.4	12.09
0	0	46	46	500.5	486.16	3	497.13	12.3	10.97
0	0	47	47	570.1	547.62	3	559.6	11.9	11.98
0	0	48	48	82.9	69.11	3	80.77	13.4	11.66
0	0	49	49	117.5	103.33	3	115.52	27.6	12.19
0	0	50	50	62.92	54.86	3	64.26	10.5	9.4
0	0	51	51	48.02	34.16	3	46.33	8.8	12.17
0	0	52	52	50	34	3	37	27.6	3
0	0	53	53	61.57	47.72	3	57.06	25.1	9.34
0	0	54	54	44.5	32.31	3	40.81	15.4	8.5
0	0	55	55	396.22	346.4	3	359.66	15.4	13.26
0	0	56	56	63.4	49.07	3	62	14.5	12.93
0	0	57	57	46.63	0	3	0	0	0
0	0	58	58	60.05	49.53	3	59.61	11	10.08
0	0	59	59	71.02	57.61	3	70.02	13.1	12.41
0	0	60	60	39.77	0	3	0	0	0
0	0	61	61	45.87	39.01	3	43.84	10.2	4.83
0	0	62	62	52.42	39.01	3	48.87	12.9	9.86
0	0	63	63	54.56	41.15	3	53.04	11.1	11.89
0	0	64	64	55.83	0	3	0	0	0
0	0	65	65	183.49	171	3	181.98	13.5	10.98
0	0	66	66	45.24	0	3	0	0	0
0	0	67	67	50	0	3	0	0	0
0	0	68	68	68.05	55.44	3	65.84	16.4	10.4
0	0	69	69	87.13	55.91	3	67.57	11.2	11.66
0	0	70	70	109.28	94.14	3	104.1	12.7	9.87
0	0	71	71	281.64	270.05	3	281.18	15.5	11.13
0	0	72	72	29.56	0	3	0	0	0
0	0	73	73	40	0	3	0	0	0

0	0	74	74	116.13	100.58	3	114.66	10.2	14.08
0	0	75	75	63.4	53.34	3	61.57	0	8.23
0	0	76	76	170.99	161.39	3	170.38	27	8.99
0	0	77	77	115.21	105.77	3	114.6	10	8.83
0	0	78	78	101.19	89.97	3	100.35	15.3	10.38
0	0	79	79	174.04	161.08	3	173.35	11.2	12.27
0	0	80	80	181.05	170.69	3	180.74	10.1	10.05
0	0	81	81	215.18	204.08	3	212.58	22.9	8.5
0	0	82	82	266.69	256.64	3	265.18	0	8.54
0	0	83	83	336.76	329.79	3	332.38	0	2.59
0	0	84	84	67.06	53.04	3	66.55	19.3	13.51
0	0	85	85	51.26	37.8	3	50.9	20.7	13.1
0	0	86	86	56.43	43.93	3	55.93	19.9	12
0	0	87	87	64.92	52.58	3	64.58	18.4	12
0	0	88	88	67.56	55.56	3	67.56	19.3	12
0	0	89	89	54.86	49.99	3	53.77	11.4	3.78
0	0	90	90	21.34	8.53	3	20.37	15.5	11.84
0	0	91	91	48.92	31.23	3	41.8	15.5	10.57
0	0	92	92	48.92	37.19	3	48.52	22.1	11.33
0	0	93	93	57	42.98	3	56.69	24.4	13.71
0	0	94	94	61.57	50.9	3	60.86	18	9.96
0	0	95	95	63.4	49.02	3	61.23	19.9	12.21
0	0	96	96	48.16	33.51	3	46.8	23	13.29
0	0	97	97	60	45.09	3	59.21	22	14.12
0	0	98	98	55	42.67	3	52.88	15	10.21
0	0	99	99	94.79	81.08	3	92.81	18.3	11.73
0	0	100	100	116.13	102.11	3	115.66	20.6	13.55

Table AP 4.4: Attributes of Coalfields

FIELD_ID	NAME
1	Western Areas
2	Wankie Concession
3	Entuba
4	Sinamatella
5	Pongora
6	Lukosi
7	Inyantue

Table AP 4.5: Attributes of Settlements

AREA	PERIMETER	SETTLE_	SETTLE_ID	NAME	FUNCTION
4043520	10199.31	2	1	Kamativi	Mine Village
215857.7	2002.464	3	3	Wankie - Sindrella	Mine Village
39125.63	909.8063	4	7	Wankie-Sindrella	Mine Village
95948.42	1171.259	5	21	St Marys	Mission Station
129811.5	1861.355	6	10	No.3 Colliery	Mine Village
159665.3	1732.015	7	18	Gwayi River Mine	Mine Village
183447.5	2003.885	8	20	Cross Roads	Business Centre
460148.5	10098.32	9	22	Hwange Airport	Airport
254613.1	2132.259	10	24	Hwange Safari Lodge	Hotel
184104.8	2825.451	11	25	Main Camp Aerodrome	Airport
6336.953	319.3935	12	28	Deka Drum	Fishing Resort
34639.63	699.492	13	16	Simangani	Clinic
274527.6	2445.57	14	8	Thompson Junction	Railway Station
726357	3459.269	15	14	ZESA-Ingagula	Residential Area
187733.6	2086.62	16	9	No.3 Low Density	Residential Area
498624.9	3229.13	17	5	No.3 Village	Mine Village
208605.9	1923.465	18	23	Marist Brothers	Mission Station
2789765	7284.201	19	11	Dete	Railway Station
713511.1	3999.257	20	12	Main Camp	Game Camp
221673.1	2695.094	21	29	Sinamatella Airstrip	Airport
307727.2	2419.747	22	19	Gwayi River Mine	Mine Village
511543.1	3913.885	23	13	Sinamatella Camp	Game Camp
1392917	4891.678	24	31	Hwange-Industrial Area	Light Industry
1969689	7658.214	25	4	Wankie-No.2	Mine Village
666990.1	3974.642	26	15	Wankie-No.5	Mine Village
964915.3	5638.947	27	17	Empumalanga	Residential Area
2021202	7809.518	28	6	Hwange-Baobab	Residential Area
10082890	20898.4	29	2	Wankie No.1	Residential Area
346157.6	2717.206	30	30	Lukosi	Business Centre

Appendix 5

GIS Database Analysis

This section illustrates manipulation and retrieval of the integrated information in the Hwange database can be manipulated and retrieved. Spatial relationships between different data sets such as lithologic units, faults, coal seams, drainage and topographic features can be modelled in the database. Five sample queries have been devised to address some of the needs and objectives of the project listed in Chapter 1 such as provision of information pertaining to coal seam characteristics, fracture patterns and lithological distributions. The solution of each query is given as a map and/ or a table with comments on the significance of each result. The queries are expressed in Structured Query Language (SQL) using the syntax used in **ESRI's *ARCVIEW*** software.

Query No.1

To determine the aerial extent of the Lower Karoo rocks in the Hwange Area where coal has been intersected by diamond drill holes which are less than 3km apart.

To address this query data is retrieved from two layers in the database, ***Lithology (Hwange)*** and ***BHS (Borehole)*** layers:

ARCVIEW 2.0: *[Seam_thickness] > 0*; **THEME PROPERTIES - Select By Theme**
Select features of active themes that [*Completely Contain*] the selected features of *[BHS]*

Comment

All the areas with boreholes that intersected coal in all the coalfields regardless of its quality are retrieved. The areas with a borehole spacing of less than 3km is also isolated. This information is important for reconnaissance mapping of the distribution of coalseams in the Hwange coalfields. Using the average coalseam thicknesses given in the database in Chapter 2 and the areas of the portions of the coalfields with borehole spacing of less than 3km, the total tonnage of insitu coal

was estimated. The table below show the estimated insitu coal tonnages in the areas isolated by using the above query.

Table A5.1

Coalfield	Area (m^2) $x10^6$	Average Seam Thickness (m)	Average Specific Gravity (t/m^3)	Volume (m^3) $x10^6$	Tonnage (Insitu Coal) $x10^6t$
Wankie Concession	568.801088	6.5	1.50	3981.607616	3882.067426
Western Areas	92.426100	7.9	1.50	730.166190	1095.249285
Entuba	28.989380	10.3	1.50	298.590614	447.885921
Sinamatella	7.469218	5	1.50	37.346090	56.019135

Fig 7.1 is a map showing areas in the Wankie (Option Area), Western Areas, Entuba, Sinamatella and Lukosi fields where coal has been intersected.

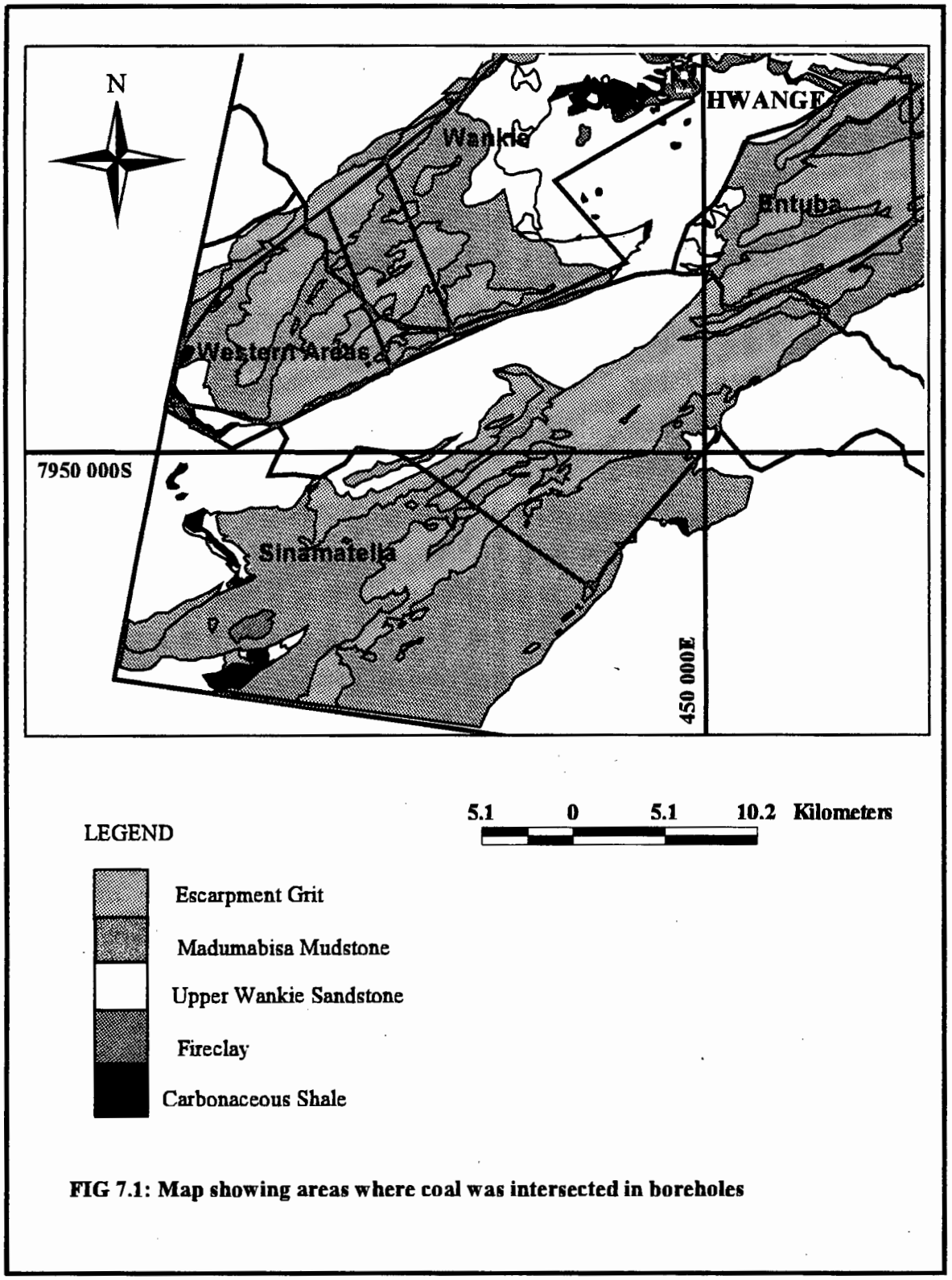

FIG 7.1: Map showing areas where coal was intersected in boreholes

Query No.2

To determine the areas in the coalfields with burnt coal which are within a distance of 2 kilometres from major fault zones.

Data is retrieved from three layers, the ***Lithology*** layer, Coalfield layer and the ***Faults*** layer. The ***Lithology*** layer contains information on burnt coal areas and the ***Fault*** layer on the locations of faults and their spacing.

ARCVIEW 2.0 *[Litho_name = "Burnt Coal"]* **THEME PROPERTIES**
Select features of active themes [*FAULTS*] [Are Within Distance of] the selected features of *[LITHOLOGY]*:Selection Distance: *2km*

Comment

Areas with burnt coal areas which are within 2 kilometres from the Entuba, Inyantue and Lukosi fault zones are retrieved. This data can aid understanding of the distribution of burnt coal areas in relation to fault zones. The areas with fault spacing less than 1 kilometre show areas which are heavily fractured and so not suitable for any mining.

Query No.3

To find all the faults in the area associated with the Zambezi Rift system and along which the lower Karoo rocks, are down faulted.

Data is retrieved from the ***Lithology*** layer and the ***Faults*** layer.

ARCVIEW 2.0 *[Fault System = Zambezi Rift]; [Subgroup = "Lower Karoo"]*
Select by Theme: Features of Active theme [*FAULTS*] [Are Within Distance of] The selected features of *[LITHOLOGY]*: Selection Distance: 0km

Comment:

Only the areas with dipslip faults down faulting the Karoo rocks are retrieved. This information aids understanding of the relationships between Karoo rocks and the different faulting episodes and fault types.

Query No.4

To isolate exploration targets and demarcate the areas into potential areas for opencast areas and underground mining within 5km of a main road or railroad.

Information to answer this query is retrieved from four layers, **Boreholes (BHS), Coalfields, Lithology,** Roads and **Faults.** The model parameters used to select suitable conditions are specified as follows:

Quality coal: Average ash content less than 15%

Open cast mining: Depth to top of coal seam less than 100m

Occurrence of fireclay, upper Wankie Sandstone and carbonaceous shales on surface also indicate shallow areas.

Underground mining: Depth to coal seam greater than 100m and less than 500m

ARCVIEW 2.0 *[% Ash < 15] ; [Rock_Name = fireclay, Upper Wankie Sandstone, Carbonaceous Shale]*

OPENCAST: [*Overburden < 100m*]

UNDERGROUND: *[Overburden > 100m] and [Overburden < 500m*]

Comment

To address this query all the information associated with shallow coal deposits as identified by the occurrence of fireclay, carbonaceous mudstones and upper Wankie sandstone on the surface and borehole intersections is used. Fig. 7.2 shows the results of this query. The depth from surface to

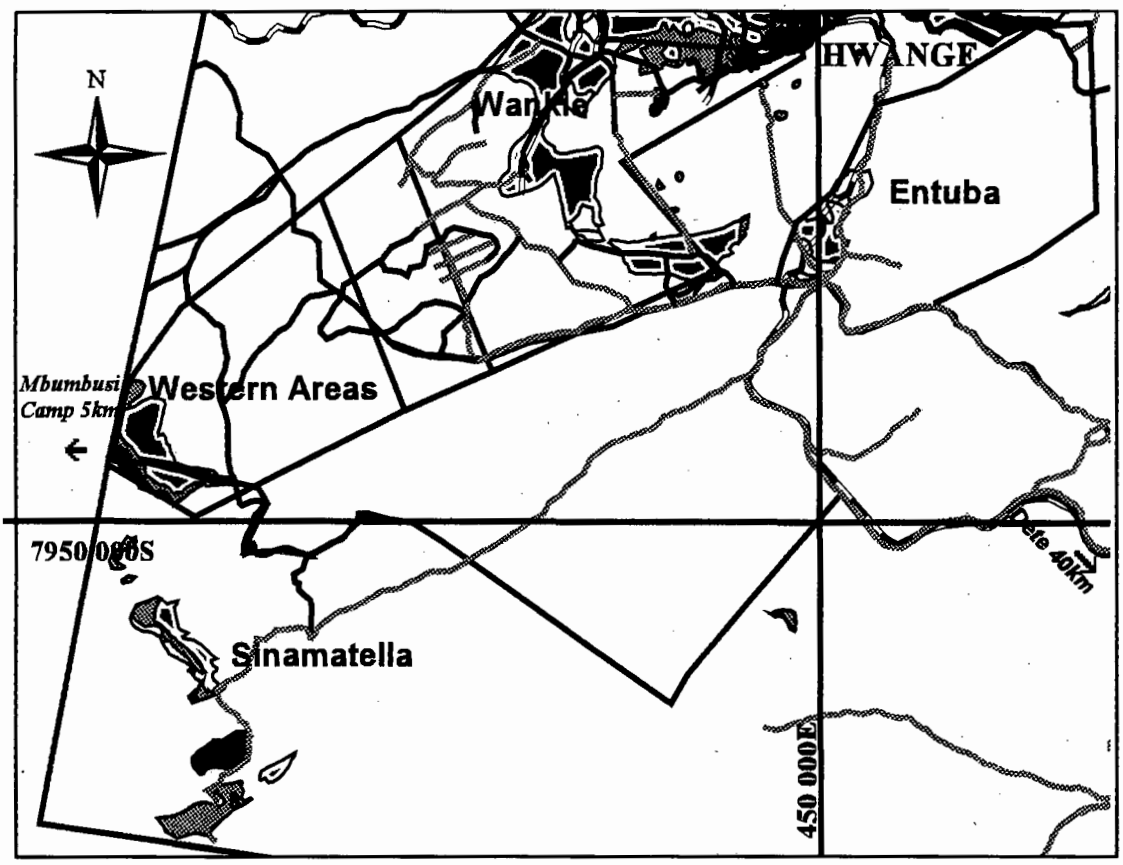

FIG 7.2: Map showing opencastable coal targets in the Hwange Area within a distance of 5km from a road or railway

the top of the main coal seam was used for assessment of variations. Parameters chosen from the maps of the Hwange area include categories of suitable sites according to coal seam depth ranging from 0 to 100 metres for opencast reserves and 100m to 500m for underground reserves. These parameters are set according to specifications in the mining industry given the available technology. Coal reserves within 5km from the main roads and railroads are more economic in terms of the economics of transport and accessibility to other facilities. Only areas in the Entuba and some parts of the Wankie field are within a distance of 5km from a main road or railroad.

Query No.5

To find areas with shallow and good quality coal (Ash < 15%) in the Lukosi, Sinamatella and Western Areas coalfields which occur in the Hwange National park.

The data is retrieved from four layers, **Borehole, Coalfield, Lithology** and **Land use (Farms)** layers.

ARCVIEW 2.0 ***[%Ash < 15]; [Field_name = "Lukosi; Sinamatella; Western Areas"]***

Select By Theme: Select features of active theme [*LITHOLOGY*]

[Completely Contain] Selected features of [*BHS*]

[Land Use = National Park]

Select By Theme: Features of active theme *[FARMS]* *[Completely Contain]*

Selected Features of *[LITHOLOGY]*

Fig 7.3 below shows the results of this query.

Comment:

The Hwange National Park is a protected area, so environmental assessment has to be done for any exploration activity carried out in the areas within the national parks. By overlaying the borehole information on the Farms (Land use) layer, it was shown that half of the shallow areas with coal seams characterised by less than 15% ash in the Western Areas coalfield and all the shallow areas in the Sinamatella field fall within the Hwange National Park.

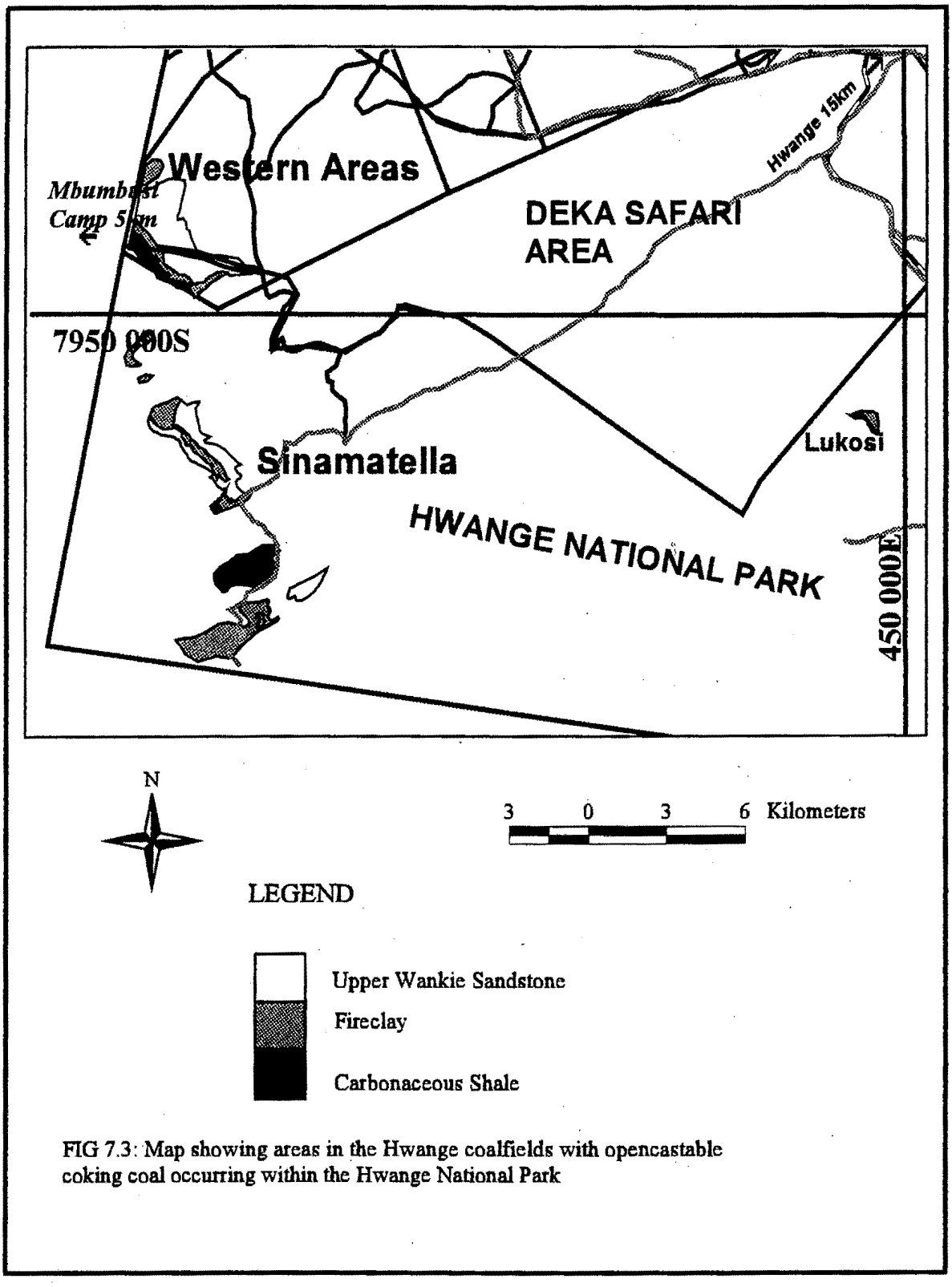

FIG 7.3: Map showing areas in the Hwange coalfields with opencastable coking coal occurring within the Hwange National Park